International Ocean Discovery Program Expedition 371 Preliminary Report

Tasman Frontier Subduction Initiation and Paleogene Climate

27 July–26 September 2017

Rupert Sutherland, Gerald R. Dickens, Peter Blum, and the Expedition 371 Scientists

IODP
INTERNATIONAL OCEAN DISCOVERY PROGRAM

Publisher's notes

Core samples and the wider set of data from the science program covered in this report are under moratorium and accessible only to Science Party members until 2 February 2019.

This publication was prepared by the *JOIDES Resolution* Science Operator (JRSO) at Texas A&M University (TAMU) as an account of work performed under the International Ocean Discovery Program (IODP). Funding for IODP is provided by the following international partners:

National Science Foundation (NSF), United States
Ministry of Education, Culture, Sports, Science and Technology (MEXT), Japan
European Consortium for Ocean Research Drilling (ECORD)
Ministry of Science and Technology (MOST), People's Republic of China
Korea Institute of Geoscience and Mineral Resources (KIGAM)
Australia-New Zealand IODP Consortium (ANZIC)
Ministry of Earth Sciences (MoES), India
Coordination for Improvement of Higher Education Personnel (CAPES), Brazil

Portions of this work may have been published in whole or in part in other IODP documents or publications.

Disclaimer

Any opinions, findings, and conclusions or recommendations expressed in this publication are those of the author(s) and do not necessarily reflect the views of the participating agencies, TAMU, or Texas A&M Research Foundation.

Copyright

Citation

Sutherland, R., Dickens, G.R., Blum, P., and the Expedition 371 Scientists, 2018. *Expedition 371 Preliminary Report: Tasman Frontier Subduction Initiation and Paleogene Climate.* International Ocean Discovery Program. https://doi.org/10.14379/iodp.pr.371.2018

ISSN
World Wide Web: 2372-9562

January 2018

Expedition 371 participants

Expedition 371 scientists

Rupert Sutherland
Co-Chief Scientist
Department of Geography, Environment, Earth Sciences
Victoria University of Wellington
New Zealand
rupert.sutherland@vuw.ac.nz

Gerald R. Dickens
Co-Chief Scientist
Department of Earth, Environmental and Planetary Sciences
Rice University
USA
jerry@rice.edu

Peter Blum
Expedition Project Manager/Staff Scientist
International Ocean Discovery Program
Texas A&M University
USA
blum@iodp.tamu.edu

Claudia Agnini
Paleontologist (nannofossils)
Dipartimento di Geoscienze
Università degli Studi di Padova
Italy
claudia.agnini@unipd.it

Laia Alegret
Paleontologist (foraminifers)
Departamento de Ciencias de la Tierra (Paleontología)
Universidad de Zaragoza
Spain
laia@unizar.es

Joyeeta Bhattacharya
Sedimentologist
Department of Earth, Environmental and Planetary Sciences
Rice University
USA
jb79@rice.edu

Aurelien Bordenave
Sedimentologist
Geological Survey of New Caledonia
New Caledonia
aurelien.bordenave@gouv.nc

Liao Chang
Paleomagnetist
School of Earth and Space Sciences
Peking University
China
liao.chang@pku.edu.cn

Julien Collot
Physical Properties Specialist
Geological Survey of New Caledonia
New Caledonia
julien.collot@gouv.nc

Margot J. Cramwinckel
Organic Geochemist/Palynologist
Department of Earth Sciences
Utrecht University
The Netherlands
m.j.cramwinckel@uu.nl

Edoardo Dallanave
Paleomagnetist
Department of Earth and Environmental Sciences, Geophysics Section
Ludwig-Maximilians-Universität München
Germany
dallanave@geophysik.uni-muenchen.de

Michelle K. Drake
Sedimentologist
Ocean Sciences Department
University of California, Santa Cruz
USA
mkdrake@ucsc.edu

Samuel J.G. Etienne
Sedimentologist
Department of Industry, Mines and Energy of New Caledonia
Geological Survey of New Caledonia
New Caledonia
samuel.etienne@gouv.nc

Martino Giorgioni
Sedimentologist
Instituto de Geociência
Universidade de Brasília
Brazil
gmartino@unb.br

Michael Gurnis
Physical Properties Specialist
Seismological Laboratory
California Institute of Technology
USA
gurnis@gps.caltech.edu

Dustin T. Harper
Stratigraphic Correlator
Department of Earth and Planetary Sciences
University of California, Santa Cruz
USA
dtharper@ucsc.edu

Huai-Hsuan May Huang
Paleontologist (ostracods)
Atmosphere and Ocean Research Institute
The University of Tokyo
Japan
huanghuaihsuan@gmail.com

Allison L. Keller
Sedimentologist
Department of Earth Sciences
University of California, Riverside
USA
akell002@ucr.edu

Adriane R. Lam
Paleontologist (foraminifers)
Department of Geosciences
University of Massachusetts
USA
arlam@geo.umass.edu

He Li
Inorganic Geochemist
Institute of Oceanology, Chinese Academy of Sciences
China
lihe@qdio.ac.cn

Hiroki Matsui
Paleontologist (foraminifers)
Department of Earth Science
Tohoku University
Japan
hmatsui531@gmail.com

Cherry Newsam
Paleontologist (nannofossils)
Department of Earth Sciences
University College London
United Kingdom
cherry.newsam.11@ucl.ac.uk

Yu-Hyeon Park
Organic Geochemist
Department of Oceanography
Pusan National University
Republic of Korea
parky@pusan.ac.kr

Kristina M. Pascher
Paleontologist (radiolarians)
GNS Science
New Zealand
kristina.pascher@gmail.com

Stephen F. Pekar
Sedimentologist
School of Earth and Environmental Sciences
Queens College (CUNY)
USA
stephen.pekar@qc.cuny.edu

Donald E. Penman
Sedimentologist
Department of Geology and Geophysics
Yale University
USA
donald.penman@yale.edu

Saneatsu Saito
Physical Properties Specialist
Research and Development Center for Ocean Drilling Science
Japan Agency for Marine-Earth Science and Technology
Japan
saito@jamstec.go.jp

Wanda R. Stratford
Physical Properties Specialist
Marine Geosciences
GNS Science
New Zealand
w.stratford@gns.cri.nz

Thomas Westerhold
Stratigraphic Correlator
Center for Marine Environmental Sciences (MARUM)
University of Bremen
Germany
twesterhold@marum.de

Xiaoli Zhou
Inorganic Geochemist
Institute of Marine and Coastal Sciences
Rutgers, The State University of New Jersey
USA
xiaoli.zhou@rutgers.edu

Observers

Gayane Asatryan
Observer/Paleontologist (radiolarians)
School of Earth and Environmental Sciences
University of Queensland
Australia
g.asatryan@uq.edu.au

Hugh E.G. Morgans
Observer/Paleontologist (foraminifers)
Paleontology and Environmental Change Section
GNS Science
New Zealand
h.morgans@gns.cri.nz

Education and outreach

Debra E. Beamish
Education/Outreach Officer
Australia
beamish5@tpg.com.au

Adam J. Kurtz
Education/Outreach Officer
USA
adamkurtz47@gmail.com

Operational and technical staff

Siem Offshore AS officials

Steve Bradley
Master of the Drilling Vessel

Jake Robinson
Master of the Drilling Vessel

Mark Robinson
Offshore Installation Manager

JRSO shipboard personnel and technical representatives

Timothy Blaisdell
Applications Developer

Susan Boehm
Thin Section Laboratory

Inva Braha
Marine Laboratory Specialist (temporary)

Lisa Brandt
Chemistry Laboratory

Chad Broyles
Curatorial Specialist

Lisa Crowder
Assistant Laboratory Officer

Douglas Cummings
Publications Specialist

Aaron de Loach
Core Laboratory

Keith Dupuis
Underway Geophysics Laboratory

Sheryl Frazier
Physical Properties Laboratory

Timothy Fulton
Imaging Specialist

Luke Furfey
Marine Laboratory Specialist (temporary)

Clayton Furman
Logging Engineer (Schlumberger)

Randy Gjesvold
Marine Instrumentation Specialist

Michael Hodge
Marine Computer Specialist

Minh Huynh
Marine Computer Specialist

Nicolette Lawler
X-Ray Laboratory

Daniel Marone
Marine Laboratory Specialist (temporary)

Aaron Mechler
Chemistry Laboratory

Mike Meiring
Electronics Specialist

Stephen Midgley
Operations Superintendent

William Mills
Laboratory Officer

Beth Novak
Paleomagnetism Laboratory

Garrick Van Rensburg
Marine Instrumentation Specialist

Rui Wang
Applications Developer

Abstract

International Ocean Discovery Program (IODP) Expedition 371 drilled six sites in the Tasman Sea of the southwest Pacific between 27 July and 26 September 2017. The primary goal was to understand Tonga-Kermadec subduction initiation through recovery of Paleogene sediment records. Secondary goals involved understanding regional oceanography and climate since the Paleogene. Six sites were drilled, recovering 2506 m of cored sediment and volcanic rock in 36.4 days of on-site drilling during a total expedition length of 58 days. Wireline logs were collected at two sites. Shipboard observations made using cores and logs represent a substantial gain in fundamental knowledge about northern Zealandia, because only Deep Sea Drilling Project Sites 206, 207, and 208 had penetrated beneath upper Eocene strata within the region.

The cored intervals at five sites (U1506–U1510) sampled nannofossil and foraminiferal ooze or chalk that contained volcanic or volcaniclastic intervals with variable clay content. Paleocene and Cretaceous sections range from more clay rich to predominantly claystone. At the final site (U1511), a sequence of abyssal clay and diatomite was recovered with only minor amounts of carbonate. The ages of strata at the base of each site were middle Eocene to Late Cretaceous, and our new results provide the first firm basis for defining formal lithostratigraphic units that can be mapped across a substantial part of northern Zealandia and related to onshore regions of New Caledonia and New Zealand.

The material and data recovered during Expedition 371 enable primary scientific goals to be accomplished. All six sites provided new stratigraphic and paleogeographic information that can be put into context through regional seismic-stratigraphic interpretation and hence provide strong constraints on geodynamic models of subduction zone initiation. Our new observations can be directly related to the timing of plate deformation, the magnitude and timing of vertical motions, and the timing and type of volcanism. Secondary paleoclimate objectives were not all completed as planned, but significant new records of southwest Pacific climate were obtained.

Introduction

The Tasman Frontier represents an extensive and under-explored area of the ocean between Australia, New Zealand, and New Caledonia (Figure **F1**). The primary goal of Integrated Ocean Drilling Program (IODP) Expedition 371 was to understand Tonga-Kermadec subduction initiation through recovery of Paleogene sediment records at six new sites across the Tasman Frontier (Figures **F1**, **F2**, **F3**, **F4**).

Subduction systems are primary drivers of plate motions, mantle dynamics, and global geochemical cycles, but little is known about how subduction starts. What are the initial conditions? How do forces and kinematics evolve? What are the short-term consequences and surface signatures: uplift, subsidence, deepwater sedimentary basins, convergence, extension, and volcanism? The early Eocene onset of subduction in the western Pacific was accompanied by a profound global reorganization of tectonic plates, with known plate motions before and after the change (Billen and Gurnis, 2005; Sharp and Clague, 2006; Steinberger et al., 2004; Whittaker et al., 2007). The Izu-Bonin-Mariana (e.g., IODP Expeditions 350, 351, and 352) and Tonga-Kermadec systems contain complementary information about subduction initiation (Figure **F1**), but the southwest Pacific has had little relevant drilling.

Eocene tectonic change occurred at a turning point in Cenozoic climate. Long-term global warming through the Paleocene–Eocene transition culminated in the Early Eocene Climate Optimum (EECO; ~53–49 Ma), which was followed by overall cooling through the remainder of the Cenozoic (Figure **F5**) (Zachos et al., 2008). A secondary scientific goal of Expedition 371 was to address the question of why Earth's climate might move between multimillion-year greenhouse and icehouse climate states. Under very high pCO_2 conditions or high climate sensitivity, global climate models (Huber and Caballero, 2011; Lunt et al., 2012) can reasonably simulate early Eocene warming in many regions (Douglas et al., 2014; Tripati et al., 2003) but not the extreme warmth previously reported in the southwest Pacific and Southern Ocean (Bijl et al., 2009; Hollis et al., 2009, 2012; Pross et al., 2012).

The Eocene–Oligocene transition and Neogene paleoceanography have been subjects of numerous scientific drilling expeditions, including Deep Sea Drilling Project (DSDP) Legs 21, 29, and 90 in the Tasman Sea (Figure **F2**), which were highly influential in the development of ideas that connected regional oceanography with thermal isolation and glaciation of Antarctica and hence global climate change (Burns and Andrews, 1973; Kennett, 1977; Kennett et al., 1975; Kennett and von der Borch, 1986). Ocean Drilling Program (ODP) Legs 181 and 189 further investigated the Eocene–Oligocene opening of the southern Tasman Sea gateway (Carter et al., 2004; Exon et al., 2004b). However, the significance of unconformities in the Tasman Sea has not, so far, included consideration of regional vertical tectonics or local faulting (Sutherland et al., 2010, 2017). Records from the Tasman Sea may also offer insights into understanding Neogene paleoceanography across the Pacific and phenomena such as the late Miocene–early Pliocene biogenic bloom (Farrell et al., 1995; Grant and Dickens, 2002).

Scientific background

Subduction initiation and global plate tectonics

Subduction initiation and changes in plate motion are linked because the largest driving and resisting tectonic forces occur within subduction zones (Becker and O'Connell, 2001; Buffett, 2006; Lithgow-Bertelloni and Richards, 1998; Stadler et al., 2010). There are two end-member classes of subduction initiation models: induced or spontaneous (Stern, 2004) (Figure **F6**). In the spontaneous model, oceanic lithosphere ages, cools, increases in density and gravitational instability, and sinks into the mantle under its own weight (Stern and Bloomer, 1992; Turcotte et al., 1977). In the induced model, externally applied compressive stress and convergence is necessary to overcome lithospheric strength before convective instability can grow and subduction initiation occurs (McKenzie, 1977; Toth and Gurnis, 1998).

Half of all presently active subduction zones on Earth initiated during the Cenozoic (Gurnis et al., 2004), so it is possible to assemble observations to address the question of how and why these margins evolved into self-sustaining subduction zones. Recent drilling results from Expedition 351 shed new light on this question, and new models suggest juxtaposition of a transcurrent fault and relict arc could have led to Izu-Bonin-Mariana subduction initiation just before 50 Ma (Leng and Gurnis, 2015). Subduction initiation at a passive continental margin has received considerable attention through the concept of a Wilson cycle (a class of the spontaneous model), but there are no known Cenozoic examples of passive margins evolving into subduction zones (Stern, 2004). Spontaneous and induced models predict different states of stress and vertical mo-

tions during their early stages, and the aim to distinguish these underpinned our drilling strategy.

The largest change in global plate motions since 83 Ma (the only period with precisely known plate kinematics) is manifest as the Emperor-Hawaii seamount chain bend (Figure **F1**). Geochronology shows that the Emperor-Hawaii bend started at ~50 Ma and may have occurred over ~8 My (Sharp and Clague, 2006). The onset of Pacific plate motion change corresponds to the timing of Pacific/Farallon plate boundary rearrangement (Caress et al., 1988) and termination of spreading in the Tasman Sea (Gaina et al., 1998), followed by a change in direction and rapid increase in rate of Australia-Antarctic spreading with consequent northward acceleration of Australia (Müller et al., 2000; Seton et al., 2012; Whittaker et al., 2007) and initiation of Australia-Pacific spreading south of New Zealand (Keller, 2003; Sutherland, 1995; Wood et al., 1996). Eocene emplacement of ophiolites and deformed flysch may record the onset of convergence in New Caledonia (Aitchison et al., 1995). Reconfiguration of plate boundaries in Antarctica (Cande et al., 2000), the Indian Ocean (Cande et al., 2010), and Asia (Aitchison et al., 2007) confirms the global extent of tectonic change.

The westward swerve in Pacific plate motion occurred at about the same time as subduction zones initiated throughout the western Pacific (Gurnis et al., 2004; Hall et al., 2003; Steinberger et al., 2004). It is the only global-scale subduction initiation event for which plate motions are known before and after, and there is a clear linkage between subduction initiation and plate motion change. Reconstructing what happened in the western Pacific is of fundamental significance for understanding subduction initiation and hence the physics of plate tectonics and mantle flow.

Eocene greenhouse climate

Paleogene sediment records have provided new insights into Earth's climate history and underpin predictions of future greenhouse climate (Lunt et al., 2014). Available data indicate that pCO_2 exceeded 1000 parts per million by volume (ppmv) in the early Eocene (Beerling and Royer, 2011), when global temperatures were ~10°C warmer than present day and the poles were largely free of ice (Zachos et al., 2008; Pagani et al., 2011; Pearson et al., 2009). Climate model simulations, using either very high greenhouse gas radiative forcing or very high climate sensitivity, yield mean annual temperatures consistent with most data for the early Eocene (Huber and Caballero, 2011; Lunt et al., 2012). However, at several sites in the southwest Pacific, both on and off shore (e.g., from Leg 189), multiple proxies yield sea-surface temperatures (SSTs) 5° to 10°C warmer than predicted by model simulations (Hollis et al., 2012; Pross et al., 2012). Such SST estimates imply very low meridional temperature gradients in the early Eocene, which has long posed a climate puzzle (Barron, 1987).

Ocean circulation might account for low SST gradients in the southwest Pacific during the early Eocene. One possibility is that modeled SST predictions are too low because the region was influenced by a warm southward-flowing current system (Hollis et al., 2012) unaccounted for in climate models. Ocean currents predicted by model simulations also could be substantially wrong if paleobathymetry is not depicted accurately (e.g., if parts of the Tasman Frontier were much shallower than today during the early Eocene). There are indications that large vertical movements in the Tasman Frontier occurred during the early Eocene (Baur et al., 2014; Sutherland et al., 2010).

The early Paleogene stratigraphic record of New Zealand has been examined in detail. The warming trend of the late Paleocene through early Eocene, the hyperthermal events of the early Eocene, the EECO, and subsequent cooling can be found in sedimentary successions of eastern New Zealand (Dallanave et al., 2015; Hancock et al., 2003; Hollis, 2006; Hollis et al., 2005; Nicolo et al., 2010, 2007; Slotnick et al., 2012).

Why did Earth's climate generally cool since about 49 Ma? Most hypotheses have invoked changes in the amount of volcanism or weathering, which would affect carbon addition to or carbon removal from the ocean and atmosphere (Brinkhuis et al., 2006; Kent and Muttoni, 2008). It has been suggested that Eocene tectonic change drove long-term Cenozoic climate change (Lee et al., 2013; Reagan et al., 2013). Prior to the early Eocene, most volcanic arcs were continental, where rising magma can react with carbonate-rich crust and generate voluminous CO_2. Initiation of widespread island-arc subduction systems around the Pacific during the early Eocene created a network of submarine plate boundaries that may have first increased and later decreased CO_2 fluxes to the atmosphere.

Post-Eocene climate evolution

Initial reports for Legs 21 and 29 (Burns and Andrews, 1973; Kennett et al., 1975) laid foundations for understanding the interplay between tectonic and oceanographic events in the region, including opening of the Tasman Sea and separation of Australia and New Zealand from Antarctica (Andrews et al., 1975; Andrews and Ovenshine, 1975; Edwards, 1973, 1975; Kennett et al., 1975; Kennett and Shackleton, 1976). Stable isotope records from Leg 29 (DSDP Sites 277 and 279) reveal a general cooling trend over the Cenozoic, with evidence for a pronounced cooling step across the Eocene–Oligocene transition. A series of landmark publications from these legs proposed that ocean circulation was a primary driver of regional and global climate through the early Cenozoic, and the role of circumpolar gateways in the evolution of Antarctic ice sheets and global climate was first hypothesized (Kennett, 1977; Kennett and Shackleton, 1976; Nelson and Cooke, 2001).

Leg 189 focused on the ocean gateway hypothesis and generated a wealth of data and debate (Exon et al., 2004a; Kennett and Exon, 2004). Some continue to argue that opening of the Tasmanian gateway and subsequent development of the Antarctic Circumpolar Current (ACC) played a crucial role in southwest Pacific oceanography and climate (Kennett and Exon, 2004), whereas others link late Paleogene cooling and ice sheet growth to a tectonically driven decline in atmospheric CO_2 (DeConto and Pollard, 2003; Huber et al., 2004).

Expedition 371 collected high-quality cores and data from the key Tasman Frontier region, where ACC-driven abyssal bottom currents and the shallow wind-driven East Australian Current (EAC) operate (Figure **F7**). Eastern flow of the EAC from Australia toward New Zealand leads to an east–west zone of surface water divergence. Drilling within the broader Indo-Pacific area has documented a phenomenon coined the late Miocene–early Pliocene "biogenic bloom" (Farrell et al., 1995; Dickens and Owen, 1999). Between about 9 and 4 Ma, the accumulation of biogenic components (e.g., carbonate, biosilica, and barite) increases significantly at many sites beneath regions of modern surface water divergence (e.g., along the Equator of the eastern Pacific [van Andel et al., 1975; Farrell et al., 1995], the far North Pacific [Rea et al., 1995], and the Oman margin [Brummer and Van Eijden, 1992]). At DSDP Site 590, which lies beneath the Tasman Front (southern boundary of the easterly flowing EAC), carbonate accumulation rates doubled between the late Miocene and early Pliocene, consistent with the bio-

genic bloom phenomenon (Grant and Dickens, 2002). The coincidence of elevated export production at numerous locations suggests far-field oceanographic teleconnections during the Neogene, such as via an acceleration of Indo-Pacific upwelling and nutrient delivery to the photic zone.

Geological setting

The seafloor beneath the Tasman Frontier in the southwest Pacific is complex with a series of bathymetric highs and lows (Figures **F1**, **F2**). The bathymetric highs, and the islands of New Zealand and New Caledonia, and perhaps the New Caledonia Trough, represent the northern part of a continent referred to as Zealandia (Mortimer et al., 2017). Unlike other continents, most of Zealandia lies underwater because the continental crust is relatively thin. East of northern Zealandia lies a lengthy subduction system, the Kermadec and Tonga Trenches.

The Tonga-Kermadec system has been studied much less than the Izu-Bonin-Mariana system but is complementary and has the following advantages for investigation by drilling: (1) the Tonga-Kermadec system formed adjacent to thin continental crust that early back-arc spreading isolated from later complication by faulting or volcanism; (2) persistent submarine conditions and moderate water depths led to preservation of fossil-rich bathyal sediment records in many places; (3) seismic reflection data demonstrate the existence of Eocene tectonic signals of change, including compression, uplift-subsidence, and volcanism; and (4) Australia-Pacific plate-motion boundary conditions are precisely known (Cande and Stock, 2004; Sutherland, 1995).

The tectonic history of the Tasman Frontier can be simplified into 4 phases with approximate ages:

- >350–100 Ma: subduction along the eastern Gondwana margin.
- 100–80 Ma: continental rifting in the Tasman Sea region.
- 80–50 Ma: oceanic rifting, passive margins, and opening of the Tasman Sea.
- 50–0 Ma: Tonga-Kermadec subduction.

Continental "basement" beneath bathymetric rises in the region is inferred to be similar to rocks found in New Zealand, New Caledonia, and eastern Australia; this inference is supported by limited dredge samples and drilling (DSDP Site 207), seismic velocities, and gravity and magnetic anomalies (Collot et al., 2012; Klingelhoefer et al., 2007; Mortimer, 2004a, 2004b; Mortimer et al., 2008; Sutherland, 1999; Tulloch et al., 1991; Wood and Woodward, 2002). The Lord Howe Rise and Challenger Plateau (Figure **F3**, **F4**) are probably composed of quartzose metasedimentary rocks and granitoids of Paleozoic age that represent the eastern edge of Gondwana (Mortimer et al., 2017). High-amplitude magnetic anomalies and a single dredge sample from the West Norfolk Ridge suggest that the southern New Caledonia Trough is underlain by a fossil arc of late Paleozoic and Mesozoic age that formed along the active margin of Gondwana (Mortimer et al., 1998; Sutherland, 1999). The geology of New Caledonia and northern New Zealand suggests that the Norfolk Ridge system is underlain by Mesozoic fore-arc accretionary rocks that formed at the convergent margin of Gondwana (Adams et al., 2009; Aitchison et al., 1998; Cluzel et al., 2010; Cluzel and Meffre, 2002; Mortimer, 2004b). Based on comparison with eastern New Zealand (Davy et al., 2008), a "fossil" Gondwana trench lay along the northeast side of the Norfolk Ridge system and the slab dipped southwest beneath the Lord Howe Rise.

The tectonic regime along the Tasman sector of the Gondwana margin changed during the Cretaceous from subduction and convergence to widespread rifting and extension. Igneous activity was widespread and of variable type and chemistry during the Cretaceous. Calc-alkaline and adakitic (high Sr/Y) activity with a subduction-related signature is characteristic of the early phase (130–110 Ma) in New Zealand and New Caledonia, whereas an intraplate rift setting characterizes later activity after ~105–100 Ma and is also recorded on the Lord Howe Rise (Bryan et al., 1997; Cluzel et al., 2010; Higgins et al., 2011; Mortimer et al., 1999; Tulloch et al., 2009). Late Cretaceous rift basins contain coastal sandstone facies overlain by transgressive marine sandstones and mudstones in New Zealand, eastern Australia, and New Caledonia and are likely present in the Tasman Frontier region (Collot et al., 2009; Herzer et al., 1999; King and Thrasher, 1996; Uruski and Wood, 1991; Uruski, 2008). The end of widespread rifting in New Zealand, New Caledonia, and Australia and the subsequent transition to passive margin conditions were contemporaneous with the onset of seafloor spreading in the Tasman Sea at ~80 Ma, but local fault activity is known to have continued to ~60 Ma in Taranaki and northern South Island, New Zealand (King and Thrasher, 1996; Laird, 1993).

Late Cretaceous to early Cenozoic seafloor spreading in the Tasman Basin is inferred from magnetic anomalies (Hayes and Ringis, 1973; Weissel and Hayes, 1977). The earliest seafloor spreading may predate Chron C33r (84–80 Ma) east of Tasmania (Royer and Rollet, 1997), but marginal seafloor along much of the western edge of the Lord Howe Rise probably formed during Chron C33r (Gaina et al., 1998; Sutherland, 1999). Seafloor spreading ceased in the central Tasman Sea during Chron C24 (53–52 Ma) or very shortly afterward (Gaina et al., 1998).

Deformation, exhumation, and emplacement of ultramafic, mafic, and sedimentary allochthons occurred in New Caledonia during the middle and late Eocene (Aitchison et al., 1995; Cluzel et al., 2001). The peak of high-pressure metamorphism in northern New Caledonia was at 44 Ma, and exhumation was largely complete by 34 Ma (Baldwin et al., 2007). Seismic-stratigraphic evidence shows that the New Caledonia Trough either formed or was substantially modified during this event, though Cretaceous sedimentary basins beneath the trough escaped Cenozoic convergent deformation in most places (Collot et al., 2008; Sutherland et al., 2010). Regional deformation and emplacement of allochthons in northern New Zealand occurred later than in New Caledonia or the Norfolk Ridge system, with the onset of tectonic activity during the late Oligocene and early Miocene (~30–20 Ma) (Bache et al., 2012; Herzer, 1995; Herzer et al., 1997; Rait et al., 1991; Stagpoole and Nicol, 2008).

Australia-Pacific plate motion is precisely known for the period since Chron C20 (43 Ma) because the plate boundary south of New Zealand was extensional and a plate circuit through Antarctica can be followed to provide additional constraints (Cande and Stock, 2004; Keller, 2003; Sutherland, 1995). Eocene convergence rates varied from <1 cm/y in New Zealand to 10 cm/y near New Caledonia (Figure **F8**). Late Eocene to Holocene subduction zone roll-back has produced back-arc basins (Loyalty, Norfolk, South Fiji, North Fiji, Havre, and Lau) and ridges interpreted as fossil and active arcs east of the Norfolk Ridge system (Loyalty, Three Kings, Lau-Colville, Tonga-Kermadec, and Vanuatu) (Crawford et al., 2003; Herzer et al., 2009; Herzer and Mascle, 1996; Mortimer et al., 2007; Schellart et al., 2006). The complexity of basin opening makes local determination of past plate boundary configurations and rates difficult. This back-arc region has mostly isolated the submerged continental part of the Tasman Frontier region from Cenozoic subduction-related deformation and volcanism.

A variety of tectonic models have been proposed to explain how various Eocene–Miocene arcs and back arcs subsequently formed between the Tonga-Kermadec Trench and Norfolk Ridge (Cluzel et al., 2006; Crawford et al., 2003; Herzer et al., 2009; Mortimer et al., 2007; Schellart et al., 2006). General agreement exists that the modern Tonga-Kermadec system evolved from a boundary lying near the Norfolk Ridge and New Caledonia in the middle Eocene. However, ideas about the exact geometry of that boundary or the nature of Cretaceous to middle Eocene plate boundaries northeast of Norfolk Ridge (Whattam et al., 2008) vary because the region has either been subducted or deformed and intruded and it is sparsely sampled.

The oldest Cenozoic volcanic rocks from the southwest Pacific with clear subduction affinities were dredged from the Tonga-Kermadec fore arc and have ages in the range of 52–48 Ma (Meffre et al., 2012). In New Caledonia, dikes with subduction affinities cut ophiolitic rocks and are interpreted to be approximately synchronous with felsic dikes that are dated at ~53 Ma (Cluzel et al., 2006). This represents the earliest evidence for subduction and predates the peak of high-pressure metamorphism at 44 Ma (Baldwin et al., 2007) and nappe emplacement in New Caledonia (Aitchison et al., 1995; Maurizot, 2012). Magnetic anomaly interpretation shows that the Tasman Basin ceased spreading at ~52–50 Ma (Gaina et al., 1998). Therefore, there is strong evidence for Pacific-wide synchronicity: the age of the Emperor-Hawaii bend, the inception of Izu-Bonin-Mariana subduction, and a change from seafloor spreading to Tonga-Kermadec subduction initiation in the Tasman Frontier.

Scientific objectives

1. *How and why does subduction initiation occur?*
   a. Did plate convergence and a period of high horizontal stress with convergent failure precede and induce subduction initiation, or did subduction initiation happen spontaneously with early extensional stresses?
   b. What vertical stresses occurred during subduction initiation, and when and where was this manifest as uplift or subsidence?
2. *Was the Eocene southwest Pacific anomalously warm, and why?*
   a. What were surface water temperatures during the early Cenozoic across the region?
   b. Were unusually high temperatures linked to regional physiographic changes and hence climate change or/and global changes in carbon cycling and hence the long-term cooling trend that begins at ~50 Ma?
3. *How does post-Eocene oceanography and climate compare to elsewhere in the Pacific?*
   a. When did the modern ocean circulation system develop as evidenced in the Tasman Frontier?
   b. Are pole-Equator climate teleconnections manifested in the Tasman Sea during the late Cenozoic?

Drilling strategy

Our drill sites were chosen foremost to test geodynamic model predictions. Periods of time in the past that had high horizontal stress may be recorded as faulted or folded strata. Anomalous vertical stress in the past caused by traction or buoyancy would have been balanced by surface uplift or subsidence and might be recorded as changes in paleodepths. Thermal or chemical anomalies in the crust or mantle in the past may be recorded by characteristic volcanic products. We aimed to sample records with these signals.

The timing and style of faulting and folding can be determined from stratigraphic relationships tied to seismic reflection data. In general, three units constrain the timing of a tectonic event: faulted strata are older than the event, unfaulted strata are younger than the event, and syntectonic growth strata record progressive faulting during the event. Growth strata are typically identified from thickness changes within a sedimentary unit that drapes faulted units, and seismic reflectors within the syntectonic unit may exhibit fanning geometries close to faults.

The only practical way of measuring elevation of the crust through time is against a sea level reference frame. Flat unconformities with regional consistency on seismic reflection (and in some cases bathymetric) data are interpreted as surfaces produced by sea level–modulated erosional processes. Samples dredged from >1500 m water depth from the Reinga Basin during the TAN1312 expedition confirm the occurrence of Paleogene bioclastic limestone with shallow-marine fossils and hence affirm the hypothesis that large (>1 km) vertical motions were associated with subduction initiation (Browne et al., 2016). We aimed to recover shallow-water (<400 m) fossils, either in place or reworked by sediment gravity flows, at our target locations to provide direct evidence of past vertical positions at precisely dated times. Tectonic and oceanographic research objectives are aligned. Fossils and geochemistry (e.g., proxy records for water temperature or chemistry) can provide independent evidence for vertical positions. Beyond direct and local constraints, models that include ocean circulation are sensitive to paleobathymetry.

Our strategy was to obtain information on transects parallel and perpendicular to where subduction initiated to constrain the different physical processes involved in subduction zone initiation (Figure **F9**). The proximal ridge includes New Caledonia, Norfolk Ridge, Reinga Basin, and northwest New Zealand (Figures **F2**, **F3**, **F4**). The proximal region is deformed and presumably was involved in the initial phase of surface convergence (Sutherland et al., 2017). Knowledge from New Caledonia, IODP Sites U1507 and U1508, and New Zealand produce a proximal boundary–parallel transect that progressively samples initial rates of predicted convergence (Bache et al., 2012).

IODP Sites U1506 and U1507 (proposed Sites LHRN-3A and NCTN-8A, respectively), combined with knowledge from New Caledonia and regional seismic reflection interpretation, should provide a boundary-perpendicular transect in the northern region (Figure **F3**), where Eocene convergence rates are thought to have been highest (Figure **F8**). IODP Sites U1508, U1509, U1510, and U1511 (proposed Sites REIS-2A, NCTS-2A, LHRS-3A, and TASS-2A, respectively), combined with knowledge from New Zealand and Australia, provide a southern transect (Figure **F4**) that has clear signs of an extended period of plate failure (Sutherland et al., 2017).

We aimed to test the hypothesis that the proximal basin, the New Caledonia Trough, subsided >2 km during the Paleogene, even though it was only subjected to minor convergent deformation (Sutherland et al., 2010). Sites U1507 and U1509 were chosen to constrain the magnitude and timing of subsidence in relation to other events. In addition, the New Caledonia Trough contains a record of detrital products derived from ridges on either side and so records the timing of deformation and emergence of those ridges (Etienne et al., in press; Bache et al., 2014).

The distal ridge, Lord Howe Rise, shows signs of minor Eocene convergent deformation, volcanism, and significant erosion surfaces (Sutherland et al., 2010). Sites U1506 and U1510 were chosen

to determine the timing and magnitude of vertical motions and hence constrain the history of dynamic topography (upper mantle flow), lithospheric buoyancy, and/or tractions related to shear zones. Different geodynamic model classes make very different predictions of vertical motion.

The distal basin, the Tasman Abyssal Plain, shows signs of local convergent deformation (Sutherland et al., 2017). The force transmitted through the tectonic plate must have been large enough to stop seafloor spreading and cause failure of the lithosphere. Site U1511 was chosen to determine the timing of this change in stress state and how it relates to other tectonic events. The timing and magnitude of force transmitted through a plate is a powerful discriminator: an induced subduction model predicts a larger and earlier compressive force than a spontaneous subduction model (Gurnis et al., 2004).

The Australia-Pacific convergence rate during the time of interest was much faster near New Caledonia than near New Zealand (Figure **F8**). Geodynamic models predict that stresses within an initiating subduction system evolve in response to the total convergence experienced (Gurnis et al., 2004), so models predict alongstrike changes in timing that can be tested using biostratigraphy. The absolute timing of observables can also be compared to known plate motions. This ability to track total convergence precisely through space and time is unique to the Tonga-Kermadec system because most subduction systems have imprecisely known kinematic histories, as the rock record has been subducted.

Site summaries

Site U1506 (northern Lord Howe Rise)

Background and objectives

Site U1506 (proposed Site LHRN-3A) is located on the northern Lord Howe Rise, ~290 km south of DSDP Sites 208 and 588 and where geophysical surveys image a regional unconformity (Sutherland et al., 2016). At Sites 208 and 588, the unconformity corresponds to a break between foraminiferal and nannofossil chalk of early Oligocene age and siliceous microfossil–bearing chalk, radiolarite, and diatomite of middle Eocene age. The primary scientific objective at Site U1506 was to test the hypothesis that the northern Lord Howe Rise transiently uplifted to near sea level during the Paleogene and has since subsided by ~1500 m. The drilling target, identified from seismic reflection data, is a buried flat-topped feature with ~100 m of relief above the regional unconformity surface. The feature has a positive polarity seismic reflection at its top but also internal reflections. We hypothesized that it could be a coral reef or wave-cut surface formed during the Eocene. Rotary drilling was chosen because consideration of the seismic reflection amplitude and seismic refraction velocity (3.2–3.8 km/s) suggested the material might be too hard for advanced piston corer (APC) or extended core barrel (XCB) coring.

Operations

Hole U1506A: 28°39.7180′S, 161°44.4240′E; water depth = 1495 m

All depth references in meters in this section refer to the drilling depth below seafloor (DSF) depth scale.

Site U1506 was the first site occupied during Expedition 371. After an 1167 nmi transit from Townsville, Australia, the ship arrived at Site U1506 at 1912 h on 3 August 2017 (UTC + 10 h). At 1948 h, the drill floor was cleared for operations, beginning Hole U1506A.

The rotary core barrel (RCB) bottom-hole assembly (BHA) was assembled and deployed, and Hole U1506A was spudded at 0600 h on 4 August. Coring proceeded to Core 29R where the expected hard formation was encountered at ~265 m. We recovered cores in half intervals (4.5–5.0 m length) below this depth to minimize risk of core loss due to jams in the bit or inner barrel.

Coring stopped after Core 36R, which arrived on the rig floor at 1345 h on 5 August. Total recovery for the 306.1 m cored in Hole U1506A was 192.38 m (63%). This included an average core recovery of 61% from Cores 1R through 28R and 79% from Cores 29R through 36R, which were recovered in half intervals (4.5–5.0 m). Hole U1506A operations ended at 1935 h and the total time spent on Hole U1506A (and Site U1506) was 47.75 h or 2.0 days. At 2000 h we departed for Site U1507.

Principal results

All depth references in meters in this section refer to the core depth below seafloor, method A (CSF-A) depth scale.

Site U1506 consists of ~265 m of Pleistocene–middle Eocene nannofossil ooze and chalk (lithostratigraphic Unit I) overlying ~40 m of volcanic rocks (lithostratigraphic Unit II; Figures **F10**, **F11**). Sediments of Unit I are further divided into three subunits.

Subunit Ia (0–258.2 m) consists of relatively homogeneous Pleistocene to upper Miocene white nannofossil ooze and chalk with foraminifers, with carbonate content ranging from 88% to 95%. Faint decimeter-scale white and grayish white color banding and rare blebs of pyrite (generally framboidal under the scanning electron microscope [SEM]) occur in this subunit. The ooze–chalk transition occurs across an interval including Cores 371-U1506A-24R through 26R (~260 m). Fine structures and texture, including bioturbation with slightly darker *Zoophycos, Planolites, Skolithos*, and *Chondrites* burrows, are better preserved and visible in the chalk than in the ooze.

Subunit Ib (258.2–264.3 m) is a ~6 m thick interval of pale yellow to white upper Oligocene nannofossil chalk with foraminifers. The Subunit Ia/Ib boundary is marked by a color change from white gray to pale yellow and a slight increase in magnetic susceptibility (MS). It also represents a ~10 My hiatus separating the late Oligocene from the late Miocene. Additionally, Subunit Ib is moderately bioturbated with common *Zoophycos* and *Planolites* trace fossils.

Subunit Ic (264.3–264.6 m) is a 34 cm thick interval of middle Eocene glauconitic nannofossil chalk with foraminifers. The Subunit Ib/Ic boundary, defined by the appearance of glauconite and a coincident color change to light greenish gray, represents a ~20 My hiatus between the middle Eocene and late Oligocene. Subunit Ic is intensely bioturbated, with burrows filled with pale yellow Oligocene nannofossil chalk from the overlying Subunit Ib.

Lithostratigraphic Unit II (264.6–305.3 m) represents the uppermost ~41 m of a volcanic rock sequence. It consists of microcrystalline to fine-grained basalt with facies alternating in ~10 m couplets of (1) dark reddish brown microcrystalline, highly vesicular, and amygdaloidal basalt with common veins and (2) dark gray fine-grained massive aphyric basalt with rare carbonate veins. Thin sections and X-ray diffraction (XRD) measurements show the basalt is dominated by Ca-plagioclase and clinopyroxene alongside various alteration minerals such as Fe-Ti oxides and chlorite. The carbonate veins and vesicle fills display a variety of composition and texture, including large (>1 cm grain size) fibrous calcite crystals and fine-grained bioclastic packstone.

Nannofossil and planktonic foraminifer biostratigraphy assign a Pleistocene to late Oligocene age to lithostratigraphic Subunits Ia and Ib. Higher resolution sampling allowed identification of a condensed interval between Samples 371-U1506A-28R-3, 75 cm, and 28R-4, 75 cm (257.25–258.75 m), that represents ~10 My. Subunit Ic is of middle Eocene age. A sample of a burrow fill within Subunit Ic (29R-2, 70 cm; 264.36 m) is late Oligocene in age, indicating erosion or nondeposition of middle Eocene to upper Oligocene sediment.

Microfossil assemblages consist of well-preserved calcareous nannofossils, planktonic and benthic foraminifers, and ostracods, indicating a depositional depth well above the lysocline. The middle Eocene benthic foraminifers are characteristic of an upper bathyal environment, about 500–1000 m shallower than the late Oligocene and younger intervals. The ostracod assemblages indicate a deep-water setting throughout Subunits Ia and Ib (representing late Oligocene and younger age) but an upper bathyal setting for Subunit Ic (middle Eocene).

Rare, heavily recrystallized reworked radiolarians were found in some core catcher samples from this site. No other siliceous microfossils were found in samples examined from this site.

A palynological reconnaissance study carried out on five samples from Hole U1506A, including one sample from the middle Eocene glauconite-rich layer in Section 371-U1506A-29R-2, yielded no palynomorphs.

Paleomagnetic measurements from ooze samples, representing most of lithostratigraphic Subunit Ia, yielded unstable paleomagnetic directions, largely due to reworking of sediments (bioturbation) and drilling disturbance associated with the RCB coring system. Integration with discrete sample-derived directions does not allow reliable correlation with the geomagnetic polarity timescale (GPTS). However, stable paleomagnetic directions with several polarity reversals were obtained in the chalk interval (below ~245 m), and clarity was improved by alternating field (AF) demagnetization at 20 mT. Principal component analysis of paleomagnetic directions after stepwise AF demagnetization of discrete samples reveals a stable remanent magnetization component above 10–20 mT, confirming observations from superconducting rock magnetometer measurements.

Lithostratigraphic Unit II yields a stable paleomagnetic signal after removing the overprint with AF demagnetization at 20 mT. A normal polarity was obtained from most volcanic rock samples. Some intervals not affected by AF demagnetization showed a reversed polarity after 20 mT demagnetization. Further analyses (e.g., thermal demagnetization) are required to investigate the paleomagnetic signal of the volcanic materials.

Gamma ray attenuation (GRA) bulk density, MS, color, and natural gamma radiation (NGR) exhibit small amplitude variations in lithostratigraphic Unit I and significantly greater amplitude variations in Unit II.

In Unit I, GRA varies between 1.6 and 1.8 g/cm^3, and porosity decreases from ~63% to 52% from the seafloor to the base of Unit I, typical of calcareous ooze and chalk. *P*-wave velocity increases gradually with depth from ~1600 to ~2000 m/s. Intermittently higher *P*-wave velocity values of ~2200 m/s occur in Cores 371-U1506A-26R and 27R, reflecting the diagenetic transition of ooze to chalk. MS is low throughout the sedimentary section, with a few local MS spikes up to 100 instrument units (IU). NGR is also generally low (1–4 counts/s) but increases to ~25 counts/s in glauconitic Subunit Ic.

Thermal conductivity shows a gradual and increasing trend with depth from 1.1 to 1.4 W/(m·K) over the uppermost ~250 m, consistent with expected values for calcareous ooze and chalk. Vane shear strength increases from ~18 kPa near the seafloor to ~40 kPa at 190 m. Compressive strength from penetrometer measurements shows very low strength in the top ~72 m of Unit I then increases and becomes variable (~60 to ~100 kPa) to 186 m.

The most significant change in physical properties spans the lithostratigraphic Unit I/II boundary. This sediment/rock contact at 265 m corresponds to major increases in bulk density (up to 2.8 g/cm^3) and *P*-wave velocity (4400–6500 m/s). This impedance contrast can be correlated with the major reflection seen in the multichannel seismic (MCS) profiles used in the site surveys (2.29 s two-way traveltime [TWT]). MS (0–1500 IU), NGR (~3–9 counts/s), bulk density, and color reflectance show much higher amplitude variations in Unit II than in Unit I. Porosity drops to 9%–20% within Unit II.

A total of 15 interstitial water (IW) samples were collected from Cores 371-U1506A-4R through 28R (26–261 m; lithostratigraphic Unit I). Sulfate concentration decreases from ~29 mM at the "mudline" to ~20 mM at depth. The ammonium profile somewhat mirrors that of sulfate, increasing from 0 to 150 µM. This suggests sulfate reduction of particulate organic carbon in the sediments. The product of this reaction, H_2S, once reacting with Fe, also explains the abundant iron sulfide mineral horizons observed in the cores. From the top to the bottom of the sedimentary section, Ca increases from 10.6 to 18.3 mM and Mg decreases from 52.9 to 36.2 mM. This could reflect reactions between pore water and basement rock. Si and Mn increase from 160 to 200 mM and from 0.4 to 3 mM, respectively, at the transition from ooze to chalk.

Headspace gas samples were collected from each core. Hydrocarbon gas concentrations in all samples were below detection limits.

Carbonate ($CaCO_3$) content is high (>88 wt%) throughout Unit I, showing an increasing trend with depth in the uppermost 70 m, with highest values (~95 wt%) between 85 and 143 m and between 200 and 228 m. Total organic carbon (TOC) percentages are low, with values ranging between 0.2 and 0.4 wt% in the top ~210 m and between 0.6 and 1.0 wt% from 219 to 247 m. Trace amounts of nitrogen are present in the uppermost two samples (0.65 and 14.32 m). No samples were taken for bulk sediment geochemistry from Subunit Ic or Unit II.

Site U1507 (northern New Caledonia Trough)

Background and objectives

Site U1507 (proposed Site NCTN-8A) is located in the New Caledonia Trough, ~460 km south of New Caledonia, ~620 km north of DSDP Site 206, and ~530 km east of Sites 208 and 588. Trending northwest–southeast and north–south, the New Caledonia Trough delineates a ~1700 km long bathymetric low on northern Zealandia (Figure **F2**). The northern and central parts of the feature have not been drilled previously. On the basis of evidence from Site 206 and the Taranaki Basin, it has been inferred that the New Caledonia Trough formed during Cretaceous rifting and subsequent subsidence. However, recent analysis of high-quality seismic reflection data has led to an alternate hypothesis: the present physiography was created mainly during Eocene subduction zone initiation. Site U1507 was chosen to determine the timing of deformation and uplift of Norfolk Ridge, to constrain the age of trough formation and sedimentary fill, and to obtain a record of regional volcanism (Sutherland et al., 2016). The intent was to core Site U1507 using the APC/XCB system to sample a downlapping sequence (at ~500–700 meters below seafloor [mbsf]) that was in-

ferred to represent an influx of sediment from the Norfolk Ridge and hence date emergence of the ridge.

Operations

Hole U1507A (26°29.3158′S, 166°31.7039′E; water depth = 3568 m)
Hole U1507B (26°29.3158′S, 166°31.7155′E; water depth = 3568 m)

All depth references in meters in this section refer to the DSF depth scale, unless noted otherwise.

Hole U1507A was cored with the APC and XCB systems. The first was used to retrieve Cores 1H through 26H with an average recovery of 106%. Temperature measurements were taken at the bottom of Cores 4H, 7H, 10H, 13H, 16H, and 19H. Deployment of orientation and temperature tools was discontinued after Core 20H, and APC coring was discontinued after Core 26H. Coring continued with the XCB system, retrieving Cores 27X through 46X with an average recovery of 55%. Total recovery for Hole U1507A was 352.7 m (83%), and the total time spent on Hole U1507A was 3.6 days.

Hole U1507B was first drilled without coring from 0 to 376 m and then cored (Cores 2R through 53R) with a recovery of 371.5 m (76%). The total time spent on Hole U1507B was 8.1 days.

After dropping the coring bit at the bottom of the hole and replacing the hole with heavy mud, three logging passes were made with a modified triple combo tool string between 75.2 and 864 m wireline log depth below seafloor (WSF): a downhole log, a 125 m uplog for calibration, and a main log up the entire hole. The modified triple combo logging tool string included MS, electrical resistivity, sonic, bulk density, and NGR tools.

Principal results

All depth references in meters in this section refer to the CSF-A depth scale.

The sedimentary sequence at Site U1507 consists of ~685 m of biogenic ooze and chalk interbedded with calcareous and volcaniclastic turbidites (lithostratigraphic Unit I), overlying ~170 m of more homogeneous clayey nannofossil chalk (lithostratigraphic Unit II; Figures **F10**, **F11**). Sediments of Unit I are further divided into three subunits, based on changes in lithology and sedimentological features, as identified by macroscopic and microscopic (smear slide, thin section, and SEM) core description.

Subunit Ia (0–401.2 m) mostly consists of white nannofossil ooze and chalk. This dominant lithology is accompanied by light greenish gray nannofossil-rich clay with volcanic ash, white gray normally graded foraminiferal ooze or limestone beds, and a restricted ~2 m thick interval of very dark greenish gray volcanic breccia and tuffaceous sandstone. Soft-sediment deformation is widespread but particularly common in the lowermost part of the subunit.

Subunit Ib (401.2–542.9 m) is primarily composed of greenish gray clayey nannofossil chalk with volcanic ash showing significant soft-sediment deformation, interbedded with dark gray clayey tuffaceous sandstone and greenish gray clayey foraminiferal limestone with volcanic clasts. This subunit differs from Subunit Ia by an overall increase in clay and volcanic content.

Subunit Ic (542.9–685.5 m) consists of dark greenish gray coarse- to fine-grained tuffaceous conglomerate, sandstone, and tuff, alternating with light greenish gray clayey nannofossil chalk with volcanic ash. The boundary with Subunit Ib is defined by the first occurrence of a thick-bedded tuffaceous conglomerate. Volcaniclastic lithologies display a range of sedimentary facies that point to deposition from various gravity flow processes from debris flows to turbidity currents. Thin sections and XRD measurements on the volcaniclastics reveal that clast lithologies consist of variable percentages of basaltic minerals, such as pyroxene, plagioclase, and olivine phenocrysts, as well as volcanic glass shards, vesicular pumice, and large benthic foraminifers.

Lithostratigraphic Unit II (685.5–855.7 m) consists of homogeneous, light greenish gray bioturbated clayey nannofossil chalk with common *Zoophycos, Nereites*, and *Spirophyton* burrows and rare foraminiferal limestone beds. The lithology is consistent with hemipelagic-dominated sedimentation. Very rare foraminiferal limestone beds, with few volcanic grains, are still encountered in this subunit. At 826–836 m, the lithology changes to a greenish gray nannofossil claystone, possibly reflecting increased carbonate dissolution.

Nannofossils and foraminifers are present throughout Holes U1507A and U1507B, providing a robust stratigraphy (Figure **F11**): Pliocene–Pleistocene (6.2–177.8 m), Miocene (187.0–432.6 m), late Oligocene (449.9–520.0 m), early Oligocene (523.1–639.1 m), and late to middle Eocene (642.3–855.7 m). The Oligocene/Miocene boundary can be approximated using the top of *Sphenolithus delphix* (~442.5 m). The Eocene/Oligocene boundary can be approximated using the top of planktonic foraminifer *Globigerina euapertura*, the benthic foraminifer *Nuttallides truempyi*, the base acme of calcareous nannofossil *Clausicoccus subdistichus*, and the top of rosette discoasters.

The occurrence of *Orbulinoides beckmanni* in samples from 835.5 to 836.1 m constrains these depths to planktonic foraminiferal Zone E12 (40.03–40.43 Ma), which effectively marks the Middle Eocene Climatic Optimum (MECO). For calcareous nannofossils, the base of *Dictyococcites bisectus* at ~836.1 m and the top of *Sphenolithus obtusus* at ~825.6 m indicate the post-MECO interval was recovered in this interval. However, Core 371-U1507B-51R (835.7–836.1 m) only recovered 38 cm (4%), so most of the MECO was washed away or lost during coring.

Radiolarians have a patchy record. Well-preserved Neogene radiolarians are found in samples from 6.2 to 54.1 m. The interval from 63.4 to 380.6 m is barren of radiolarians. The interval from 380.6 to 523.2 m contains varying amounts of radiolarians, ranging from trace to common, with some samples barren of radiolarians. Low-latitude index species are absent or rare.

Benthic foraminifers indicate paleodepths that gradually range from abyssal in the most recent part of the sequence to lower bathyal in the Oligocene and Eocene. In some intervals (e.g., ~205.6 m), their assemblages contain a mixture of deepwater and relatively shallow-water taxa with different preservation states. A palynological reconnaissance study, carried out on 10 core catcher samples throughout the sedimentary sequence, showed that deposits at Site U1507 are effectively barren of palynomorphs. Ostracods were rare to common between 6.2 and 279.7 m in Hole U1507A and absent in Hole U1507B, except for one sample.

Paleomagnetic measurements on section halves from Holes U1507A and U1507B show variable quality for different lithostratigraphic units. In Hole U1507A, the natural remanent magnetization (NRM) intensity is in the range of 10^{-2} A/m and increases from 234 m downhole by about one order of magnitude. NRM inclination is mostly positive, likely the effect of a present-day geomagnetic overprint. After AF demagnetization cleaning at 20 mT, the interval from 0 to 54.1 m is characterized by dominantly normal polarity

with some intervals of reversed polarity. Between 53.7 and 215.6 m, some swings between positive and negative inclination are observed, without a clear bimodal clustering, and from 216 m downhole inclinations are less stable. This may reflect some combination of drilling-related deformation, depositional processes, and weak magnetization. The average inclination for Hole U1507A is around −20°, and no reliable shipboard magnetostratigraphy can be obtained for this hole.

High-quality paleomagnetic data were obtained on sediments from Hole U1507B, with a well-defined series of normal and reversed polarity intervals in lithostratigraphic Unit I. Inclination values for Unit I after 20 mT AF demagnetization have two clear peaks clustered around −40° and 45°. The overall high-quality paleomagnetic data from Hole U1507B can be attributed to the high NRM intensity and good recovery of lithified sediment cores. Integration with biostratigraphic results shows that the interval between 433.3 and 682.9 m contains most polarity chrons from Chron C6Br in the early Miocene through Chron C16n in the late Eocene.

Sediments from lithostratigraphic Unit II generally show scattered inclination values without recognizable bimodal distribution. Two inclination changes at 759.3 and 834.0 m are tentatively correlated with the bases of Chrons C17n and C18n, respectively.

Anisotropy of magnetic susceptibility (AMS) was measured on 123 discrete samples from Site U1507, which were collected in the most undisturbed intervals and often on top of turbidite layers. The soft and magnetically weak sediments from Hole U1507A did not yield well-defined orientations of the AMS tensor. Cube samples from lithified sediment, however, show a clear oblate magnetic fabric, where the minimum axis of the AMS ellipsoid is statistically oriented perpendicular to the bedding.

Cores recovered from Holes U1507A and U1507B were analyzed with the full suite of physical property measurements. Downhole temperature measurements were made in Hole U1507A, and wireline logging was completed using a modified triple combo tool string in Hole U1507B.

Bulk density increases with depth from the seafloor (1.5 g/cm^3) to the bottom of the hole (2.4 g/cm^3) with local decreases to ~1.6 g/cm^3 observed between ~420 and ~500 m. Moisture and density–derived porosity values correspondingly decrease from ~70% in nannofossil ooze at the top of Hole U1507A to ~25% at the base of Hole U1507B in nannofossil chalk. Grain density is ~2.71 g/cm^3 to ~300 m and then varies between 2.7 and 2.8 g/cm^3 to ~700 m, except for the interval ~420–500 m, where grain density conspicuously drops to 2.6–2.7 g/cm^3. In lithostratigraphic Unit II, grain density decreases again to ~2.5–2.7 g/cm^3.

P-wave velocity measured on cores gradually increases downhole in Subunit Ia, with a more rapid increase around 290 m corresponding to the diagenesis of ooze to chalk. From ~400 to 520 m, *P*-wave velocities increase from 2000 to 2500 m/s, and stay at similar values to the base of the hole. *P*-wave velocity from wireline logging increases from 2300 to 2700 m/s within Unit II, with a negative excursion to ~2400 m/s associated with the MECO at ~835 m.

Thermal conductivity increases gradually with depth from 1.1 to 1.8 W/(m·K) in Subunit Ia and shows a decreasing trend in Subunits Ib and Ic. In Hole U1507A, six temperature measurements were made with the advanced piston corer temperature tool (APCT-3), yielding a temperature gradient of 46.9°C/km.

MS is low (< 50 IU) in Subunits Ia and Ib and high (up to 1000 IU) within Subunit Ic. Below 680 m, values decrease to ~40 IU and are constant in the lowermost part of the hole. NGR measured on cores and by wireline logging show matching downhole variations. NGR is low, except for positive excursions of ~20–40 counts/s between 400 and 520 m and between 520 and 680 m.

Changes in color reflectance occur at the base of Subunit Ia, where all parameters decrease, reflecting the darker and greener clay-rich sediments. A slight increase in lightness (L*) is observed at the top of Unit II.

Headspace gas samples were routinely collected from each core from Holes U1507A and U1507B. Hydrocarbon gas concentrations in all samples were below detection limits.

A total of 56 IW samples were collected from Cores 371-U1507A-1H through 45X (51 samples) and 371-U1507B-6R through 14R (5 samples). The results show a distinctive difference between above and below 250 m, corresponding to the change from APC to XCB or rotary coring. The IW constituent profiles are smooth in the upper 250 m and become scattered below 250 m. Despite this issue, Mg, K, and SO_4^{2-} generally decrease, whereas Ca increases downhole. Dissolved Sr increases smoothly in the upper 160 m and then remains approximately constant with depth. The negative correlation between dissolved Ca and Mg concentrations suggests reactions between volcanic material and pore water in the sediment column. The downhole decrease in SO_4^{2-} suggests sulfate reduction of particulate organic carbon, which also explains the rise in dissolved NH_4^+ with depth.

Samples for solid sediment analysis were taken at a sampling resolution of at least one sample per core from Holes U1507A and U1507B. Carbonate contents are very high (>90 wt%) throughout Subunit Ia. Decreasing carbonate contents (30–70 wt%) toward the middle of Subunit Ib and Ic correlate well with changes in other properties, such as decreasing reflectance L*, increasing MS, and increasing NGR. Interbedded darker colored layers are represented by lower total carbon and carbonate contents (~20 wt%). Carbonate contents within Unit II are high, varying between 50 and 80 wt%. TOC contents are low (averaging 0.4 wt%) throughout the sediment column and do not differ significantly between units.

Linear sedimentation rates (LSRs) and mass accumulation rates were calculated for Site U1507 using paleomagnetic and calcareous nannofossil datums (Figure **F11**). The record recovered at Site U1507 is remarkably continuous despite numerous turbidite deposits and seismic reflectors, and it includes the entirety of the Oligocene. LSRs in the mid to late Eocene vary between ~30 and 60 m/My but decrease near the Eocene–Oligocene transition to ~15–20 m/My. An extended duration of low LSRs (~12 m/My) characterizes the Oligocene to middle Miocene, except for two short time intervals of enhanced LSRs (30–29 Ma and 25–23 Ma). After 9.5 Ma, LSRs stepwise increase to 40 m/My at 7.4 Ma and remain at these high values until 4.0 Ma. This pulse in sedimentation, which is characterized by constant high carbonate contents, may correspond to the late Miocene to early Pliocene biogenic bloom as documented at other sites. The uppermost 4 My at Site U1507 are represented by a relatively condensed section with LSRs <4 m/My.

Mass accumulation rates follow the trend observed in LSRs and vary between 2 and 12 g/cm^2/ky.

Site U1508 (Reinga Basin)

Background and objectives

Site U1508 (proposed Site REIS-2A) is located ~130 km west of Cape Reinga, the northern tip of Northland, New Zealand. The location is on the northeast margin of Reinga Basin (Bache et al., 2012), which contains folded Eocene strata that have been dredged but never drilled (Browne et al., 2016). The site was chosen to sample a record of deformation, uplift, subsidence, and early arc volca-

nism in a southern region proximal to Tonga-Kermadec subduction initiation (Sutherland et al., 2016). The overall objective was to sample Miocene–Eocene strata, which includes an onlap surface that marks the onset of deformation. A high-amplitude seismic reflector near the base of the borehole has regional significance for stratigraphic correlation and was hypothesized to represent a major change in sedimentation during the Eocene.

Operations

Hole U1508A (34°26.8902′S, 171°20.6073′E; water depth = 1609 m)
Hole U1508B (34°26.8975′S, 171°20.5990′E; water depth = 1609 m)
Hole U1508C (34°26.8905′S, 171°20.5889′E; water depth = 1609 m)

All depth references in meters in this section refer to the DSF depth scale, unless noted otherwise.

We completed the 546 nmi transit from Site U1507 to U1508 and arrived at 2300 h on 20 August 2017 (UTC + 10 h). An APC/XCB BHA was made up and APC coring in Hole U1508A started at 0900 h on 21 August. Temperature measurements were taken on Cores 7H, 9H, 10H, 12H, 14H, and 17H. Core 23H had to be drilled over for 40 min to release it from the formation, and Hole U1508A was ended at 1140 h on 22 August. Total recovery for the 210.3 m cored was 201.1 m (96%). The time spent on Hole U1508A was 36.0 h or 1.5 days.

The ship was offset by ~20 m to the southwest. An RCB BHA was made up and drilling without coring in Hole U1508B started at 1745 h on 22 August, reaching the target (186.6 m) at 2245 h on 22 August. Coring in Hole U1508B began with Core 2R. While retrieving Core 38R (503.4 m) at 0700 h on 24 August, we stopped operations due to a medical emergency and began recovering the drill string. Cores 2R through 38R penetrated from 186.6 to 503.4 m and recovered 133.32 m (42%). The time spent on Hole U1508B was 49.5 h or 2.1 days.

The 302 nmi transit to Auckland began at 1354 h on 24 August. During the trip, the clock was advanced twice, to UTC + 12 h (Auckland time). On the way back from the medical evacuation, the clock was set back 1 h, to UTC + 11 h, and remained that way for the rest of the Expedition 371 drilling operations. The trip back to Site U1508 was completed at 0600 h on 27 August. An RCB BHA was deployed and Hole U1508C was initiated ~20 m northwest of Hole U1508B at 1150 h. The top 450 m of Hole U1508C was drilled without coring, except for two spot-cored intervals at 278.0–292.6 m (Cores 2R through 4R) and 316.0–330.7 m (Cores 6R and 7R) to better recover key intervals. At 0730 h on 28 August, we resumed RCB coring until penetration rates slowed to ~2 m/h. Although short of the desired target depth, we decided to stop coring and conduct wireline logging at 0300 h on 31 August. Collectively, Cores 2R through 38R and the two drilled intervals penetrated from 278.0 to 704.5 m and recovered 185.04 m of sediment (65% of cored intervals).

The bit was dropped at the bottom of the hole at 0325 h on 31 August, the hole was displaced with 194 barrels of 11.0 lb/gal mud, and the open end of the drill string was set at 86.7 m. At 0900 h, we deployed the same modified triple combo logging tool string configuration as used in Hole U1507B with the exception that no source was installed in the density tool. Logging went well until ~1230 h when the tool string became stuck at ~270 m WSF. The logging line was cut at the rig floor and terminated with connectors that would allow assembly of drill pipe over the logging line to wash down and over the logging tools with the open-ended BHA. After the logging tools were free at 2105 h, the tool string arrived back on the rig floor at 0315 h on 1 September. After the drill string was recovered, the ship began the transit to Site U1509 at 0730 h on 1 September.

Principal results

All depth references in meters in this section refer to the CSF-A depth scale.

The sedimentary sequence at Site U1508 consists of ~700 m of heterogeneous strata divided into three lithostratigraphic units (I, II, and III).

Lithostratigraphic Unit I (0.0–90.1 m) consists of ~90 m of foraminiferal ooze with varying amounts of nannofossils and coarse-grained bioclasts. An increase in the occurrence of millimeter-sized bioclasts comprised mainly of bryozoans starts at ~49 m and extends to the bottom of this unit. The Unit I/II boundary at 90.1 m is defined by an abrupt change from foraminiferal ooze with bioclasts to clayey nannofossil ooze with biosilica.

Lithostratigraphic Unit II (90.1–379.3 m) consists of ~290 m of calcareous ooze and chalk with varying amounts of clay and is divided into two subunits. Subunit IIa (90.1–200.6 m) comprises light greenish clayey nannofossil ooze with varying contents of foraminifers and sponge spicules. Subunit IIb (200.6–379.3 m) is nannofossil-rich foraminiferal ooze and chalk with lithic and volcanic grains increasing to ~336 m and then decreasing downhole, resulting in a pure foraminiferal chalk in the lowermost 30 m of the subunit.

The lithostratigraphic Unit II/III boundary at 379.3 m is identified by an abrupt downhole decrease in grain size to nannofossil chalk with varying amounts of foraminifers. Unit III (379.3–701.9 m) is composed of moderately bioturbated nannofossil chalk, which is further divided into two subunits. Subunit IIIa (379.3–491.6 m) consists of moderately to heavily bioturbated clayey nannofossil chalk and contains at least 50 sporadic centimeter-scale cherty limestone intervals. Subunit IIIb (493.8–701.9 m) is characterized by a downhole decrease in clay content and color brightening, with cherty limestone last observed at ~503 m. Subunit IIIb comprises nannofossil chalk, and from ~685 m downhole it is sufficiently lithified to be classified as a nannofossil limestone.

Calcareous nannofossils are abundant in most of the studied samples. Planktonic foraminifers dominate over benthic foraminifers, which are present in most samples. Radiolarians are few to rare in most samples, barren in some samples from Holes U1508A and U1508B, and few to abundant in the lower half of Hole U1508A. Ostracods are abundant to common in Unit I and Subunit IIb and rare to barren in Subunits IIa, IIIa, and IIIb. Preservation of all fossil groups decreases downhole, ranging from excellent to good in the upper part of Hole U1508A and from moderate to poor in Hole U1508C.

Calcareous nannofossil and planktonic foraminiferal datums, occasionally supplemented by radiolarian biostratigraphy, allow age assignments to all studied samples (Figure **F11**). Lithostratigraphic Unit I is Pleistocene–Pliocene in age. The interval between 96 and 210 m, nearly coincident with lithostratigraphic Subunit IIa, is Miocene in age. Samples between 187 and 373 m are Miocene to Oligocene in age. Nannofossil biostratigraphy points to an early Miocene to late Oligocene hiatus (Zones NN4–NN1) of ~6 My in both Holes U1508B (312–321 m) and U1508C (316–321 m). The interval from 379 to 497 m in Hole U1508B is late to middle Eocene age. In Hole U1508C, the interval from 450 to 480 m is late Eocene age and the

interval from 484 to 686 m is middle Eocene age. Nannofossils, planktonic foraminifers, and radiolarians indicate an early Eocene age near the bottom of the sequence (686–702 m). Age-diagnostic dinocyst species corroborate the age constraints determined by nannofossils and planktonic foraminifers.

Benthic microfossils (ostracods and foraminifers) indicate a lower bathyal paleoenvironment throughout most of the sedimentary sequence and slightly shallower paleodepths (deep middle bathyal) during the Oligocene and late Eocene. Palynological assemblages contain moderately to well-preserved palynomorphs, predominantly inner neritic to pelagic dinocysts. Terrestrial palynomorph content is much higher in the Pliocene to late Oligocene than in the early Oligocene to Eocene, indicating a significant change in offshore transport. Reworked microfossils, in particular of early Paleogene age, commonly occur downhole from the mid-Miocene in all fossil groups.

Pass-through paleomagnetic measurements from Unit I (0–90 m) are affected by core disturbance and have extremely weak magnetization (~10^{-5}–10^{-3} A/m), resulting in random NRM inclinations. NRM inclinations in Subunit IIa (~90–210 m) show a series of polarity swings but no clear polarity pattern. In contrast, high-quality paleomagnetic data were obtained from Subunit IIb from ~250 to 380 m with well-defined geomagnetic reversals. From lithostratigraphic Subunit IIb to Unit III, the NRM intensity drops to ~10^{-4}–10^{-3} A/m, resulting in poor paleomagnetic behavior for many cores. Reliable paleomagnetic data were obtained from some intervals in Hole U1508C, including 278–324 and ~650–700 m. Integration with biostratigraphy allows a series of paleomagnetic reversals in Holes U1508B and U1508C (Subunit IIb and Unit III) to be correlated with the GPTS back to ~48 Ma.

Samples from Hole U1508A have a poorly defined orientation of the AMS tensor, whereas most samples from Holes U1508B and U1508C exhibit a well-defined oblate AMS fabric with the minimum axis of the AMS ellipsoids statistically oriented perpendicular to the bedding plane.

Variations in physical properties define three distinctive boundaries at ~90, ~200, and ~500 m and are correlated with two strong reflections on MCS data and three lithostratigraphic boundaries. The upper interval, corresponding to lithostratigraphic Unit I, is characterized by low density of ~1.5 g/cm^3, high porosity of ~65%–75%, and increasing velocity from ~1500 to ~1700 m/s. All these values show a baseline shift at the Unit I/II boundary (~90 m) to higher bulk density values (~1.65 g/cm^3), lower porosity values (~60%–65%), and lower velocity values (~1600 m/s) that remain constant throughout Subunit IIa down to ~200 m. Within the uppermost part of Subunit IIb (~200–250 m), bulk density decreases from ~1.75 to ~1.55 g/cm^3, porosity increases from ~60% to ~70%, and shear strength decreases from ~100 to ~30 kPa, whereas *P*-wave velocity increases from ~1600 to 1900 m/s. Below the Subunit IIIa/IIIb boundary at 500 m, bulk density gradually increases from 2.0 to 2.3 g/cm^3, porosity gradually decreases to ~25%, and *P*-wave velocity increases from ~2200 to 2600 m/s. At the very base of Subunit IIIb where the transition from chalk to limestone occurs (680–700 m), velocity and bulk density sharply increase to ~3600 m/s and 2.45 g/cm^3, respectively.

NGR and color reflectance data reveal complementary trends to the density, porosity, and velocity measurements, including the three distinctive boundaries at ~90, ~200, and ~500 m. NGR increases and the color changes at ~90 m. NGR decreases and then increases around ~200 m. MS from wireline logging and core measurements are low throughout the entire section, except for the interval from ~240 to ~380 m (Subunit IIb), which contains lithic constituents. This interval also has higher amplitude (up to ~20 counts/s) NGR variations.

Five in situ temperature measurements in Hole U1508A revealed a gradient of ~55°C/km.

Headspace gas samples were routinely collected from each core in Hole U1508A and from deeper cores in Hole U1508C. Methane was above the detection limit from ~460 m downhole and progressively increased below ~500 m. Methane concentration was ~6000 ppmv and ethane concentration was 36 ppmv at the base of Hole U1508C.

A total of 75 IW samples were collected from Site U1508 by three different methods: whole-round squeezing, Rhizon sampling, and half-round squeezing. The latter were ~15 cm intervals taken from core working halves 1–2 days after recovery and crushed in plastic bags. These half-round samples yield reasonable results for some dissolved species, notably sulfate. Rhizon results generally lie close to those from squeezed samples at nearby depths. The manganese concentration profile does not show a peak within the uppermost meter or so, which suggests the true mudline is missing. Adjacent samples from the upper ~100 m of the section show large variance because the sediment is unconsolidated foraminiferal sand, which makes collection of uncontaminated pore water difficult. Nonetheless, most constituents do not vary much in concentration over the uppermost 275 m. Below 275 m, sulfate concentrations decrease downhole linearly and ammonium, barium, and strontium concentrations increase linearly or exponentially. The concomitant loss of sulfate and rise in methane from ~500 m downhole suggests a deep zone of anaerobic oxidation of methane (AOM), which also may explain the abundant macroscopic pyrite at this depth interval.

Bulk sediment carbonate content varies considerably with depth, having 100 m–scale fluctuations between highs of ~95 wt% and lows of ~40 wt%, which relate to the lithostratigraphic units. TOC contents are 0.76 ± 0.36 wt%, without any consistent downhole trend.

All cores from Holes U1508A–U1508C were correlated to the downhole logging data (at the wireline log matched depth below seafloor [WMSF] depth scale) using one tie per core. An offset table allows users to approximate depths of core data at the CSF-A depth scale to the WMSF depth scale of the downhole logging data.

LSRs were calculated for Site U1508 using calcareous nannofossil datums and polarity chron boundaries from 0 to 48 Ma (Figure **F11**). LSRs in the Pliocene–Pleistocene vary between ~10 and 80 m/My and average ~20 m/My during the early to late Miocene. The succession is condensed for most of the Oligocene despite a short interval from 23 to 26 Ma. LSRs for the late to middle Eocene are steady at ~20 m/My.

Site U1509 (southern New Caledonia Trough)

Background and objectives

Site U1509 (proposed Site NCTS-2A) is located ~640 km west of the northern tip of New Zealand, ~300 km south of Site 206, and ~200 km north of DSDP Site 592. The location is on the western margin of the New Caledonia Trough at the base of the Lord Howe Rise slope, near the mouth of a canyon that drains around the northeast end of a small submerged spur (Sutherland et al., 2016). This spur, inferred to have been created by deformation, is underlain by the northeast-dipping limb of a west-verging fold that exposes strata that can be traced beneath the axis of the New Caledonia Trough. Site U1509 was chosen to determine the timing

of Cenozoic folding in the southern New Caledonia Trough and to obtain stratigraphic constraints on the timing of vertical tectonic movements and volcanism.

Operations

Hole U1509A (34°39.1312′S, 165°49.6599′E; water depth = 2911 m)

All depth references in meters in this section refer to the DSF depth scale.

We arrived at Site U1509 at 1030 h on 2 September 2017 (UTC + 11 h), completing the 273 nmi transit from Site U1508. RCB coring in Hole U1509A was initiated at 2145 h on 2 September. The decision to use the RCB system was made after considering target depth, time constraints, and success at previous sites. Coring continued until 2345 h on 6 September and reached 690.7 m (Core 74R). Total recovery in Hole U1509A was 462.86 m (67%).

Planned wireline logging in Hole U1509A was canceled due to ship heave exceeding 3.0 m. Hole U1509A was ended at 1434 h, after a total of 127.5 h or 5.3 days. At 1630 h on 7 September, the ship began a ~200 nmi transit to the north to avoid severe weather forecast for 9–10 September; this weather also impacted operations at the remaining drilling sites.

Principal results

All depth references in meters in this section refer to the CSF-A depth scale.

The sedimentary sequence at Site U1509 consists of ~415 m of calcareous ooze, chalk, and limestone (Unit I) overlying ~275 m of claystone (Unit II).

Lithostratigraphic Unit I is divided into three subunits. Subunit Ia (0–99.6 m) consists of calcareous ooze and chalk with rare tuffaceous beds. RCB coring led to soupy and mousse-like drilling disturbance in the soft sediments of the upper ~50 m of this subunit, followed by biscuiting, horizontal cracking, fracturing, and pulverization in the more indurated lower sediment of the unit. The ooze–chalk transition was observed, remarkably, at ~55 m. Subunit Ib (99.6–139.28 m) comprises calcareous chalk showing significant soft-sediment deformation (i.e., slumps). Subunit Ic (139.28–414.57 m) consists of calcareous chalk and limestone with biosilica and several silicified (chert) intervals. Subunit Ic is characterized distinctively by tilted bedding (apparent dip of ~20°). From Subunit Ic downhole, preferential fracturing of cores was seen along primary deformation structures such as shear zones, microfaults, and tilted bedding. The chalk–limestone transition occurs within Subunit Ic at around 385 m.

Lithostratigraphic Unit II is divided into two subunits. Subunit IIa (414.57–614.2 m) consists of claystone with nannofossils and silt. Subunit IIb (614.2–689.68 m) consists of massive brown claystone with minor bioturbation and agglutinated benthic foraminifers. Similar to Subunit Ic, tilted bedding is observed throughout Unit II.

Nannofossil and planktonic foraminifer preservation and abundance generally decrease downhole, with these groups absent below 617.6 and 536.0 m, respectively. Radiolarians are rare to abundant and well preserved in the upper 393 m but are rare and poorly preserved farther downhole. Benthic foraminifer abundance is low, and preservation decreases downhole in the upper 249 m and remains poor below. Only agglutinated taxa are found in sediments below 617.6 m. Ostracods are common to rare with moderate to poor preservation in the upper 178 m and are rare to barren below. A palynological reconnaissance study focused on Unit II and recovered rich and well-preserved assemblages.

Nannofossil and foraminifer datums yielded Miocene (22.41–82.47 m), Oligocene (90.13–248.63 m), Eocene (259.98–407.07 m), and Paleocene (418.53–609.27 m) ages for the sequence in Hole U1509A (Figure **F11**). The interval from 617.6 to 689.6 m is barren of age-diagnostic nannofossils and planktonic foraminifer taxa but contains Late Cretaceous dinocysts and agglutinated benthic foraminifers. Benthic foraminifers indicate deposition in a lower bathyal–abyssal environment during the Pleistocene to Eocene and at middle bathyal depths during the Paleocene and Cretaceous.

NRM intensity of most sediment cores from Hole U1509A is weak, mostly around 10^{-4} A/m. This results in generally noisy paleomagnetic data from the pass-through magnetometer. However, step-wise AF demagnetization of some discrete samples gives reliable paleomagnetic data. Integrating these data with biostratigraphy, the observed magnetic polarities at 110 to ~260 m are tentatively correlated to Chrons C9 through C13 of GPTS2012. The claystone interval of Subunit IIb produces higher quality pass-through data compared to intervals above. Cores from Subunit IIb have a normal magnetic polarity.

Physical property measurements in Hole U1509A exhibit gradual changes in bulk density and *P*-wave velocity with depth, except across a layer of limestone between ~390 and 415 m. Through the ooze and chalk, above the limestone, *P*-wave velocity and bulk density increase with depth from 1500 to 1900 m/s and from 1.55 to 1.90 g/cm^3, respectively. The transition from ooze to chalk is shallow (~55 m) and correlates with a *P*-wave velocity increase of ~100 m/s. The limestone of Subunit Ic represents a discrete interval where *P*-wave velocity and density increase by ~40% and porosity decreases sharply. *P*-wave velocity, bulk density, and MS are approximately constant in the Unit II claystone below the limestone. A gradual decrease in porosity with depth is also observed. NGR values show high variance in Unit II (from 8 to 30 counts/s), reflecting changes in clay composition and abundance.

A total of 23 IW samples were collected from Hole U1509A. Profiles of some species show trends similar to those at Site U1508. For example, sulfate concentrations decrease and ammonium concentrations increase downhole, suggesting sulfate reduction of particulate organic matter and release of nitrogen to pore waters. Furthermore, at ~370 m, sulfate concentrations drop below 1.0 mM and methane concentrations start to rise. This suggests further sulfate consumption by AOM at a deep sulfate–methane transition (SMT). Reduction of sulfate leads to production of hydrogen sulfide, which reacts with iron to form pyrite (Snyder et al., 2007), which is present in many cores from this hole. Below the SMT, headspace methane concentrations increase to 15,000 ppmv and dissolved Ba concentrations increase to 0.4 mM. Such values are common to slope environments of many continental margins.

Bulk sediment chemistry corresponds to lithostratigraphic units. Unit I is characterized by carbonate contents that decrease downhole from ~94 wt% at 20 m to ~65 wt% between 360 and 380 m. Carbonate content varies little in the uppermost 200 m, but by more than 10% in the lower part. Carbonate content drops drastically across the Unit I–II transition (415 m), to average values of 18 and 0.5 wt% in Subunits IIa and IIb, respectively. TOC contents are ~0.3 wt% in Unit I and Subunit IIa and ~1.0 wt% in Upper Cretaceous Subunit IIb.

Site U1510 (southern Lord Howe Rise)

Background and objectives

Site U1510 (proposed Site LHRS-3A) is located on the southern Lord Howe Rise, ~850 km west of northern New Zealand and ~495 km south of Site 206. Site U1510 is ~80 km west of Site 592 and ~105 km northwest of Site 207. Seismic reflection data can be used to tie stratigraphy at the three sites but with some uncertainty caused by unconformities and deformation (Sutherland et al., 2016). Site U1510 was chosen to determine the timing of Cenozoic folding on the southern Lord Howe Rise and to constrain the timing of regional tectonic movements and volcanism. The primary drilling objectives at Site U1510 were to (1) constrain the depths and ages for the top and base of the syntectonic seismic unit; (2) determine the nature of the lowest seismic unit and pretectonic state of the southern Lord Howe Rise; and (C) collect evidence for volcanism or vertical movements, especially including sediments representing nearby shallow water of any age. A secondary objective was to collect a continuous late Neogene record for paleoceanographic studies.

Operations

Hole U1510A (36°19.7385′S, 164°33.5220′E; water depth = 1238 m)
Hole U1510B (36°19.7392′S, 164°33.5347′E; water depth = 1238 m)

All depth references in meters in this section refer to the DSF depth scale.

After the 380 nmi transit in heavy winds and seas from a waiting on weather location, the ship arrived at Site U1510 at 0918 h on 12 September 2017 (UTC + 11 h).

An APC/XCB BHA was deployed and coring in Hole U1510A started at 1915 h on 12 September. Cores 1H through 17H penetrated from 0 to 150.5 m and recovered 147.9 m (98%). We stopped deploying the orientation tool after Core 15H. Temperature measurements were taken on Cores 4H, 7H, 10H, 13H, and 17H. We continued with XCB coring until 1930 h on 14 September. Cores 18X through 52X penetrated from 150.5 to 483.4 m and recovered 108.1 m (32%). Recovery over portions of this depth interval was seriously compromised because of frequent chert layers. Coring in Hole U1510A concluded on 14 September with a total penetration of 483.4 m and total recovery of 260.0 m (53%). The time spent on Hole U1510A was 60 h or 2.5 days.

The ship was offset 20 m to the east and APC coring in Hole U1510B began at 2300 h on 14 September and ended at 0215 h on 15 September. Cores 1H through 7H penetrated from 0 to 66.3 m and recovered 64.7 m (98%). An APCT-3 temperature measurement was taken on Core 7H. Operations in Hole U1510B and at Site U1510 ended at 0815 h on 15 September. The time spent on Hole U1510B was 10.75 h or 0.4 days. At 0842 h the ship began the transit to Site U1511.

Principal results

All depth references in meters in this section refer to the CSF-A depth scale.

Lithostratigraphic Unit I (0–138.0 m) is composed of calcareous ooze and is divided into two subunits. Subunit Ia (0–60.0 m) consists of subtle color banding between light gray and white calcareous ooze. Subunit Ib (60.0–138.0 m) is a white homogeneous calcareous ooze. The Unit I/II boundary is defined by the first occurrence of chert at 138 m.

Lithostratigraphic Unit II (138.0–418.1 m) consists of ~340 m of calcareous ooze and chalk interbedded with cherty limestone and chert. Unit II is divided into three subunits. Subunit IIa is a ~9.5 m thick white homogeneous nannofossil ooze with bioclasts. The upper ~30 cm of Subunit IIa consists of centimeter-sized extraclasts composed of chert, cherty limestone, and lithic clasts. Although this interval could be affected by drilling disturbance (i.e., "fall-in" at the top of the core), it also contains the first occurrence of chert; similar material had not been found in the cores above. Subunit IIb (147.5–349.4 m) is a 201.9 m thick interval of light gray, moderately bioturbated clayey calcareous chalk with scattered shallow-water bioclasts interbedded with cherty limestone. Subunit IIc (349.4–478.1 m) is a 128.7 m thick homogeneous white nannofossil chalk interbedded with chert and sparse volcaniclastic beds in the lower portion of the subunit.

Core recovery in Unit I was near 100%, with coring disturbance limited to up-arching and soupy sediments. Recovery dropped to ~20% in Subunits IIa and IIb due to the presence of chert and cherty limestone and the use of the XCB coring system, with drilling disturbance including severe fracturing of chert and cherty limestone intervals and moderate to severe biscuiting of the calcareous chalk intervals.

Nannofossils are generally abundant with moderate preservation. Planktonic foraminifer abundance and preservation decrease downhole (from 215 and 187 m, respectively) with a few barren samples. Radiolarians are rare throughout, except for a short middle Miocene interval (109.6 to 119.7 m) where radiolarians are common. Radiolarian preservation is good in the upper 135 m and poor farther downhole. Benthic foraminifers were recovered at generally low abundance from all cores, with very good preservation for the Neogene and generally poor preservation for the Paleogene. Ostracods are very abundant in most samples with good preservation from 0 to ~150 m and with poor preservation below. Due to weather constraints on processing, no samples from Site U1510 were analyzed for palynology. Paleodepth was lower bathyal from the Pleistocene through the Eocene. During the late and middle Eocene, a significant component of the benthic fauna appears to be derived from shallower (shelf, upper bathyal, and middle bathyal) sources.

Based on nannofossil and foraminifer biostratigraphy, the following ages were determined for the sequence in Hole U1510A: Pleistocene (5.0–33.5 m), Pliocene (43.1–70.3 m), Miocene (72.3–135.4 m), and late, middle, and early Eocene (138.8–147.7, 150.5–438.9, and 448.9–478.2 m, respectively).

Low NRM intensity of most cores, low core recovery, and significant core disturbance from XCB coring make it difficult to establish shipboard magnetostratigraphy at Site U1510.

Physical property measurements show a gradual increase in bulk density and *P*-wave velocity with depth in the nannofossil and foraminiferal ooze of Unit I. In Subunits IIa and IIb, from 140 to ~350 m, physical property measurements are less reliable and sparse due to drilling disturbance and low recovery, respectively. Bulk density (~1.75 g/cm^3) and *P*-wave velocity (~1750 m/s) increase downhole to 300 m and then decrease again to the base of Subunit IIb, where fewer chert layers are observed. MS and NGR both increase downhole in these two subunits then decrease toward the base of Subunit IIb. *P*-wave velocity peaks and spikes in NGR in Subunit IIc correlate with sandstone and claystone. Near the base of the hole (~470 m) where sediments become more lithified, density and velocity increase and porosity decreases.

Headspace samples from Site U1510 yielded hydrocarbon gas concentrations below detection limits.

A total of 118 IW samples were taken from Site U1510 by squeezing whole-round sediment and by Rhizon sampling (Dickens et al., 2007). Ca concentrations increase and Mg and K concentrations decrease downhole, similar to Sites U1506 and U1507. These profiles may result from the reaction of pore water with volcanic material in the sediment. Sulfate and ammonium concentration profiles mirror each other, suggesting sulfate reduction of organic matter. Dissolved Sr, Si, Li, and B concentrations increase downhole, likely reflecting dissolution of biogenic carbonate and silica. Dissolved Mn and Fe concentrations decrease within the uppermost meter, suggesting the true mudline is missing. Dissolved Fe concentrations in Rhizon samples decrease rapidly over the upper 8 to 10 m, consistent with the odor of H_2S at ~10 m.

Carbonate content is >90 wt% in Unit I and in Subunits IIa and IIc, corresponding to calcareous ooze and chalk lithologies. In Subunit IIb, carbonate content decreases downhole toward the middle of the subunit, along with decreasing L* and increasing NGR. Interbedded cherty and tuffaceous layers are distinguished by carbonate contents of <50 and <20 wt%, respectively. TOC content is mostly below detection limit but is represented by somewhat higher values (0.35 wt%) below 400 m.

Coring of Hole U1510B was monitored in near real time through out-of-sequence measurement of whole-round sections. Using primarily NGR data, cores from Holes U1510A and U1510B were depth shifted to construct a composite depth scale. A spliced record was generated using the composite scale, which provides a continuous record of the top ~44 m of sediment at Site U1510.

Site U1511 (Tasman Abyssal Plain)

Background and objectives

Site U1511 (proposed Site TASS-2A) is located on the Tasman Abyssal Plain, ~945 km east of Australia and ~990 km northwest of New Zealand. Site U1511 lies west of the Lord Howe Rise on oceanic crust of Late Cretaceous age that is thought to have formed during Chron C33 (74–84 Ma). Regional seismic reflection data reveal a thick (>800 m) sequence of sediments deformed by reverse faults and folds (Sutherland et al., 2016). Site U1511 was chosen to find the age of this deformation and to provide the second comprehensive record of sedimentation on the Tasman Abyssal Plain. The primary drilling objectives at Site U1511 were to sample (1) the top of the middle seismic unit to constrain the age of folding and (2) the rest of the sedimentary sequence to develop an understanding of this significant abyssal location. The only previous scientific borehole into Tasman Abyssal Plain sediments was drilled in 1973 at DSDP Site 283, 870 km to the southwest and on conjugate crust of Late Cretaceous age east of southeast Australia.

Operations

Hole U1511A (37°33.6665′S, 160°18.9380′E; water depth = 4847 m)

Hole U1511B (37°33.6656′S, 160°18.9379′E; water depth = 4847 m)

All depth references in meters in this section refer to the DSF depth scale.

The ship completed the transit from Site U1510 and arrived at Site U1511 at 1248 h on 16 September 2017 (UTC + 11 h). RCB coring in Hole U1511A began at 0425 h on 17 September. After retrieving Core 3R, the drill string had to be pulled clear of the seafloor due to excessive heave and wind. Cores 1R through 3R penetrated from 0 to 26.6 m and recovered 7.9 m (30%). A total of 19.25 h or 0.8 days were spent on Hole U1511A.

After waiting for 17 h because of weather, Hole U1511B was initiated at 0145 h on 18 September by washing down (i.e., drilling without coring and without a center bit installed) to 19.8 m. Coring resumed at 0215 h on 18 September, and Cores 2R through 7R penetrated from 19.8 to 77.2 m. A center bit was deployed and the interval from 77.2 to 192.2 m was drilled without coring to ensure we could reach the target depth in the remaining time of the expedition. Coring resumed at 1500 h on 18 September, and Cores 9R through 41R penetrated from 192.2 to 508.8 m. At 1600 h on 20 September, coring was suspended due to excessive heave and the drill string was raised above the bottom of the hole. As the swell began to subside at 1030 h on 21 September, the drill string was lowered back to the bottom of the hole. After pumping a 25 barrel mud sweep, coring resumed at 1600 h on 21 September and ended with the recovery of the last core (47R) at 0450 h on 22 September. The total cored interval in Hole U1511B was 431.4 m and recovery was 279.3 m (65%). Two intervals were drilled without coring for a total of 134.8 m.

The rig floor was secured for transit to Hobart at 1630 h on 22 September, ending Hole U1511B and Site U1511. A total of 110.75 h or 4.6 days were spent on Hole U1511B. The total time at Site U1511 was 130.0 h or 5.4 days. This included 40.5 h lost because of weather.

Principal results

All depth references in meters in this section refer to the CSF-A depth scale.

Three lithostratigraphic units were described and are differentiated by the presence or absence of microfossils. Unit I (0–77.2 m) is ~80 m of gray to brown clay, with calcareous nannofossils restricted to the lowermost 40 cm of the unit. Unit II (201.9–403.4 m) is separated from Unit I by a ~120 m drilled interval and consists of ~200 m of greenish gray to yellowish brown diatomite with minor abundances of clay and other siliceous microfossils (radiolarians, sponge spicules, ebridians, and silicoflagellates). Unit III (403.4–560.7 m) is ~150 m of claystone. A ~30 m reddish brown interval near the top of Unit III contains minor abundances of radiolarians. A ~40 m grayish green interval near the bottom of the unit contains minor abundances of calcareous nannofossils.

A variety of secondary minerals are present throughout Site U1511, attesting to diagenesis and alteration. Manganese nodules and black specks of sulfides occur in Unit I, whereas sporadic centimeter-scale nodules and specks of pink rhodochrosite occur in Unit II. Several centimeter-scale intervals of greenish gray claystone within Units II and III contain sand-sized grains of native copper surrounded by dark green halos. The lower part of Unit II also contains cristobalite and an interval of red and pink fluorapatite. Furthermore, a color gradient across Unit III from red and reddish brown at the top of the unit to greenish gray toward the base, with alternations of the two colors in the intervening interval, seems to be related to trace amounts of redox-sensitive metal oxides. These minerals suggest a complex history of diagenesis and alteration, the latter likely mediated by past fluid flow.

Calcareous nannofossils and planktonic foraminifers are generally absent throughout Site U1511. When present, their abundances and preservation states are varied. Radiolarians are present from 192 to 547 m and are abundant from 209 to 394 m, with good preservation. Below, radiolarians are less abundant and poorly preserved.

Benthic foraminifers are sparse in the Pliocene to lower Eocene interval, where a low-diversity agglutinated assemblage was recog-

nized. The transition to a higher diversity Paleocene to lowermost Eocene assemblage was observed at the contact between lithostratigraphic Units II and III. The Paleocene interval contains both agglutinated and calcareous taxa. Samples are barren of ostracods and palynomorphs. Given the overall microfossil assemblages, the location of Site U1511 has probably been abyssal and beneath or near the carbonate compensation depth (CCD) since the Paleocene.

Rare nannofossils and planktonic foraminifers found through the Pliocene, Miocene, lower Oligocene, and Paleocene intervals were used to constrain age where possible (Figure **F11**). Based on planktonic foraminifers, Pliocene (7.5–7.6 m), lower Pliocene to upper Miocene (7.5–47.6 m), and possible Miocene (65.6–65.7 m) strata were recognized. Based on calcareous nannofossils, the lower Oligocene (192.2–204.0 m) was identified; however, sediments from this level may have come from the drilled interval and may not be in situ.

Based on radiolarian biostratigraphy, upper Eocene (209–235 m), lower to middle Eocene (235–389 m), and Paleocene (432–539 m) strata were recognized. The lower to middle Paleocene (538.8–539.4 m) was also identified based on nannofossil biostratigraphy.

High-quality paleomagnetic data were obtained across intervals of Units II and III. From Cores 371-U1511B-14R through 30R (~240–400 m), all polarity reversals from the base of Chron C17n.3n to Chron C21n are identified, indicating that Unit II in Hole U1511B spans from ~38 to 47.5 Ma (Bartonian–Lutetian). Four magnetic polarity reversals within Core 38R can be successfully correlated with Chrons C24n.1n to C24.2n (~53 Ma).

The remanence intensity of sediments from Units II and III exhibits possible cycles. These variations appear related to lithologic color changes, where brown intervals generally have a higher magnetization compared to the lower magnetization in the gray sediment intervals. Such changes may be related to magnetic mineral diagenesis. Many samples in Unit III show magnetically hard NRM behavior that is resistant to AF demagnetization. Such a hard remanence component is carried by hematite, which probably contributes to the reddish sediment color in Unit III.

Cube samples from Units II and III show reliable AMS data and distinct patterns for Units II and III. Samples from Unit II indicate a random orientation of the AMS tensor, which probably reflects a random deposition of minerals without sediment compaction. In contrast, sediments from Unit III exhibit a well-defined oblate AMS fabric, as typical for compacted sedimentary rocks.

Porosity decreases downhole from 80% to 65% in Unit I along a trend typical for pelagic clay. This trend continues in Unit III (from 60% to 45%). However, in Unit II porosity is offset to extremely high values (70%–83%). This general profile is mirrored in bulk density and is attributed to the diatomite with clay in Unit II. *P*-wave velocity increases linearly downhole, with the exception of two peaks in the lower part of Unit II (1750 m/s) and the middle part of Unit III (1850 m/s). MS values vary between 5 and 50 IU in Unit I and near the top of Unit III and are much lower in Unit II and in the lower part of Unit III. NGR shows a similar trend and both MS and NGR appear to correspond to clay content. All color reflectance parameters (L*, a*, and b*) increase downhole from 200 to 300 m and then decrease from 300 to 400 m, corresponding to the diatomite in Unit II. A step increase in bulk density (1.50–1.75 g/cm^3), MS, NGR, and a* and b*, associated with a decrease in porosity (from 70% to 52%), is attributed to a red claystone interval in the top of Unit III (~410 m).

Headspace samples from Site U1511 yielded no light hydrocarbon gas concentrations above detection limits.

Low contents of carbonate (<15 wt%) and TOC (<0.4 wt%) prevail throughout the sedimentary column at Site U1511. Carbonate contents only rise >1 wt% in samples from two intervals: at the bottom of Unit I (71–77 m) and within the lower half of Unit III (490–539 m).

A total of 50 IW samples were collected at Site U1511 by two methods: squeezing and Rhizon sampling. At the precision required to understand basic processes at Site U1511, squeeze and Rhizon samples give similar profiles for most dissolved species. These profiles show some general trends, as well as some unusual features. This reflects a combination of lithology and multiple processes.

As also observed at other Expedition 371 sites, modest oxidation of particulate organic carbon leads to production of alkalinity and NH_4^+ and removal of SO_4^{2-}. Limited dissolution of biogenic silica occurs, which increases dissolved H_4SiO_4 (particularly in Unit II). Dissolved Ca increases and dissolved Mg and K decrease downhole, suggesting reactions with silicate minerals. However, the change in Ca relative to Mg with respect to depth is much greater at Site U1511 than at other Expedition 371 sites, which probably results from reactions with underlying basalt rather than sediment or continental crust. Many species display an inflection in concentrations at ~200 m and a major drop in concentrations at ~400 m. The first change probably results from the major increase in porosity associated with diatomite; the latter change probably represents the conversion of biosilica to cristobalite and the release of water. Dissolved Mn increases slightly in the upper 80 m but sharply below 200 m, reaching an extreme of 357 µM at 421 m. Such high values suggest dissolution of Mn oxides in the lower layer of the sediment column. Ammonium concentrations are below the detection limit across the uppermost 20 m, which may indicate a deep horizon of ammonia oxidation.

Physical property, paleomagnetic, and biostratigraphic data were compiled to locate middle Eocene climate events in Hole U1511B. Interpretation of magnetic inclination and radiolarian assemblages indicates the MECO was recovered in sediment of Core 371-U1511B-16R. The putative C19r hyperthermal event (Edgar et al., 2007) may be present in sediment of Core 18R, based on natural magnetic remanence data.

Summary of scientific results

Regional stratigraphy

Expedition 371 retrieved the sedimentary section at six sites (Table **T1**) in a vast remote region (Figure **F2**). Only two continents on Earth remain largely unexplored: Antarctica and Zealandia. The observations made at these six sites represent a substantial gain in fundamental knowledge about northern Zealandia, which is similar in size to India (Mortimer et al., 2017). The only previous boreholes in the region that penetrated strata older than late Eocene were at DSDP Sites 206, 207, and 208 (Shipboard Scientific Party et al., 1973a, 1973b, 1973c), and these sites were drilled in 1971, before regional seismic reflection data were available and their context was understood.

At five sites, we sampled nannofossil and foraminiferal ooze and chalk that contained volcanic or volcaniclastic intervals with variable clay content (Figure **F10**). The Paleocene and Cretaceous sections are generally clay rich or predominantly claystone. At the final site (U1511), a sequence of abyssal clay and diatomite was recovered with only minor carbonate. The ages at the base of the deepest hole at each site varied from Eocene to Cretaceous, and sedimentation rates were moderate to high (5–20 m/My) for the lower bathyal and

abyssal environments within which most sediments accumulated (Figures **F11**, **F12**).

Our new results provide the first substantial basis for definition of formal lithostratigraphic units that can be mapped across a substantial part of northern Zealandia and related to onshore regions of New Caledonia and New Zealand.

Paleogeography and vertical tectonic motions

Flat unconformities have been mapped across large parts of the Lord Howe Rise using seismic reflection data and have been tentatively interpreted as surfaces produced by sea level–modulated erosion (Sutherland et al., 2010). Similar surfaces also have been identified in the Reinga Basin (Bache et al., 2012). Our discovery of shallow-water (<400 m) fossils at several sites near these horizons provides the first compelling evidence of substantial vertical motions during the Cenozoic. The detailed age models we have constructed and paleoenvironmental interpretations we have made will allow us to construct new paleogeographic maps of northern Zealandia, with broad implications for studies of tectonics, climate, and biogeography.

Ocean circulation and sedimentation models are sensitive to paleobathymetry, and geodynamic models make predictions of vertical motions that control paleogeography. Therefore, our primary and secondary science objectives are closely aligned. Our new observations of sediment distribution combined with fossils provide independent evidence for past vertical positions and paleogeography. Our new data confirm the hypothesis that Eocene vertical motions were dramatic and regional in nature. Importantly, the paleogeography of the early Eocene and older cannot be easily inferred from looking at the present physiography.

Timing and style of deformation

The southern four sites (U1508–U1511) are located adjacent to reverse faults and folds. For all four sites, high-quality age models were constructed that can be tied to seismic reflection images and hence provide strong constraints on the time period when faulting and folding occurred. Additional postexpedition work is required to model ties between depth and TWT on seismic reflection sections, but preliminary estimates suggest that faulting and folding occurred during the late Eocene to early Oligocene. At Sites U1508 and U1510, there is some evidence that faulting and folding started somewhat earlier (during the middle Eocene) than at the other sites.

New Caledonia Trough subsidence

Existing subduction initiation models do not predict the New Caledonia Trough feature, which we have now confirmed from our observations at Sites U1507 and U1509 was either created or greatly modified during the Eocene. Future work will focus on the development of a new class of subduction initiation geodynamic model that can fit our observations.

Volcanic history

The Pacific Ring of Fire was created during the Eocene when subduction initiated throughout the western Pacific. In the Izu-Bonin-Mariana system, the onset of volcanic activity associated with the new subduction system started at ~52 Ma (Arculus et al., 2015b). Our proximal sites (U1507 and U1508) are located in appropriate locations to record the onset of volcanic activity in the upper Eocene and Oligocene (i.e., well after 52 Ma). Additional postexpedition analyses are required to determine the precise age and type of volcanic activity.

Paleoceanography and diagenesis

Thirty years ago and following the three previous scientific drilling expeditions to the Tasman Sea (DSDP Legs 22, 29, and 90), Kennett and von der Borch (1986) summarized the Cenozoic paleoceanography of the region. The work remains staple reading but also highlights three well-known biases within the paleoceanographic community: (1) the proportion of text that discusses the Paleogene as compared to the Neogene is approximately 26%, whereas the Paleogene represents ~65% of the combined geological time; (2) the findings come from extrapolations across a vast and poorly mapped area, but the sites were selected to minimize stratigraphic complexity; and (3) the detailed records come without full disclosure of diagenetic reactions that can modify the signal. Expedition 371 presents an opportunity to address each of these issues and for fresh interpretations and balanced perspectives on a classic region for Cenozoic climate study. We find that sediment accumulation and diagenesis across the Tasman Sea are highly variable in space and time. Some of this heterogeneity relates to tectonic history, as described above.

Quaternary sediment cycles and bryozoan fossils

Two sites hold Quaternary records amenable for paleoceanographic study. The upper section of Site U1510 on the southern Lord Howe Rise was recovered by APC coring in two holes that can be spliced together to form a 44.5 m continuous section spanning most of the late Pleistocene. The section contains calcareous ooze with obvious cycles in physical properties, such as color and grain size. Site U1508, northwest of northern New Zealand has a nearly 100 m thick Pleistocene section. Though rotary cored, layers with macroscopic fragments of bryozoans and other shallow-water organisms present an intriguing and unusual find. The site is at a "temperate carbonate" margin (Nelson and Hancock, 1984) that provides an opportunity to study coupling between sedimentology and large-amplitude variations in sea level.

Late Miocene to early Pliocene biogenic bloom

Four sites recovered carbonate-rich sediment in which to assess the so-called late Miocene–early Pliocene biogenic bloom. This phenomenon, which is recognized from sediment sections at multiple ocean drilling sites, can be described as follows: at zones of surface water divergence in the Indian and Pacific Oceans, the accumulation rates of biogenic components to the seafloor was significantly elevated between about 8 and 3 Ma. Similar to previously drilled DSDP sites from the Tasman Sea, carbonate accumulation rates rose dramatically at northern Sites U1506 and U1507 from 8 to 3 Ma. However, a condensed interval marks the stratigraphic records at southern Sites U1509 and U1510. This may indicate underlying changes in deepwater flow during the late Miocene and early Pliocene.

Eocene to Oligocene interval and presence of biogenic silica

Previous drilling in the Tasman Sea recovered little sediment that was deposited between the middle Eocene and middle Oligocene. This led to the widely accepted idea of a regional unconformity caused by intensification of deepwater currents. We apparently

recovered complete Oligocene sections at Sites U1507 and U1509 in the New Caledonia Trough, with all calcareous biozones and most polarity chrons identified at the first site. However, a hiatus of variable duration was found at shallow sites on Lord Howe Rise between the upper Eocene and upper Oligocene at Site U1508 and between the upper Eocene and middle Miocene at Site U1510. Notably, the middle Eocene through lower Oligocene interval, where found, including Site U1511 on the Tasman Abyssal Plain, contains biosilica or chert. Postexpedition effort will be placed on understanding whether these observations support unusual oceanography or a different paleogeography to that in existing computer simulations.

Regional Paleogene climate records

Several Paleogene sediment sections exposed in New Zealand and New Caledonia have become the focus of paleoclimate research. This has primarily arisen because, once placed onto accurate age models, lithologic variations at key sites, such as Mead Stream in South Island, correspond to established changes in global climate. Several Expedition 371 sites contain lithostratigraphic records where changes in sediment composition appear to correlate with those now uplifted on land. This is particularly true for Site U1508 in the Reinga Basin.

Eocene warm worlds and hyperthermals

Earth surface temperatures peaked during several time intervals of the early and middle Eocene. These events especially include the MECO (~40.5 Ma), the EECO (53–49 Ma), and a series of geological brief "hyperthermals," such as the Paleocene/Eocene Thermal Maximum (PETM; 56 Ma). These events generally were not recovered at most sites during Expedition 371. At Sites U1507 and U1508, poorly recovered horizons seem to mark the MECO. Sites U1508 and U1510 terminated near the top of the lower Eocene for reasons of operational time. At Site U1509, almost the entire early Eocene appears to have slumped on a surface approximately coincident with the PETM. It is possible that lithologic changes associated with warm events, such as clay-rich horizons and surrounding chert, make them difficult to recover in deep holes. Despite the above difficulties, an apparently complete MECO interval was recovered from the Tasman Abyssal Plain at Site U1511.

Paleocene and Maastrichtian claystones

Paleogene calcareous green claystone was found at Sites U1509 and U1511. At the former site, coring also recovered dark brown Maastrichtian claystone. Considering exposed sections on land and past drill sites in the region, Paleogene clays accumulated over a widespread area of Zealandia. At Site U1511 and some locations, these clays contain modest organic carbon.

Thermogenic gas

Routine headspace gas sampling revealed significant concentrations of light hydrocarbon gases in deep sediments at two locations. Methane concentrations began increasing below ~500 m within the middle Eocene nannofossil chalk at Site U1508 and below ~400 m within the Eocene calcareous claystone at Site U1509. At both locations, ethane and propane were also detected, although the C_1/C_2 ratio did not drop below 100. The suites of hydrocarbons measured were not classified as "anomalous" but do suggest burial of strata containing organic carbon and thermogenic hydrocarbon production in the Reinga Basin and the southern New Caledonia Trough.

Deep anaerobic oxidation of methane

Upward-migrating gas at Sites U1508 and U1509 (above) impacts pore water chemistry significantly. At both sites, dissolved sulfate concentrations steadily decrease, almost linearly, from near seawater values at some shallow depth to zero at the depth where methane concentrations begin to rise. These deep SMTs, ~500 m at Site U1508 and ~400 m at Site U1509, probably represent locations of AOM. Abundant pyrite is found in sediment near the SMTs, and dissolved Ba concentrations rise steeply beneath the SMTs. Interestingly, at Site U1508, sulfate concentrations begin decreasing at ~290 m rather than at the seafloor, possibly because of major changes in the porosity of sediment. In any case, these two Expedition 371 sites, along with a few other sites recently drilled elsewhere, significantly expand the subbottom depth range over which AOM can occur.

Sediment compaction and ooze–chalk transition

Calcareous ooze, dominantly comprising microscopic calcite shells, blankets a large area of the modern seafloor above the CCD. With time and burial, this ooze can become compacted and altered to chalk and ultimately limestone. Reduction in porosity (Figure **F13**) and lithification over the transition zone from ooze to chalk has long fascinated the marine geoscience community, as it affects the velocity of seismic waves, the recovery of core, and the nature of calcareous components. Analysis of previous DSDP drilling emphasized the complex nature of the ooze–chalk transition in the Tasman Sea. Cores and data from Expedition 371 provide new empirical data to quantify relationships between sediment composition, burial history, compaction, and diagenesis and may help clarify our understanding of the underlying processes. The ooze–chalk transition was found at approximately 235, 290, 200, 55, and 150 m at Sites U1506, U1507, U1508, U1509, and U1510, respectively. The very shallow transition in middle Miocene sediment at Site U1509 probably reflects missing overburden that was lost by slumping. The other depths appear related to differences in age, compaction, and sediment composition.

Iron oxide and copper mineralization

Vivid red-orange (2.5YR 5/6) claystone and native copper surrounded by dark green halos were found in multiple intervals of lower Eocene sediment at Site U1511. The striking color of the claystones comes from hematite, as determined from rock magnetic properties. Although the thickest and most striking horizon approximately coincides with the EECO (see above), both observations and theoretical arguments suggest the unusual mineralogy is not primary but the product of alteration. Presumably, saline fluids lacking dissolved oxygen and sulfur but carrying dissolved iron and copper precipitated minerals as they passed through the sediment, perhaps along fractures. Notably, seismic profiles show that Eocene and older strata at the site are folded and faulted. Native copper has been described at previous scientific drill sites, and a commonality seems to be proximal folding and faulting.

Rotary drilling and pore water collection

Coring with the APC system in multiple holes and the construction of spliced records has become a common approach for drilling expeditions with paleoceanography or biogeochemistry objectives. To achieve the Expedition 371 goals, which required deep drilling (and ultimately within a significantly shortened time window), the sedimentary records at most sites were recovered mostly in one

hole, often using the RCB system. Although not ideal, good first-order sedimentary records and pore water profiles could be generated at most sites. Notably, at sites where intervals were cored using both the XCB and RCB methods, the latter generally gave better quality cores in a shorter time period. To obtain reasonably good and detailed pore water profiles with minimal impact to the sedimentary record, Rhizon samples were taken at some sites and squeeze samples were taken from the bases of core Sections 1, 6, or both. Such sampling generally avoids splice intervals (i.e., the core gaps created by IW sampling fall into "off-splice" intervals).

Operations

Port call

Expedition 371 started at 0812 h (all times are UTC + 10 h) on 27 July 2017 with the first line ashore at Wharf 10 in Townsville, Australia. The Co-Chief Scientists and IODP staff moved onto the ship and began port call activities, including meetings with the offgoing staff and discharging and receiving cargo.

The rest of the Expedition 371 scientists boarded the ship in the morning of 28 July and, after checking into their cabins, received various introductory presentations as well as laboratory safety tours. The Siem Offshore crew change was completed. Fresh food and other catering supplies were loaded on board. Three public ship tours were held. Toward the end of the day, we began loading 450 metric tons of marine gas oil, which was transported alongside by trucks and then pumped on board.

Fueling was finished at 0100 h on 29 July. We made progress on the subsea camera hydraulic system upgrade but were not able to complete it during this short port call. The Expedition 371 scientists received several presentations, including an introduction to the project science from the Co-Chief Scientists, an overview of the education and outreach (E&O) plans from the two E&O Officers aboard, and an introduction to the expedition work plan from the Expedition Project Manager (EPM). The Captain and other senior Siem Offshore personnel met with the scientists and provided ship safety information. The EPM then led the scientists on laboratory tours for an overview of scientific equipment, procedures, and work responsibilities. The passage plan for the expedition transits was completed and arrangements were made with the agent and immigration for a departure at 0700 h on 30 July.

The ship left Townsville with the last line released at 0712 h on 30 July. The first fire and life boat safety drill was held for all aboard. The Co-Chief Scientists and EPM met with each laboratory team to discuss requirements, tasks, and issues, and the teams began to prepare for their work.

Site U1506

Hole locations, water depths, and the number of cores recovered are listed in Table **T1**. All times are local ship time (UTC + 10 h). All depth references in meters in this section refer to the DSF depth scale, unless noted otherwise.

Site U1506 was the first site occupied during Expedition 371. After an 1167 nmi transit from Townsville, Australia, the ship arrived at Site U1506 at 1912 h on 3 August 2017. The thrusters were lowered and the dynamic positioning system was engaged. At 1948 h, the drill floor was cleared for operations, beginning Hole U1506A. At 2033 h, a seafloor positioning beacon was deployed.

The RCB BHA was assembled and deployed. All drill string tubulars were strapped and drifted during the pipe trip. The top drive was picked up and a wiper "pig" was pumped through the drill string to clean debris from the inside of the drill string prior to coring. The core barrel was deployed and Hole U1506A was spudded at 0600 h on 4 August.

The seafloor depth was determined to be 1505.8 m drilling depth below rig floor (DRF) based on tagging it with the drill string, establishing a water depth of 1495 m. RCB coring proceeded at 9.5–9.7 m intervals through Core 28R (263.1 m). Core 29R encountered the expected hard formation at ~265 m. We recovered cores in half intervals (4.5–5.0 m length) below this depth to minimize the risk of core loss due to jams in the bit or inner barrel. We obtained an average core recovery of 76% in this depth interval.

We decided to stop coring after Core 36R, which arrived on the rig floor at 1345 h on 5 August. Total recovery for the 306.1 m drilled in Hole U1506A was 192.38 m (63%). A single 15 barrel mud sweep of high-viscosity gel mud was pumped during drilling in this hole. The drill string was retrieved, disassembled, and inspected; the acoustic beacon was recovered; and the rig floor was secured for transit, ending Hole U1506A operations at 1935 h. The time spent on Hole U1506A (and Site U1506) was 47.75 h or 2.0 days.

At 2000 h we departed for Site U1507.

Site U1507

Hole locations, water depths, and the number of cores recovered are listed in Table **T1**. All times are local ship time (UTC + 10 h). All depth references in meters in this section refer to the DSF depth scale, unless noted otherwise.

The 286 nmi transit from Site U1506 concluded with the arrival at Site U1507 at 2200 h on 6 August 2017. After lowering the thrusters and switching to dynamic positioning mode, the rig floor was cleared for operations, beginning Hole U1507A at 2225 h. The rig crew assembled an APC/XCB BHA by 0130 h on 7 August, picked up drill pipe and the top drive, and deployed the bit just above the seafloor. A wiper pig was pumped through the drill string to clean out potential debris. The nonmagnetic APC core barrels were dressed with core liners in preparation to spudding Hole U1507A at 1040 h.

The mudline core recovered 6.2 m, establishing a water depth of 3568 m. APC coring continued to Core 26H. Given the force required to retrieve the last few APC cores and the overdrilling required on Core 26H, we switched to XCB coring at 1815 h on 8 August. Given the depth objectives for Site U1507 (>700 m), we decided against using the more time consuming half-APC coring system. Recovery of Cores 1H through 26H ranged from 99% to 106% and averaged 104% (total of 243.7 m cored and 252.7 m recovered). Temperature measurements were taken with Cores 4H, 7H, 10H, 13H, 16H, and 19H. The deployment of orientation and temperature tools was discontinued after Core 20H.

Coring continued in Hole U1507A with the XCB system. Toward the end of 9 August (at ~425 m) it took ~100–150 min to cut a core. Moreover, the quality of the cores was poor, with prominent biscuiting and abundant fracturing. At 0000 h, we decided to terminate Hole U1507A, pull the drill string, and start an RCB hole at the depth where XCB coring became particularly difficult (~375 m). Recovery for the XCB cores varied from 6% to 97% and averaged 55% (total of 181.7 m cored and 100.1 m recovered). The drill string was retrieved from Hole U1507A and cleared the rig floor at 0940 h on 10 August, ending Hole U1507A. The time spent on Hole U1507A was 83.25 h or 3.5 days.

The ship was offset 20 m to the east of Hole U1507A. An RCB BHA was made up with a center bit installed in the core barrel that would allow us to drill without coring for the first 375 m. We in-

cluded a mechanical bit release (MBR) that would allow us to drop the bit at the bottom of the hole and then wireline log without retrieving the entire drill string. Drill pipe was deployed, and by 1800 h on 10 August the bit was just above the seafloor. After picking up the top drive, we pulled the core barrel with center bit and pumped a wiper pig through the drill string to clean out debris observed during drill string assembly. The core barrel with center bit was then dropped back in place and drilling in Hole U1507B began at 2045 h on 10 August. Drilling without coring in Hole U1507B reached 376 m by 0630 h on 11 August. The center bit was removed from the core barrel, and coring began at 0730 h and concluded at 1000 h on 17 August. Cores 2R through 53R penetrated from 376.0 to 864.4 m with a total recovery of 371.5 m (76%). Recovery for the RCB cores varied between 1% and 109%. Importantly, the quality of the RCB cores was superior to those collected by XCB drilling over the 50 m overlap interval. Mud sweeps were pumped for hole cleaning on every third core starting with Core 8R. At the end of coring, Hole U1507B was cleaned with a 25 barrel high-viscosity mud sweep in preparation for logging.

Wireline logging began with a wireline trip for the rotary shifting tool (RST) to activate the MBR and drop the coring bit at the bottom of the hole. The bit was released at 1130 h on 17 August. The RST was recovered, and a second wireline trip was conducted with the reverse RST to reposition the MBR sleeve into the circulating position. The tool was recovered and the sinker bars removed. From 1230 to 1315 h, the hole was displaced with 245 barrels of 11.0 ppg mud. The top drive was set back, the end of drill pipe was raised to the logging depth of 75.2 m, and the rig floor was prepared for logging.

Assembly of the modified triple combo logging tool string began at 1700 h. The tool string included MS, electrical resistivity, sonic, bulk density, and NGR tools. The neutron porosity tool often run in the triple combo and the microresistivity imaging (Formation MicroScanner) tool, often run in a separate string together with the sonic tool, were omitted from the logging plan for this hole. The tools were assembled and tested at 1815 h and the tool string was lowered into Hole U1507B.

The wireline active heave compensator was switched on once the tools reached open hole. A downhole log was performed from just above the seafloor to the bottom of the hole at ~864 m WSF. The hole was then logged up for a 124 m calibration pass, run back to the bottom, and logged up to just below the end of the pipe where the caliper was closed prior to entering the BHA. The tools were pulled from the hole and were back at the surface at 0200 h on 18 August. By 0345 h, all logging equipment was rigged down and the rig crew began retrieving the drill string.

Hole conditions were excellent for logging, with a hole diameter close to the bit diameter (~10 inches) all the way from the bottom of the hole (846.4 m WSF) to ~490 m WSF. Hole conditions were still good up to 234 m WSF, where a bridge with a hole diameter of only ~6 inches was encountered. Additional bridges were indicated in the caliper log further uphole and just below the base of the drill string. The tool string passed these obstructions successfully and acquired high-quality measurements throughout the open hole. However, several hours of remediation work (washing) would have been required before the Versatile Seismic Imager (VSI) tool could have been run as planned, with limited chance of success, significant daylight time restrictions, and a poor weather forecast. Given the quality of the standard logs, particularly the sonic log, the primary logging scientific objective of tying cores to seismic reflection images had been substantially achieved, so we canceled the VSI run.

While the drill string was recovered, the seafloor positioning beacon was released and recovered. With bad weather expected during the transit to the next site, the drill collars were disassembled and secured in the drill collar rack. At 1130 h on 18 August, the end of the drill string cleared the rig floor. The rig floor was secured for transit at 1150 h, ending Hole U1507B and Site U1507. A total of 194 h or 8.1 days were spent on Hole U1507B.

While raising the thrusters, a hydraulic malfunction occurred and was repaired, and the transit to Site U1508 began at 1330 h on 18 August.

Site U1508

Hole locations, water depths, and the number of cores recovered are listed in Table **T1**. All times are local ship time (UTC + 10 h for Holes U1508A and U1508B and UTC + 11 h for Hole U1508C). All depth references in meters in this section refer to the DSF depth scale, unless noted otherwise.

We completed the 546 nmi transit from Site U1507 to Site U1508 at an average speed of 9.5 kt and arrived at 2300 h on 20 August 2017. Thrusters and hydrophones were lowered for dynamic positioning and the rig floor was cleared for operations at 2342 h. At 0130 h on 21 August, we deployed an acoustic beacon for hole positioning. An APC/XCB BHA was made up and the drill string was assembled and deployed to just above the seafloor. The top drive was installed, and the nonmagnetic core barrels dressed with core liners and the orientation tool were deployed. APC coring in Hole U1508A started at 0900 h on 21 August.

After shooting Core 10H at 1520 h, the core line parted just above the sinker bar. The wireline was cut and a new rope socket was installed. An RCB core barrel was dressed with a fishing shoe, and by 1800 h on 21 August the sinker bars and core barrel with Core 10H had been recovered in two wireline trips.

Use of the core orientation tool was postponed until we cut Core 13H because of sandy hole conditions and was discontinued after Core 17H because of unstable hole conditions. Temperature measurements were taken on Cores 7H, 9H, 10H, 12H, 14H, and 17H.

Core 23H had to be drilled over for 40 min to release it from the formation. At 0600 h on 22 August, we started to retrieve the drill string and the bit cleared the rig floor at 1140 h, ending Hole U1508A. Total recovery for the 210.3 m cored in Hole U1508A was 201.13 m (96%). The time spent on Hole U1508A was 36.0 h or 1.5 days.

The ship was offset by ~20 m to the southwest. An RCB BHA was made up and deployed, and the drill pipe was assembled until the bit was just above the seafloor. The top drive was picked up and drilling without coring in Hole U1508B started at 1745 h on 22 August, with a center bit installed in the core barrel. At ~75 m, the drill string became stuck while making a connection. After pumping a mud sweep, we were able to free the drill string. A total of 85 barrels of mud were pumped for the next ~100 m of drilling. Drilling ahead without coring reached the target (186.6 m) at 2245 h on 22 August, the center bit was retrieved, and an RCB core barrel was dropped to begin coring with Core 2R. After achieving low recovery on Cores 23R through 25R and reaching a zone of particular science interest at ~417 m, we decided to cut half cores for Cores 26R through 33R. When recovery began to improve, we switched back to full-length cores with Core 34R.

RCB coring continued to Core 38R (503.4 m), when at 0700 h on 24 August a medical emergency was declared and drill string recovery began. Cores 2R through 38R penetrated from 186.6 to 503.4 m and recovered 133.32 m (42%). Mud sweeps were pumped for hole

cleaning on every third core starting with Core 5R. Core recovery varied from 3% to 104% throughout Hole U1508B.

The acoustic beacon was released and recovered, the drill string was retrieved and set back in the derrick, and the rig floor was secured, ending Hole U1508B at 1320 h on 24 August. The time spent on Hole U1508B was 49.5 h or 2.1 days.

After securing the rig floor for transit, the hydrophones and thrusters were raised and the 302 nmi transit to Auckland began at 1354 h on 24 August. The clocks were advanced 1 h for the first time at 1400 h, and a second time at 0200 h on 25 August. We arrived at the dock in Auckland at 2106 h on 25 August (UTC + 12 h). The medical evacuee, accompanied by two doctors and the port agent, and a crew member disembarked. The ship left Auckland at 0218 h on 26 August to return to Site U1508. The clock was set back 1 h during the transit (UTC + 11 h) and remained that way for the remainder of the Expedition 371 drilling operations. We completed the 302 nmi transit at an average speed of 10.9 kt and arrived at 0600 h on 27 August. Dynamic positioning was established and the drill floor was cleared for operations at 0712 h. The RCB BHA was assembled and deployed to the seafloor and Hole U1508C was initiated ~20 m northwest of Hole U1508B at 1150 h, with a center bit installed in the core barrel.

The plan was to drill to ~480 m, ~20 m above total depth of Hole U1508B, and resume coring. We also decided to spot core two scientifically interesting intervals that had particularly low recovery in Hole U1508B. After drilling without coring to 278 m, we pulled the center bit and collected core from 278 to 292.6 m (Cores 2R through 4R) at half-core intervals. The center bit was deployed again to drill ahead from 292.6 to 316.0 m before cutting a half core and a full core (6R and 7R) from 316.0 to 330.7 m. The center bit was deployed again and drilling without coring advanced from 330.7 to 450.0 m. At 0730 h on 28 August, we retrieved the center bit and resumed RCB coring until penetration rates slowed to ~2 m/h. Although short of the desired target depth, at 0300 h on 31 August we decided to stop coring and conduct wireline logging. Collectively, Cores 2R through 38R, and the two interspersed drilled intervals, penetrated from 278.0 to 704.5 m and recovered 185.04 m of sediment (65% of cored intervals).

At the end of coring, the hole was cleaned with a 30 barrel high-viscosity mud sweep. Next, the RST was deployed to trigger the MBR and drop the bit at the bottom of the hole (0325 h). The reverse RST was deployed to shift the MBR sleeve back into the circulation position (0430 h). Next, the hole was displaced with 194 barrels of 11.0 ppg mud and the end of the drill string was set at 86.7 m. An additional 10 barrels of mud were pumped to ensure the entire hole was displaced with heavy mud.

At 0745 h on 31 August, assembly of the modified triple combo logging tool string began. This was the same configuration as used in Hole U1507B with the exception that no source was installed in the density tool. The logging tools were deployed at 0900 h and data were collected while lowering the tool string to the bottom of the hole. After logging up 128 m for a calibration run, the tools were run back to the bottom of the hole and the main logging pass began. At ~1230 h, the tool string became stuck at ~270 m WSF. The logging line was cut at the rig floor and terminated with connectors that would allow assembly of drill pipe over the logging line to wash down and over the logging tools with the open-ended BHA. The logging tools were free at 2105 h. The tool was pulled to 155 m WSF using the T-bar procedure, when sufficient logging line had been retrieved to make a connection with the aft coring line, which was used to pull the logging tools to the surface. The logging tools were recovered and cleaned by 0315 h on 1 September. The drill string was recovered and the end of pipe cleared the rig floor at 0650 h. The positioning beacon was recovered, the rig floor was secured for transit, the thrusters and hydrophones were raised, and the transit to Site U1509 began at 0730 h on 1 September.

Site U1509

Hole locations, water depths, and the number of cores recovered are listed in Table **T1**. All times are local ship time (UTC + 11 h). All depth references in meters in this section refer to the DSF depth scale.

We arrived at Site U1509 at 0630 h on 2 September 2017, completing the 273 nmi transit from Site U1508. After lowering thrusters and hydrophones and establishing dynamic positioning, the rig floor was cleared for operations at 0700 h. While the RCB BHA was being assembled, a seafloor positioning beacon was deployed. The drill string was deployed to just above the seafloor and the top drive was engaged. A wiper pig was pumped through the drill pipe in an attempt to remove excessive rust observed during drill string assembly.

Coring in Hole U1509A began at 1825 h on 2 September and continued until 2345 h on 6 September to a total depth of 690.7 m (Core 74R). The hole was cleaned with 10–15 barrel mud sweeps, which were pumped on every third core for Cores 9R through 49R. Starting with Core 50R the frequency and volume of mud sweeps were increased to every other core and 20–25 barrels, respectively. Total recovery in Hole U1509A was 462.86 m (67%).

In preparation for logging, Hole U1509A was cleaned with a 30 barrel high-viscosity mud sweep. The RST was deployed to trigger the MBR and drop the bit at the bottom of the hole (0015 h on 7 September). The reverse RST was deployed to shift the MBR sleeve back into the circulation position (0145 h). Next, the hole was displaced with 214 barrels of 10.5 ppg mud, the top drive was set back, and the drill string was pulled back to the logging depth of 81 m (0530 h). The modified triple combo logging tool string was rigged up when at 0645 h the operational decision was made to stop logging operations based on ship heave exceeding 3.0 m. The drill string was retrieved and the rig was secured for transit by 1434 h, ending Hole U1509A and Site U1509. A total of 127.5 h or 5.3 days were spent on Hole U1509A. After recovering the seafloor positioning beacon and retrieving positioning thrusters and hydrophones at 1630 h on 7 September, the ship began the ~200 nmi transit to the north to avoid severe weather that was forecast for 9–10 September at the remaining proposed drilling sites.

Site U1510

Hole locations, water depths, and the number of cores recovered are listed in Table **T1**. All times are local ship time (UTC + 11 h). All depth references in meters in this section refer to the DSF depth scale.

After the 380 nmi transit in heavy winds and seas from a waiting on weather location, the ship arrived at Site U1510 at 0918 h on 12 September 2017. The thrusters were lowered, dynamic positioning was established, and the drill floor was cleared for operations at 0936 h. No seafloor positioning beacon was deployed at this site.

An APC/XCB BHA was assembled and deployed. After the first 7 stands of drill pipe were added, the iron roughneck clamping valve refused to unclamp from the drill pipe. While the repair was taking place, drill pipe assembly continued using the rig tongs instead of the iron roughneck for the next 23 stands. When the iron roughneck repair was complete, the remaining 8 stands of drill pipe were

run. The top drive was picked up, the nonmagnetic core barrels were dressed with core liners, and the orientation tool was installed. Coring in Hole U1510A started at 1915 h on 12 September.

APC coring continued through Core 17H, which stroked out only ~3 m because the cutting shoe impacted a chert layer. At 0645 h on 13 September, we decided to switch to XCB coring. We stopped deploying the orientation tool after Core 15H. Temperature measurements were taken on Cores 4H, 7H, 10H, 13H, and 17H. The APC cored interval penetrated from 0 to 150.5 m and recovered 147.9 m (98%).

XCB coring continued until 1930 h on 14 September. Cores 18X through 52X penetrated from 150.5 to 483.4 m and recovered 108.1 m (32%). Recovery was compromised seriously because of frequent chert layers.

Coring in Hole U1510A concluded with a total penetration of 483.4 m and total recovery of 260.0 m (53%). The drill pipe was retrieved from Hole U1510A, clearing the rig floor at 2135 h on 14 September and ending Hole U1510A. The time spent on Hole U1510A was 60 h or 2.5 days.

The ship was offset 20 m to the east and APC coring in Hole U1510B began at 2300 h on 14 September with Core 1H and ended at 0215 h on 15 September with Core 7H. Nonmagnetic core barrels were used for Cores 1H through 7H and a single APCT-3 temperature measurement was taken on Core 7H. Cores 1H through 7H penetrated from 0 to 66.3 m and recovered 64.7 m (98%). The drill string was recovered and the rig floor was secured for transit at 0815 h, ending Hole U1510B and operations at Site U1510. The time spent on Hole U1510B was 10.75 h or 0.4 days.

The thrusters were raised and at 0842 h on 15 September the ship began the transit to Site U1511.

Site U1511

Hole locations, water depths, and the number of cores recovered are listed in Table **T1**. All times are local ship time (UTC + 11 h). All depth references in meters in this section refer to the DSF depth scale.

The ship completed the 216 nmi transit from Site U1510 at an average speed of 7.7 kt and arrived at Site U1511 at 1248 h on 16 September 2017. The thrusters were lowered and dynamic positioning was established. No acoustic beacon was deployed at Site U1511.

Logging was eliminated from the operations plan following the stuck logging tool incident earlier in the cruise. After losing ~2000 m of logging wireline, we could no longer reach the combination of water depth and hole depth to log Site U1511.

Operations in Hole U1511A began at 1334 h on 16 September with the assembly of an RCB BHA. Drill pipe assembly was completed at 0245 h on 17 September and a wiper pig was pumped through the pipe to clean out potential debris. RCB coring in Hole U1511A began at 0425 h. After retrieving Core 3R at 0810 h, we had to pull the drill string clear of the seafloor due to excessive heave and wind. Cores 1R through 3R penetrated from 0 to 26.6 m and recovered 7.9 m (30%). A total of 19.25 h or 0.8 days were spent on Hole U1511A.

After waiting from 0845 h on 17 September to 0145 h on 18 September (17 h) for the weather to improve, with the drill string suspended just above the seafloor, we began Hole U1511B by washing down (i.e., drilling without coring and without a center bit installed) to 19.8 m, near the total depth of Hole U1511A (26.6 m). We resumed coring from 0215 to 1015 h on 18 September and Cores 2R through 7R penetrated from 19.8 to 77.2 m. At 1015 h, we deployed a center bit and drilled without coring from 77.2 to 192.2 m to accelerate penetration and reach the target depth in the time remaining for operations on Expedition 371. At 1500 h on 18 September, we resumed coring and Cores 9R through 41R penetrated from 192.2 to 508.8 m. At 1630 h on 20 September, coring was suspended due to excessive heave and the drill string was raised ~37 m above the bottom of the hole (472 m), while maintaining circulation and rotation in the hole. While waiting for the weather to improve, the ship was having difficulties maintaining position. At 0315–0630 h on 21 September, the drill string was raised to 163 mbsf as a precaution. As the swell began to subside, the drill string was lowered back to the bottom of the hole at 1030–1400 h. After pumping a 25 barrel mud sweep and recovering the wash barrel, coring resumed at 1600 h on 21 September, following 23.5 h of waiting, and ended with the recovery of the last core (47R) at 0450 h on 22 September.

During the course of drilling and coring in Hole U1511B, a total of 265 barrels of high-viscosity mud were pumped in 15–20 barrel mud sweeps for hole cleaning. The cored interval was 431.4 m and recovery was 279.3 m (65%). The two intervals drilled without coring amount to 134.8 m.

The rig floor was secured for transit to Hobart at 1630 h on 22 September, ending Hole U1511B and Site U1511. A total of 110.75 h or 4.6 days were spent on Hole U1511B. The total time spent at Site U1511 was 130.0 h or 5.4 days. This included 40.5 h lost because of weather.

Expedition 371 ended with the first line ashore at 0930 h on 26 September.

Education, outreach, and media

E&O immediately before, during, and immediately after an IODP expedition present a wonderful but challenging aspiration. Clearly, media exposure helps the broad public to understand the necessity of ocean drilling.

The current IODP framework importantly includes an E&O component. However, the translation of these efforts to maximize science impact remains uncertain.

Expedition 371 received special media attention, in part because a paper entitled “Zealandia: Earth’s Hidden Continent” (Mortimer et al., 2017) was widely circulated in media and its basic contents were widely read across the globe before the expedition. Anticipating high media attention, we thought to have two education and outreach personnel (a teacher and a videographer) with somewhat overlapping work-shifts and also to document the experience.

Video conferencing

A total of 52 ship to shore video links were established with 41 different international education institutions: 22 in the USA, 22 in Australia, 4 in New Zealand, and 5 in Europe and South America. Approximately 2600 students and teachers participated (Table **T2**). In addition, 8 video links were made with media outlets that reached an audience exceeding 100,000 (Table **T2**).

Other conferencing events

ABC filmed three ship to shore links with the goal of compiling a documentary on the *JOIDES Resolution* education and outreach program run by IODP:

Pascack Hills High School, New Jersey, USA
Monterey Peninsula, California, USA
Pennsylvania State College, Pennsylvania, USA

Education projects completed at sea

- A senior high school task was prepared with the topic of interpreting a sedimentary sequence from drill hole data and reconstructing a terrestrial Cretaceous landscape. Students determine what major tectonic events may have occurred for the present sequence to have subsided into a marine sedimentary basin.
- A lower to middle primary school task was prepared with the topic of interviewing a geoscientist and looking at how they travel back through time to recreate a paleolandscape.

Videography

The videographer operated the camera for all Zoom sessions and assisted in social media posting by delivering photos and videos and setting up scientists with accounts for posting blogs.

Seven video clips were uploaded to YouTube and the *JOIDES Resolution* website (Table **T3**). These videos cover different topics from leaving port in Townsville, drone footage of the ship, and the drilling and core sampling process. The video titled "Exploring Zealandia" has reached more than 4900 acknowledged views so far since being uploaded. During the expedition, 15 interviews with scientists, technical staff, and the drill crew also were recorded.

Media impact

Expedition 371 had significant media activity (international TV, radio, web, and newspapers) associated with both port calls. A full analysis of the Townsville port call was not attempted, but a brief search of Google News and an analysis done for GNS Science identified >150 media stories that reached an audience of at least two million people (Table **T4**). Stories ran in the major newspapers of many countries (e.g., New York Times, Le Figaro, Vangardia, Sydney Morning Herald, etc.). Both Co-Chief Scientists and several of the scientists wrote stories and/or communicated with journalists numerous times during the expedition (e.g., the story written by Sutherland in *The Conversation* obtained 20,000 views in the week it was written; and was republished by media organizations).

It was a challenge for the Co-Chief Scientists and many of the scientists involved to manage the time involved in outreach activities and to monitor/quantify the very high levels of media interest during the expedition. Certainly, two people are needed to conduct appropriate E&O activities during IODP expeditions with heavy media attention. This is in part because, at a basic level, one person needs to film and one person needs to interview. How the overall effort should be balanced between a focus on small intimate groups or a focus on large generic populations is a great question. We also acknowledge interesting problems in terms of assessment, namely that a video might be downloaded and presented elsewhere (e.g., in a classroom environment) so as to be seen by many, but a more personal contact might impact an individual to become the next great oceanographer.

Preliminary scientific assessment and further work

The primary drilling objectives of the expedition were mostly completed. All six sites provide new regional stratigraphic and paleogeographic information that can be put into regional context through seismic-stratigraphic interpretation and hence provide strong constraints on geodynamic models of subduction zone initiation. Our new observations can be related directly to the timing of plate failure, the magnitude and timing of vertical motions, and the timing and type of volcanism.

Secondary paleoclimate objectives were not completed as planned for three primary reasons: (1) the selected sites targeted tectonic objectives, (2) the stratigraphy in this vast region is (with hindsight) more complicated than predicted, and (3) complications due to weather and other unforeseen factors. Nonetheless, significant new records of southwest Pacific oceanography and climate in the past were obtained. Sediments that were cored were more indurated and diagenetically altered than expected. Core recovery was poorer than expected. Operational issues resulted in a lack of time, and hence it was not possible to build spliced intervals. Notably, strata deposited during Eocene hyperthermal events were systematically poorly recovered, even when recovery was good above and below. This was possibly due to higher clay and lower carbonate content (based on wireline logs at Sites U1507 and U1508). We recovered a MECO section at Site U1511, but the site is affected by diagenesis and fluid-mediated reactions. Site U1511 also appears barren of organic carbon suitable for biomarker analysis and has little biogenic carbonate preserved. Miocene sediment that was recovered provides a useful supplement to material collected during Leg 90. A Pliocene–Quaternary spliced section at Site U1510 has orbital cycles evident in physical properties and may provide a significant climate record at a key location.

All sites were cored to near planned target depths, but operations did not go precisely as anticipated. The original plan included 3.0 days of port call, 12.5 days of transit, and 45.5 days of operations. We lost operational time due to weather, longer transits than planned, stuck logging tools, and a medical emergency, leaving a total of 36.4 days of on-site operations. The breaks in drilling resulted in lower overall efficiency due to time spent tripping drill pipe and re-establishing coring (e.g., through starting a new hole and drilling down with overlap). Wireline logging tools became stuck at Site U1508 and required 2 km of logging cable to be cut from the winch, which meant it was impossible to log subsequent Site U1511 due to the water depth. Our logging program was abandoned due to sea conditions at Sites U1509 and U1510. We intended to double APC/XCB core at four sites, but a combination of time pressure and hard sediments made this impossible at any site. Despite these operational challenges, the first-order results obtained are highly significant and Expedition 371 can be considered a success.

Regional stratigraphy resulting from Expedition 371 creates a new framework for understanding the continent of Zealandia, the onshore geology of New Caledonia and New Zealand, and sediment cores collected at DSDP sites in the region. Our results likely will influence a wide range of future studies and provide a new basis for understanding fundamental processes of plate tectonics and paleoclimate.

References

Adams, C.J., Cluzel, D., and Griffin, W.L., 2009. Detrital-zircon ages and geochemistry of sedimentary rocks in basement Mesozoic terranes and their cover rocks in New Caledonia, and provenances at the Eastern Gondwanaland margin. *Australian Journal of Earth Sciences,* 56(8):1023–1047. **https://doi.org/10.1080/08120090903246162**

Aitchison, J.C., Ali, J.R., and Davis, A.M., 2007. When and where did India and Asia collide? *Journal of Geophysical Research: Solid Earth,* 112(B5):B05423. **https://doi.org/10.1029/2006JB004706**

Aitchison, J.C., Clarke, G.L., Meffre, S., and Cluzel, D., 1995. Eocene arc-continent collision in New Caledonia and implications for regional southwest Pacific tectonic evolution. *Geology,* 23(2):161–164. **https://doi.org/10.1130/0091-7613(1995)023<0161:EAC-CIN>2.3.CO;2**

Aitchison, J.C., Ireland, T.R., Clarke, G.L., Cluzel, D., Davis, A.M., and Meffre, S., 1998. Regional implications of U/Pb SHRIMP age constraints on the tectonic evolution of New Caledonia. *Tectonophysics,* 299(4):333–343. **https://doi.org/10.1016/S0040-1951(98)00211-X**

Andrews, P.B, Gostin, V.A., Hampton, M.A., Margolis, S.V., and Ovenshine, A.T., 1975. Synthesis—sediments of the Southwest Pacific Ocean, Southeast Indian Ocean, and South Tasman Sea. *In* Kennett, J.P., Houtz, R.E. et al., *Initial Reports of the Deep Sea Drilling Project,* 29: Washington, DC (U.S. Govt. Printing Office), 1147–1153. **https://doi.org/10.2973/dsdp.proc.29.143.1975**

Andrews, P.B., and Ovenshine, A.T., 1975. Terrigenous silt and clay facies: deposits of the early phase of ocean basin evolution. *In* Kennett, J.P., Houtz, R.E. et al., *Initial Reports of the Deep Sea Drilling Project,* 29: Washington, DC (U.S. Government Printing Office), 1049–1063. **https://doi.org/10.2973/dsdp.proc.29.131.1975**

Arculus, R.J., Ishizuka, O., Bogus, K., Aljahdali, M.H., Bandini-Maeder, A.N., Barth, A.P., Brandl, P.A., do Monte Guerra, R., Drab, L., Gurnis, M.C., Hamada, M., Hickey-Vargas, R.L., Jiang, F., Kanayama, K., Kender, S., Kusano, Y., Li, H., Loudin, L.C., Maffione, M., Marsaglia, K.M., McCarthy, A., Meffre, S., Morris, A., Neuhaus, M., Savov, I.P., Sena Da Silva, C.A., Tepley, F.J., III, van der Land, C., Yogodzinski, G.M., and Zhang, Z., 2015a. Expedition 351 summary. *In* Arculus, R.J., Ishizuka, O., Bogus, K., and the Expedition 351 Scientists, *Proceedings of the International Ocean Discovery Program, Expedition 351: Izu-Bonin-Mariana Arc Origins:* College Station, TX (International Ocean Discovery Program). **https://doi.org/10.14379/iodp.proc.351.101.2015**

Arculus, R.J., Ishizuka, O., Bogus, K.A., Gurnis, M., Hickey-Vargas, R., Aljahdali, M.H., Bandini-Maeder, A.N., et al., 2015b. A record of spontaneous subduction initiation in the Izu-Bonin-Mariana arc. *Nature Geoscience,* 8:728–733. **https://doi.org/10.1038/ngeo2515**

Bache, F., Mortimer, N., Sutherland, R., Collot, J., Rouillard, P., Stagpoole, V., and Nicol, A., 2014. Seismic stratigraphic record of transition from Mesozoic subduction to continental breakup in the Zealandia sector of eastern Gondwana. *Gondwana Research,* 26(3–4):1060–1078. **https://doi.org/10.1016/j.gr.2013.08.012**

Bache, F., Sutherland, R., Stagpoole, V., Herzer, R., Collot, J., and Rouillard, P., 2012. Stratigraphy of the southern Norfolk Ridge and the Reinga Basin: a record of initiation of Tonga–Kermadec–Northland subduction in the southwest Pacific. *Earth and Planetary Science Letters,* 321–322:41–53. **https://doi.org/10.1016/j.epsl.2011.12.041**

Baldwin, S.L., Rawling, T., and Fitzgerald, P.G., 2007. Thermochronology of the New Caledonian high-pressure terrane: implications for middle Tertiary plate boundary processes in the southwest Pacific. *Special Paper—Geological Society of America,* 419:117–134. **https://doi.org/10.1130/2006.2419(06)**

Barron, E.J., 1987. Eocene Equator-to-pole surface ocean temperatures: a significant climate problem? *Paleoceanography,* 2(6):729–739. **https://doi.org/10.1029/PA002i006p00729**

Baur, J., Sutherland, R., and Stern, T., 2014. Anomalous passive subsidence of deep-water sedimentary basins: a prearc basin example, southern New Caledonia Trough and Taranaki Basin, New Zealand. *Basin Research,* 26(2):242–268. **https://doi.org/10.1111/bre.12030**

Becker, T.W., and O'Connell, R.J., 2001. Predicting plate velocities with mantle circulation models. *Geochemistry, Geophysics, Geosystems,* 2(12):1060. **https://doi.org/10.1029/2001GC000171**

Beerling, D.J., and Royer, D.L., 2011. Convergent Cenozoic CO_2 history. *Nature Geoscience,* 4(7):418–420. **https://doi.org/10.1038/ngeo1186**

Bijl, P.K., Schouten, S., Sluijs, A., Reichart, G.-J., Zachos, J.C., and Brinkhuis, H., 2009. Early Palaeogene temperature evolution of the southwest Pacific Ocean. *Nature,* 461(7265):776–779. **https://doi.org/10.1038/nature08399**

Billen, M.I., and Gurnis, M., 2005. Constraints on subducting plate strength within the Kermadec Trench. *Journal of Geophysical Research: Solid Earth,* 110(B5):B05407. **https://doi.org/10.1029/2004JB003308**

Brinkhuis, H., Schouten, S., Collinson, M.E., Sluijs, A., Sinninghe Damsté, J.S., Dickens, G.R., Huber, M., et al., 2006. Episodic fresh surface waters in the Eocene Arctic Ocean. *Nature,* 441(7093):606–609. **https://doi.org/10.1038/nature04692**

Browne, G.H., Lawrence, M.J.F., Mortimer, N., Clowes, C.D., Morgans, H.E.G., Hollis, C.J., Beu, A.G., Black, J.A., Sutherland, R., and Bache, F., 2016. Stratigraphy of Reinga and Aotea basins, NW New Zealand: constraints from dredge samples on regional correlations and reservoir character. *New Zealand Journal of Geology and Geophysics,* 59(3):396–415. **https://doi.org/10.1080/00288306.2016.1160940**

Brummer, G.J.A., and van Eijden, A.J.M., 1992. "Blue-ocean" paleoproductivity estimates from pelagic carbonate mass accumulation. *Marine Micropaleontology,* 19(1–2):99–117. **https://doi.org/10.1016/0377-8398(92)90023-D**

Bryan, S.E., Constantine, A.E., Stephens, C.J., Ewart, A., Schön, R.W., and Parianos, J., 1997. Early Cretaceous volcano-sedimentary successions along the eastern Australian continental margin: implications for the break-up of eastern Gondwana. *Earth and Planetary Science Letters,* 153(1–2):85–102. **https://doi.org/10.1016/S0012-821X(97)00124-6**

Buffett, B.A., 2006. Plate force due to bending at subduction zones. *Journal of Geophysical Research: Solid Earth,* 111(B9):B09405. **https://doi.org/10.1029/2006JB004295**

Burns, R.E., and Andrews, J.E., 1973. Regional aspects of deep sea drilling in the southwest Pacific. *In* Burns, R.E., Andrews, J.E., et al., *Initial Reports of the Deep Sea Drilling Project,* 21: Washington, DC (U.S. Govt. Printing Office), 897–906. **https://doi.org/10.2973/dsdp.proc.21.128.1973**

Cande, S.C., Patriat, P., and Dyment, J., 2010. Motion between the Indian, Antarctic and African plates in the early Cenozoic. *Geophysical Journal International,* 183(1):127–149. **https://doi.org/10.1111/j.1365-246X.2010.04737.x**

Cande, S.C., and Stock, J.M., 2004. Pacific–Antarctic–Australia motion and the formation of the Macquarie plate. *Geophysical Journal International,* 157(1):399–414. **https://doi.org/10.1111/j.1365-246X.2004.02224.x**

Cande, S.C., Stock, J.M., Müller, R.D., and Ishihara, T., 2000. Cenozoic motion between east and west Antarctica. *Nature,* 404(6774):145–150. **https://doi.org/10.1038/35004501**

Caress, D.W., Menard, H.W., and Hey, R.N., 1988. Eocene reorganization of the Pacific-Farallon spreading center north of the Mendocino Fracture Zone. *Journal of Geophysical Research: Solid Earth,* 93(B4):2813–2838. **https://doi.org/10.1029/JB093iB04p02813**

Carter, R.M., McCave, I.N., and Carter, L., 2004. Leg 181 synthesis: fronts, flows, drifts, volcanoes, and the evolution of the southwestern gateway to the Pacific Ocean, eastern New Zealand. *In* Richter, C. (Ed.), *Proceedings of the Ocean Drilling Program, Scientific Results,* 181: College Station, TX (Ocean Drilling Program), 1–111. **https://doi.org/10.2973/odp.proc.sr.181.210.2004**

Cluzel, D., Adams, C.J., Meffre, S., Campbell, H., and Maurizot, P., 2010. Discovery of Early Cretaceous rocks in New Caledonia: new geochemical and U-Pb zircon age constraints on the transition from subduction to marginal breakup in the southwest Pacific. *Journal of Geology,* 118(4):381–397. **https://doi.org/10.1086/652779**

Cluzel, D., Aitchison, J.C., and Picard, C., 2001. Tectonic accretion and underplating of mafic terranes in the late Eocene intraoceanic fore-arc of New Caledonia (southwest Pacific): geodynamic implications. *Tectonophysics,* 340(1–2):23–59. **https://doi.org/10.1016/S0040-1951(01)00148-2**

Cluzel, D., and Meffre, S., 2002. The Boghen Terrane (New Caledonia, SW Pacific): a Jurassic accretionary complex. Preliminary U-Pb radiochronological data on detrital zircon. *Comptes Rendus Geoscience,* 334(11):867–874. **https://doi.org/10.1016/S1631-0713(02)01823-0**

Cluzel, D., Meffre, S., Maurizot, P., and Crawford, A.J., 2006. Earliest Eocene (53 Ma) convergence in the southwest Pacific: evidence from pre-obduction dikes in the ophiolite of New Caledonia. *Terra Nova,* 18(6):395–402. **https://doi.org/10.1111/j.1365-3121.2006.00704.x**

Collot, J., Geli, L., Lafoy, Y., Vially, R., Cluzel, D., Klingelhoefer, F., and Nouzé, H., 2008. Tectonic history of northern New Caledonia Basin from deep offshore seismic reflection: relation to late Eocene obduction in New Caledonia, southwest Pacific. *Tectonics,* 27(6):TC6006. **https://doi.org/10.1029/2008TC002263**

Collot, J., Herzer, R., Lafoy, Y., and Géli, L., 2009. Mesozoic history of the Fairway-Aotea Basin: implications for the early stages of Gondwana fragmentation. *Geochemistry, Geophysics, Geosystems,* 10(12):Q12019. **https://doi.org/10.1029/2009GC002612**

Collot, J., Vendé-Leclerc, M., Rouillard, P., Lafoy, Y., and Géli, L., 2012. Map helps unravel complexities of the southwestern Pacific Ocean. *Eos, Transactions of the American Geophysical Union,* 93(1):1–2. **https://doi.org/10.1029/2012EO010001**

Crawford, A.J., Meffre, S., and Symonds, P.A., 2003. 120 to 0 Ma tectonic evolution of the southwest Pacific and analogous geological evolution of the 600 to 220 Ma Tasman fold belt system. *In* Hillis, R.R., and Müller, R.D. (Eds.), *Evolution and Dynamics of the Australian Plate.* Special Paper - Geological Society of America, 372:383–403. **https://doi.org/10.1130/0-8137-2372-8.383**

Dallanave, E., Agnini, C., Bachtadse, V., Muttoni, G., Crampton, J.S., Strong, C.P., Hines, B.R., Hollis, C.J., and Slotnick, B.S., 2015. Early to middle Eocene magneto-biochronology of the southwest Pacific Ocean and climate influence on sedimentation: insights from the Mead Stream section, New Zealand. *Geological Society of America Bulletin,* 127(5–6):643–660. **https://doi.org/10.1130/B31147.1**

Davy, B., Hoernle, K., and Werner, R., 2008. Hikurangi Plateau: crustal structure, rifted formation, and Gondwana subduction history. *Geochemistry, Geophysics, Geosystems,* 9(7):Q07004. **https://doi.org/10.1029/2007GC001855**

DeConto, R.M., and Pollard, D., 2003. Rapid Cenozoic glaciation of Antarctica induced by declining atmospheric CO_2. *Nature,* 421(6920):245–249. **https://doi.org/10.1038/nature01290**

Dickens, G.R., and Owen, R.M., 1999. The latest Miocene–early Pliocene biogenic bloom: a revised Indian Ocean perspective. *Marine Geology,* 161(1):75–91. **https://doi.org/10.1016/S0025-3227(99)00057-2**

Dickens, G.R., Koelling, M., Smith, D.C., Schneiders, L., and the IODP Expedition 302 Scientists, 2007. Rhizon sampling of pore waters on scientific drilling expeditions: an example from the IODP Expedition 302, Arctic Coring Expedition (ACEX). *Scientific Drilling,* 4:22–25. **http://dx.doi.org/10.2204/iodp.sd.4.08.2007**

Douglas, P.M.J., Affek, H.P., Ivany, L.C., Houben, A.J.P., Sijp, W.P., Sluijs, A., Schouten, S., and Pagani, M., 2014. Pronounced zonal heterogeneity in Eocene southern high-latitude sea surface temperatures. *Proceedings of the National Academy of Sciences of the United States of America,* 111(18):6582–6587. **https://doi.org/10.1073/pnas.1321441111**

Edgar, K.M., Wilson, P.A., Sexton, P.F., and Suganuma, Y., 2007. No extreme bipolar glaciation during the main Eocene calcite compensation shift. *Nature,* 448(7156):908–911. **https://doi.org/10.1038/nature06053**

Edwards, A.R., 1973. Southwest Pacific regional unconformities encountered during Leg 21. *In* Burns, R.E., Andrews, J.E., et al., *Initial Reports of the Deep Sea Drilling Project,* 21: Washington, DC (U.S. Government Printing Office), 701–720. **https://doi.org/10.2973/dsdp.proc.21.120.1973**

Edwards, A.R., 1975. Further comments on the Southwest Pacific Paleogene regional unconformities. *In* Andrews, J.E., Packham, G., et al., *Initial Reports of the Deep Sea Drilling Project,* 30: Washington (U.S. Government Printing Office), 663–666. **https://doi.org/10.2973/dsdp.proc.30.122.1975**

Etienne, S., Collot, J., Sutherland, R., Patriat, M., Bache, F., Rouillard, P., Henrys, S., Barker, D., and Juan, C., in press. Deepwater sedimentation and Cenozoic deformation in the southern New Caledonia Trough (northern Zealandia, SW Pacific). *Marine and Petroleum Geology.* **https://doi.org/10.1016/j.marpetgeo.2017.12.007**

Exon, N.F., Brinkhuis, H., Robert, C.M., Kennett, J.P., Hill, P.J., and Macphail, M.K., 2004a. Tectono-sedimentary history of uppermost Cretaceous through Oligocene sequences from the Tasmanian region: a temperate Antarctic margin. *In* Exon, N.F., Kennett, J.P., and Malone, M. (Eds.), *The Cenozoic Southern Ocean: Tectonics, Sedimentation, and Climate Change between Australia and Antarctica.* Geophysical Monograph, 151:319–344. **https://doi.org/10.1029/151GM18**

Exon, N.F., Kennett, J.P., and Malone, M. (Eds.), 2004b. The Cenozoic Southern Ocean: tectonics, sedimentation and climate change between Australia and Antarctica. *Geophysical Monograph,* 151.

Farrell, J.W., Raffi, I., Janecek, T.R., Murray, D.W., Levitan, M., Dadey, K.A., Emeis, K.-C., Lyle, M., Flores, J.-A., and Hovan, S., 1995. Late Neogene sedimentation patterns in the eastern equatorial Pacific Ocean. *In* Pisias, N.G., Mayer, L.A., Janecek, T.R., Palmer-Julson, A., and van Andel, T.H. (Eds.), *Proceedings of the Ocean Drilling Program, Scientific Results,* 138: College Station, TX (Ocean Drilling Program), 717–756. **https://doi.org/10.2973/odp.proc.sr.138.143.1995**

Gaina, C., Müller, D.R., Royer, J.-Y., Stock, J., Hardebeck, J., and Symonds, P., 1998. The tectonic history of the Tasman Sea: a puzzle with 13 pieces. *Journal of Geophysical Research: Solid Earth,* 103(B6):12413–12433. **https://doi.org/10.1029/98JB00386**

Grant, K.M., and Dickens, G.R., 2002. Coupled productivity and carbon isotope records in the southwest Pacific Ocean during the late Miocene–early Pliocene biogenic bloom. *Palaeogeography, Palaeoclimatology, Palaeoecology,* 187(1–2):61–82. **https://doi.org/10.1016/S0031-0182(02)00508-4**

Gurnis, M., Hall, C., and Lavier, L., 2004. Evolving force balance during incipient subduction. *Geochemistry, Geophysics, Geosystems,* 5(7):Q07001. **https://doi.org/10.1029/2003GC000681**

Hall, C.E., Gurnis, M., Sdrolias, M., Lavier, L.L., and Dietmar Müller, R., 2003. Catastrophic initiation of subduction following forced convergence across fracture zones. *Earth and Planetary Science Letters,* 212(1–2):15–30. **https://doi.org/10.1016/S0012-821X(03)00242-5**

Hancock, H.J.L., Dickens, G.R., Strong, C.P, Hollis, C.J., and Field, B.D., 2003. Foraminiferal and carbon isotope stratigraphy through the Paleocene–Eocene transition at Dee Stream, Marlborough, New Zealand. *New Zealand Journal of Geology and Geophysics,* 46(1):1–19. **https://doi.org/10.1080/00288306.2003.9514992**

Hayes, D.E., and Ringis, J., 1973. Seafloor spreading in the Tasman Sea. *Nature,* 243(5408):454–458. **https://doi.org/10.1038/243454a0**

Herzer, R.H., 1995. Seismic stratigraphy of a buried volcanic arc, Northland, New Zealand and implications for Neogene subduction. *Marine and Petroleum Geology,* 12(5):511–531. **https://doi.org/10.1016/0264-8172(95)91506-K**

Herzer, R.H., Chaproniere, G.C.H., Edwards, A.R., Hollis, C.J., Pelletier, B., Raine, J.I., Scott, G.H., Stagpoole, V., Strong, C.P., Symonds, P., Wilson, G.J., and Zhu, H., 1997. Seismic stratigraphy and structural history of the Reinga Basin and its margins, southern Norfolk Ridge system. *New Zealand Journal of Geology and Geophysics,* 40: 425–451. **https://doi.org/10.1080/00288306.1997.9514774**

Herzer, R.H., Davy, B.W., Mortimer, N., Quilty, P.G., Chaproniere, G.C.H., Jones, C.M., Crawford, A.J., and Hollis, C.J., 2009. Seismic stratigraphy and structure of the Northland Plateau and the development of the Vening Meinesz transform margin, SW Pacific Ocean. *Marine Geophysical Researches,* 30(1):21–60. **https://doi.org/10.1007/s11001-009-9065-1**

Herzer, R.H., and Mascle, J., 1996. Anatomy of a continent-backarc transform—the Vening Meinesz Fracture Zone northwest of New Zealand. *Marine Geophysical Researches,* 18(2):401–427. **https://doi.org/10.1007/BF00286087**

Herzer, R.H., Sykes, R., Killops, S.D., Funnell, R.H., Burggraf, D.R., Townend, J., Raine, J.I., and Wilson, G.J., 1999. Cretaceous carbonaceous rocks from the Norfolk Ridge system, southwest Pacific: implications for regional petroleum potential. *New Zealand Journal of Geology and Geophysics,* 42(1):57–73. **https://doi.org/10.1080/00288306.1999.9514831**

Higgins, K., Hashimoto, T., Fraser, G., Rollet, N., and Colwell, J., 2011. Ion microprobe (SHRIMP) U-Pb dating of Upper Cretaceous volcanics from the northern Lord Howe Rise, Tasman Sea. *Australian Journal of Earth Sciences,* 58(2):195–207. **https://doi.org/10.1080/08120099.2011.543150**

Hollis, C.J., 2006. Radiolarian faunal turnover through the Paleocene–Eocene transition, Mead Stream, New Zealand. *Eclogae Geologicae Helvetiae,* 99(1):S79–S99. **https://doi.org/10.1007/s00015-006-0604-3**

Hollis, C.J., Dickens, G.R., Field, B.D., Jones, C.M., and Strong, C.P., 2005. The Paleocene–Eocene transition at Mead Stream, New Zealand: a southern Pacific record of early Cenozoic global change. *Palaeogeography, Palaeoclimatology, Palaeoecology,* 215(3–4):313–343. **https://doi.org/10.1016/j.palaeo.2004.09.011**

Hollis, C.J., Handley, L., Crouch, E.M., Morgans, H.E.G., Baker, J.A., Creech, J., Collins, K.S., Gibbs, S.J., Huber, M., Schouten, S., Zachos, J.C., and Pancost, R.D., 2009. Tropical sea temperatures in the high latitude South Pacific during the Eocene. *Geology,* 37(2):99–102. **https://doi.org/10.1130/G25200A.1**

Hollis, C.J., Taylor, K.W.R., Handley, L., Pancost, R.D., Huber, M., Creech, J.B., Hines, B.R., Crouch, E.M., Morgans, H.E.G., Crampton, J.S., Gibbs, S., Pearson, P.N., and Zachos, J.C., 2012. Early Paleogene temperature history of the Southwest Pacific Ocean: reconciling proxies and models. *Earth and Planetary Science Letters,* 349–350:53–66. **https://doi.org/10.1016/j.epsl.2012.06.024**

Huber, M., Brinkhuis, H., Stickley, C.E., Döös, K., Sluijs, A., Warnaar, J., Schellenberg, S.A., and Williams, G.L., 2004. Eocene circulation of the Southern Ocean: was Antarctica kept warm by subtropical waters? *Paleoceanography,* 19(4):PA4026. **https://doi.org/10.1029/2004PA001014**

Huber, M., and Caballero, R., 2011. The early Eocene equable climate problem revisited. *Climate of the Past,* 7(2):603–633. **https://doi.org/10.5194/cp-7-603-2011**

Keller, W.R., 2003. Cenozoic plate tectonic reconstructions and plate boundary processes in the southwest Pacific [Ph.D. dissertation]. California Institute of Technology. **http://resolver.caltech.edu/CaltechETD:etd-01102005-223039**

Kennett, J.P., 1977. Cenozoic evolution of Antarctic glaciation, the circum-Antarctic Ocean, and their impact on global paleoceanography. *Journal of Geophysical Research: Oceans and Atmospheres,* 82(27):3843–3860. **https://doi.org/10.1029/JC082i027p03843**

Kennett, J.P., and Exon, N.F., 2004. Paleoceanographic evolution of the Tasmanian seaway and its climatic implications. *In* Exon, N.F., Kennett, J.P., and Malone, M.J. (Eds.), *The Cenozoic Southern Ocean: Tectonics, Sedimentation, and Climate Change between Australia and Antarctica*. Geophysical Monograph, 151:345–367. **https://doi.org/10.1029/151GM19**

Kennett, J.P., Houtz, R.E., Andrews, P.B., Edwards, A.R., Gostin, V.A., Hajós, M., Hampton, M., Jenkins, D.G., Margolis, S.V., Ovenshine, A.T., and Perch-Nielsen, K., 1975. Cenozoic paleoceanography in the southwest Pacific Ocean, Antarctic glaciation, and the development of the Circum-Antarctic Current. *In* Kennett, J.P., Houtz, R.E., et al., *Initial Reports of the Deep Sea Drilling Project,* 29: Washington, DC (U.S. Government Printing Office), 1155–1169. **https://doi.org/10.2973/dsdp.proc.29.144.1975**

Kennett, J.P., and Shackleton, N.J., 1976. Oxygen isotopic evidence for the development of the psychrosphere 38 Myr ago. *Nature,* 260(5551):513–515. **https://doi.org/10.1038/260513a0**

Kennett, J.P., and von der Borch, C.C., 1986. Southwest Pacific Cenozoic paleoceanography. *In* Kennett, J.P., von der Borch, C.C., et al., *Initial Reports of the Deep Sea Drilling Project,* 90: Washington, DC (U.S. Government Printing Office), 1493–1517. **https://doi.org/10.2973/dsdp.proc.90.148.1986**

Kent, D.V., and Muttoni, G., 2008. Equatorial convergence of India and early Cenozoic climate trends. *Proceedings of the National Academy of Sciences of the United States of America,* 105(42):16065–16070. **https://doi.org/10.1073/pnas.0805382105**

King, P.R., and Thrasher, G.P., 1996. Cretaceous–Cenozoic geology and petroleum systems of the Taranaki Basin, New Zealand. *Institute of Geological & Nuclear Sciences Monograph,* 2.

Klingelhoefer, F., Lafoy, Y., Collot, J., Cosquer, E., Géli, L., Nouzé, H., and Vially, R., 2007. Crustal structure of the basin and ridge system west of New Caledonia (southwest Pacific) from wide-angle and reflection seismic data. *Journal of Geophysical Research: Solid Earth,* 112(B11):B11102. **https://doi.org/10.1029/2007JB005093**

Laird, M.G., 1993. Cretaceous continental rifts: New Zealand region. *In* Ballance, P.F. (Ed.), *Sedimentary Basins of the World* (Volume 2): *South Pacific Sedimentary Basins*: Amsterdam (Elsevier), 37–49.

Lee, C.-T.A., Shen, B., Slotnick, B.S., Liao, K., Dickens, G.R., Yokoyama, Y., Lenardic, A., Dasgupta, R., Jellinek, M., Lackey, J.S., et al., 2013. Continental arc–island arc fluctuations, growth of crustal carbonates, and long-term climate change. *Geosphere,* 9(1):21–36. **https://doi.org/10.1130/GES00822.1**

Leng, W., and Gurnis, M., 2015. Subduction initiation at relic arcs. *Geophysical Research Letters,* 42(17):7014–7021. **https://doi.org/10.1002/2015GL064985**

Lithgow-Bertelloni, C., and Richards, M.A., 1998. The dynamics of Cenozoic and Mesozoic plate motions. *Reviews of Geophysics,* 36(1):27–78. **https://doi.org/10.1029/97RG02282**

Lunt, D.J., Dunkley Jones, T., Heinemann, M., Huber, M., LeGrande, A., Winguth, A., Loptson, C., Marotzke, J., Roberts, C.D., Tindall, J., Valdes, P., et al., 2012. A model-data comparison for a multi-model ensemble of early Eocene atmosphere-ocean simulations: EoMIP. *Climate of the Past,* 8(2):1716–1736. **https://doi.org/10.5194/cpd-8-1229-2012**

Lunt, D.J., Otto-Bliesner, B., Poulsen, C.J., Rosenbloom, N., and Tabor, C.R., 2014. *Pre-Pliocene PMIP Working Group: Results So Far, and Questions for Discussion.* Working Group Report of the Paleoclimate Modelling Intercomparison Project.

Maurizot, P., 2012. Palaeocene age for the Adio Limestone, New Caledonia: stratigraphic and regional context. *New Zealand Journal of Geology and Geophysics,* 56(1):16–26. **https://doi.org/10.1080/00288306.2012.735677**

McKenzie, D.P., 1977. The initiation of trenches: a finite amplitude instability. *In* Talwani, M., and Pitman, W.C., III (Eds.), *Island Arcs, Deep Sea Trenches and Back-Arc Basins*. Maurice Ewing Series, 1:57–61. **http://www.agu.org/books/me/v001/ME001p0057/ME001p0057.pdf**

Meffre, S., Falloon, T.J., Crawford, T.J., Hoernle, K., Hauff, F., Duncan, R.A., Bloomer, S.H., and Wright, D.J., 2012. Basalts erupted along the Tongan fore arc during subduction initiation: evidence from geochronology of dredged rocks from the Tonga fore arc and trench. *Geochemistry, Geophysics, Geosystems,* 13(12):Q12003. **https://doi.org/10.1029/2012GC004335**

Mortimer, N., 2004a. Basement gabbro from the Lord Howe Rise. *New Zealand Journal of Geology and Geophysics,* 47(3):501–507. **https://doi.org/10.1080/00288306.2004.9515072**

Mortimer, N., 2004b. New Zealand's geological foundations. *Gondwana Research,* 7(1):261–272. **https://doi.org/10.1016/S1342-937X(05)70324-5**

Mortimer, N., Campbell, H.J., Tulloch, A.J., King, P.R., Stagpoole, V.M., Wood, R.A., Rattenbury, M.S., et al., 2017. Zealandia: Earth's hidden continent. *GSA Today,* 27(3):27–35. **https://doi.org/10.1130/GSATG321A.1**

Mortimer, N., Hauff, F., and Calvert, A.T., 2008. Continuation of the New England orogen, Australia, beneath the Queensland Plateau and Lord Howe Rise. *Australian Journal of Earth Sciences,* 55(2):195–209. **https://doi.org/10.1080/08120090701689365**

Mortimer, N., Herzer, R.H., Gans, P.B., Laporte-Magoni, C., Calvert, A.T., and Bosch, D., 2007. Oligocene–Miocene tectonic evolution of the South Fiji Basin and Northland Plateau, SW Pacific Ocean: evidence from petrology and dating of dredged rocks. *Marine Geology,* 237(1–2):1–24. **https://doi.org/10.1016/j.margeo.2006.10.033**

Mortimer, N., Herzer, R.H., Gans, P.B., Parkinson, D.L., and Seward, D., 1998. Basement geology from Three Kings Ridge to West Norfolk Ridge, southwest Pacific Ocean: evidence from petrology, geochemistry and isotopic dating of dredge samples. *Marine Geology,* 148(3–4):135–162. **https://doi.org/10.1016/S0025-3227(98)00007-3**

Mortimer, N., Tulloch, A.J., Spark, R.N., Walker, N.W., Ladley, E., Allibone, A., and Kimbrough, D.L., 1999. Overview of the Median Batholith, New Zealand: a new interpretation of the geology of the Median Tectonic Zone and adjacent rocks. *Journal of African Earth Sciences,* 29(1):257–268. **https://doi.org/10.1016/S0899-5362(99)00095-0**

Müller, R.D., Gaina, C., Tikku, A., Mihut, D., Cande, S.C., and Stock, J.M., 2000. Mesozoic/Cenozoic tectonic events around Australia. *In* Richards, M.A., Gordon, R.G., and Van Der Hilst, R.D. (Eds.), *The History and Dynamics of Global Plate Motions.* Geophysical Monograph, 121:161–188. **https://doi.org/10.1029/GM121p0161**

Nelson, C.S., and Cooke, P.J., 2001. History of oceanic front development in the New Zealand sector of the Southern Ocean during the Cenozoic—a synthesis. *New Zealand Journal of Geology and Geophysics,* 44(4):535–553. **https://doi.org/10.1080/00288306.2001.9514954**

Nelson, C.S., and Hancock, G.E., 1984. Composition and origin of temperate skeletal carbonate sediments on South Maria Ridge, northern New Zealand. *New Zealand Journal of Marine and Freshwater Research,* 18(2):221–239. **https://doi.org/10.1080/00288330.1984.9516044**

Nicolo, M.J., Dickens, G.R., and Hollis, C.J., 2010. South Pacific intermediate water oxygen depletion at the onset of the Paleocene-Eocene Thermal Maximum as depicted in New Zealand margin sections. *Paleoceanography,* 25(4). **https://doi.org/10.1029/2009PA001904**

Nicolo, M.J., Dickens, G.R., Hollis, C.J., and Zachos, J.C., 2007. Multiple early Eocene hyperthermals: their sedimentary expression on the New Zealand continental margin and in the deep sea. *Geology,* 35(8):699–702. **https://doi.org/10.1130/G23648A.1**

Pagani, M., Huber, M., Liu, Z., Bohaty, S.M., Henderiks, J., Sijp, W., Krishnan, S., and DeConto, R.M., 2011. The role of carbon dioxide during the onset of Antarctic glaciation. *Science,* 334(6060):1261–1264. **https://doi.org/10.1126/science.1203909**

Pearson, P.N., Foster, G.L., and Wade, B.S., 2009. Atmospheric carbon dioxide through the Eocene–Oligocene climate transition. *Nature,* 461(7267):1110–1113. **https://doi.org/10.1038/nature08447**

Pross, J., Contreras, L., Bijl, P.K., Greenwood, D.R., Bohaty, S.M., Schouten, S., Bendle, J.A., et al., 2012. Persistent near-tropical warmth on the Antarctic continent during the early Eocene epoch. *Nature,* 488(7409):73–77. **https://doi.org/10.1038/nature11300**

Rait, G., Chanier, F., and Waters, D.W., 1991. Landward- and seaward-directed thrusting accompanying the onset of subduction beneath New Zealand. *Geology,* 19(3):230–233. **https://doi.org/10.1130/0091-7613(1991)019<0230:LASDTA>2.3.CO;2**

Rea, D.K., Basov, I.A., Krissek, L.A., and the Leg 145 Scientific Party, 1995. Scientific results of drilling the North Pacific transect. *In* Rea, D.K., Basov, I.A., Scholl, D.W., and Allan, J.F. (Eds.), *Proceedings of the Ocean Drilling Program, Scientific Results,* 145: College Station, TX (Ocean Drilling Program), 577–596. **https://doi.org/10.2973/odp.proc.sr.145.146.1995**

Reagan, M.K., McClelland, W.C., Girard, G., Goff, K.R., Peate, D.W., Ohara, Y., and Stern, R.J., 2013. The geology of the southern Mariana fore-arc crust: implications for the scale of Eocene volcanism in the western Pacific. *Earth and Planetary Science Letters,* 380:41–51. **http://dx.doi.org/10.1016/j.epsl.2013.08.013**

Rintoul, S.R., Hughes, C., and Olbers, D., 2001. The Antarctic circumpolar current system. *In* Siedler, G., Church, J., and Gould, J. (Eds.), *Ocean Circulation and Climate.* International Geophysics, 77:271–302. **https://doi.org/10.1016/S0074-6142(01)80124-8**

Royer, J.-Y., and Rollet, N., 1997. Plate-tectonic setting of the Tasmanian region. *In* Exon, N.F., and Crawford, A.J. (Eds.), *West Tasmanian Margin and Offshore Plateaus: Geology, Tectonic and Climatic History, and Resource Potential.* Australian Journal of Earth Sciences, 44(5):543–560. **https://doi.org/10.1080/08120099708728336**

Schellart, W.P., Lister, G.S., and Toy, V.G., 2006. A Late Cretaceous and Cenozoic reconstruction of the Southwest Pacific region: tectonics controlled by subduction and slab rollback processes. *Earth-Science Reviews,* 76(3–4):191–233. **https://doi.org/10.1016/j.earscirev.2006.01.002**

Seton, M., Müller, R.D., Zahirovic, S., Gaina, C., Torsvik, T., Shephard, G., Talsma, A., Gurnis, M., Turner, M., Maus, S., and Chandler, M., 2012. Global continental and ocean basin reconstructions since 200 Ma. *Earth-Science Reviews,* 113(3–4):212–270. **https://doi.org/10.1016/j.earscirev.2012.03.002**

Sharp, W.D., and Clague, D.A., 2006. 50-Ma initiation of Hawaiian-Emperor Bend records major change in Pacific plate motion. *Science,* 313(5791):1281–1284. **https://doi.org/10.1126/science.1128489**

Shipboard Scientific Party, 1973a. Site 206. With contributions by D. Burns and P.N. Webb. *In* Burns, R.E., Andrews, J.E., et al., *Initial Reports of the Deep Sea Drilling Project,* 21: Washington, DC (U.S. Government Printing Office), 103–195. **https://doi.org/10.2973/dsdp.proc.21.106.1973**

Shipboard Scientific Party, 1973b. Site 207. With contributions by D. Burns, W.A. Watters, and P.N. Webb. *In* Burns, R.E., Andrews, J.E., et al., *Initial Reports of the Deep Sea Drilling Project,* 21: Washington, DC (U.S. Government Printing Office), 197–269. **http://dx.doi.org/10.2973/dsdp.proc.21.107.1973**

Shipboard Scientific Party, 1973c. Site 208. With contributions by D. Burns and P.N. Webb. *In* Burns, R.E., Andrews, J.E., et al., *Initial Reports of the Deep Sea Drilling Project,* 21: Washington, DC (U.S. Government Printing Office), 271–331. **https://doi.org/10.2973/dsdp.proc.21.108.1973**

Slotnick, B.S., Dickens, G.R., Nicolo, M.J., Hollis, C.J., Crampton, J.S., Zachos, J.C., and Sluijs, A., 2012. Large-amplitude variations in carbon cycling and terrestrial weathering during the latest Paleocene and earliest Eocene: the record at Mead Stream, New Zealand. *The Journal of Geology,* 120(5):487–505. **https://doi.org/10.1086/666743**

Snyder, G.T, Hiruta, A., Matsumoto, R., Dickens, G.R., Tomaru, H., Takeuchi, R., Komatsubara, J., Ishida, Y., and Yu, H., 2007. Pore water profiles and authigenic mineralization in shallow marine sediments above the methane-charged system on Umitaka Spur, Japan Sea. *Deep-Sea Research, Part II,* 54(11–13):1216–1239. **https://doi.org/10.1016/j.dsr2.2007.04.001**

Stadler, G., Gurnis, M., Burstedde, C., Wilcox, L.C., Alisic, L., and Ghattas, O., 2010. The dynamics of plate tectonics and mantle flow: from local to global scales. *Science,* 329(5995):1033–1038. **https://doi.org/10.1126/science.1191223**

Stagpoole, V., and Nicol, A., 2008. Regional structure and kinematic history of a large subduction back thrust: Taranaki Fault, New Zealand. *Journal of Geophysical Research: Solid Earth,* 113(B1):B01403. **https://doi.org/10.1029/2007JB005170**

Steinberger, B., Sutherland, R., and O'Connell, R.J., 2004. Prediction of Emperor–Hawaii Seamount locations from a revised model of global plate motion and mantle flow. *Nature,* 430(6996):167–173. **https://doi.org/10.1038/nature02660**

Stern, R.J., 2004. Subduction initiation: spontaneous and induced. *Earth and Planetary Science Letters,* 226(3–4):275–292. **http://dx.doi.org/10.1016/j.epsl.2004.08.007**

Stern, R.J., and Bloomer, S.H., 1992. Subduction zone infancy: examples from the Eocene Izu-Bonin-Mariana and Jurassic California arcs. *Geological Society of America Bulletin,* 104(12):1621–1636. **https://doi.org/10.1130/0016-7606(1992)104<1621:SZIEFT>2.3.CO;2**

Sutherland, R., 1995. The Australia-Pacific boundary and Cenozoic plate motions in the SW Pacific: some constraints from Geosat data. *Tectonics,* 14(4):819–831. **https://doi.org/10.1029/95TC00930**

Sutherland, R., 1999. Basement geology and tectonic development of the greater New Zealand region: an interpretation from regional magnetic data. *Tectonophysics,* 308(3):341–362. **https://doi.org/10.1016/S0040-1951(99)00108-0**

Sutherland, R., Collot, J., Bache, F., Henrys, S., Barker, D., Browne, G., Lawrence, M., Morgans, H., Hollis, C., and Clowes, C., 2017. Widespread compression associated with Eocene Tonga-Kermadec subduction initiation. *Geology,* 45(4)3255–358. **https://doi.org/10.1130/G38617.1**

Sutherland, R., Collot, J., Lafoy, Y., Logan, G.A., Hackney, R., Stagpoole, V., Uruski, C., et al., 2010. Lithosphere delamination with foundering of lower crust and mantle caused permanent subsidence of New Caledonia Trough and transient uplift of Lord Howe Rise during Eocene and Oligocene initiation of Tonga-Kermadec subduction, western Pacific. *Tectonics,* 29(2). **https://doi.org/10.1029/2009TC002476**

Sutherland, R., Dickens, G.R., and Blum, P., 2016. *Expedition 371 Scientific Prospectus: Tasman Frontier Subduction Initiation and Paleogene Climate.* International Ocean Discovery Program. **http://dx.doi.org/10.14379/iodp.sp.371.2016**

Sutherland, R., Dickens, G.R., and Blum, P., 2016. Expedition 371 Scientific Prospectus: Tasman Frontier Subduction Initiation and Paleogene Climate. International Ocean Discovery Program. http://dx.doi.org/10.14379/iodp.sp.371.2016

Toth, J., and Gurnis, M., 1998. Dynamics of subduction initiation at preexisting fault zones. *Journal of Geophysical Research: Solid Earth,* 103(B8):18053–18067. **https://doi.org/10.1029/98JB01076**

Tripati, A.K., Delaney, M.L., Zachos, J.C., Anderson, L.D., Kelly, D.C., and Elderfield, H., 2003. Tropical sea-surface temperature reconstruction for the early Paleogene using Mg/Ca ratios of planktonic foraminifera. *Paleoceanography,* 18(4):1101–1113. **https://doi.org/10.1029/2003PA000937**

Tulloch, A.J., Kimbrough, D.L., and Wood, R.A., 1991. Carboniferous granite basement dredged from a site on the southwest margin of the Challenger

Plateau, Tasman Sea. *New Zealand Journal of Geology and Geophysics,* 34(2):121–126. **https://doi.org/10.1080/00288306.1991.9514449**

Tulloch, A.J., Ramezani, J., Mortimer, N., Mortensen, J., van den Bogaard, P., and Maas, R., 2009. Cretaceous felsic volcanism in New Zealand and Lord Howe Rise (Zealandia) as a precursor to final Gondwana break-up. *In* Ring, U., and Wernicke, B. (Eds.), *Extending a Continent: Architecture, Rheology and Heat Budget.* Geological Society Special Publication, 321(1):89–118. **https://doi.org/10.1144/SP321.5**

Turcotte, D.L., Haxby, W.F., and Ockendon, J.R., 1977. Lithospheric instabilities. *In* Talwani, M., and Pitman, W.C., III (Eds.), *Island Arcs, Deep Sea Trenches and Back-Arc Basins.* Maurice Ewing Series, 1:63–69. **http://onlinelibrary.wiley.com/doi/10.1029/ME001p0063/summary**

Uruski, C., and Wood, R., 1991. A new look at the New Caledonia Basin, an extension of the Taranaki Basin, offshore North Island, New Zealand. *Marine and Petroleum Geology,* 8(4):379–391. **https://doi.org/10.1016/0264-8172(91)90061-5**

Uruski, C.I., 2008. Deepwater Taranaki, New Zealand: structural development and petroleum potential. *Exploration Geophysics,* 39(2):94–107. **https://doi.org/10.1071/EG08013**

van Andel, T.H., Heath, G.R., and Moore, T.C., Jr., 1975. Cenozoic history of the central equatorial Pacific Ocean: a synthesis based on Deep Sea Drilling Project data. *In* Sutton, G.H., Manghnani, M.H., Moberly, R., and Mcafee, E.U. (Eds.), *The Geophysics of the Pacific Ocean Basin and its Margin.* Geophysical Monograph, 19:281–295. **https://doi.org/10.1029/GM019p0281**

Weissel, J.K., and Hayes, D.E., 1977. Evolution of the Tasman Sea reappraised. *Earth and Planetary Science Letters,* 36(1):77–84. **https://doi.org/10.1016/0012-821X(77)90189-3**

Whattam, S.A., Malpas, J., Ali, J.R., and Smith, I.E.M., 2008. New SW Pacific tectonic model: cyclical intraoceanic magmatic arc construction and near-coeval emplacement along the Australia-Pacific margin in the Cenozoic. *Geochemistry, Geophysics, Geosystems,* 9(3):Q03021. **https://doi.org/10.1029/2007GC001710**

Whittaker, J.M., Müller, R.D., Leitchenkov, G., Stagg, H., Sdrolias, M., Gaina, C., and Goncharov, A., 2007. Major Australian-Antarctic plate reorganization at Hawaiian-Emperor Bend time. *Science,* 318(5847):83–86. **https://doi.org/10.1126/science.1143769**

Wood, R., and Woodward, D., 2002. Sediment thickness and crustal structure of offshore western New Zealand from 3D gravity modelling. *New Zealand Journal of Geology and Geophysics,* 45(2):243–255. **https://doi.org/10.1080/00288306.2002.9514971**

Wood, R.A., Lamarche, G., Herzer, R.H., Delteil, J., and Davy, B., 1996. Paleogene seafloor spreading in the southeast Tasman Sea. *Tectonics,* 15(5):966–975. **https://doi.org/10.1029/96TC00129**

Zachos, J.C., Dickens, G.R., and Zeebe, R.E., 2008. An early Cenozoic perspective on greenhouse warming and carbon-cycle dynamics. *Nature,* 451(7176):279–283. **https://doi.org/10.1038/nature06588**

Table T1. Hole summary, Expedition 371. Drilled intervals were purposefully drilled without collecting core. DSF = drilling depth below seafloor. APC = advanced piston corer, XCB = extended core barrel, RCB = rotary core barrel.

Hole	Latitude	Longitude	Water depth (m)	Penetration DSF (m)	Cored interval (m)	Recovered length (m)	Recovery (%)	Drilled interval (m)	Total cores (*N*)	APC cores (*N*)	XCB cores (*N*)	RCB cores (*N*)	Time on hole (days)
U1506A	28°39.7180′S	161°44.4240′E	1495	306.1	306.1	192.5	63		36	0	0	36	2.1
U1507A	26°29.3158′S	166°31.7039′E	3568	425.4	425.4	352.7	83		46	26	20	0	3.6
U1507B	26°29.3158′S	166°31.7155′E	3568	864.4	488.4	371.5	76	376.0	52	0	0	52	8.1
U1508A	34°26.8902′S	171°20.6073′E	1609	210.3	210.3	201.1	96		23	23	0	0	1.5
U1508B	34°26.8975′S	171°20.5990′E	1609	503.4	316.7	133.3	42	186.7	37	0	0	37	2.1
U1508C	34°26.8905′S	171°20.5889′E	1609	704.5	283.8	184.8	65	420.7	35	0	0	35	5.0
U1509A	34°39.1312′S	165°49.6599′E	2911	690.7	690.7	462.8	67		74	0	0	74	5.2
U1510A	36°19.7385′S	164°33.5220′E	1238	483.4	483.4	255.9	53		52	17	35	0	2.5
U1510B	36°19.7392′S	164°33.5347′E	1238	66.3	66.3	64.7	98		7	7	0	0	0.4
U1511A	37°33.6665′S	160°18.9380′E	4847	26.6	26.6	7.9	30		3	0	0	3	0.8
U1511B	37°33.6656′S	160°18.9379′E	4847	566.2	431.4	279.3	65	134.8	45	0	0	45	5.1
			Totals:	4847.3	3729.1	2506.4	67	1118.2	410	73	55	282	36.4

Table T2. Video conferencing, Expedition 371. (Continued on next page.)

Date (2017)	Ship time (h)	Location (city, state, and country broadcasting to)	Organization/School name	Age level	Attendees (*N*)	Topic
3 Aug	0500	Washington, DC, USA	Smithsonian/teachers workshop	Adult	25	Plate tectonics, biostratigraphy, climate
9 Aug	0300	Los Angeles CA, USA	Cerritos College	17–30	30	Education
9 Aug	1000	Brisbane, QLD, Australia	Corinda SHS	16–17	25	Plate tectonics
10 Aug	1425	Sydney, NSW, Australia	Barker College, NSW	17–18	25	Plate tectonics, biostratigraphy, climate
14 Aug	0935	Sydney, NSW, Australia	Barker College, NSW	17–18	30	Plate tectonics, biostratigraphy, climate
15 Aug	0430	Cornwall, UK	Royal Geological Society	Adult	20	Stratigraphy
17 Aug	1320	Sydney, NSW, Australia	Barker College, NSW	17–18	30	Plate tectonics
17 Aug	1315	Brisbane, QLD, Australia	Kelvin Grove SHS	11–18	50	History of the earth
18 Aug	1200	Canberra, ACT, Australia	Geoscience (Australia)	Adult	50	Technology/climate change
21 Aug	1130	Brisbane, QLD, Australia	Kenmore State School (STEM) Year 6	10–11	25	Life on the ship
21 Aug	1400	Brisbane, QLD, Australia	Kenmore State School (STEM) Year 5/6	9–10	25	Life on the ship
21 Aug	1000	Gladstone, QLD, Australia	Chanel College	12–13	25	Biostratigraphy, climate change, life on the ship
24 Aug	1000	Rockhampton, QLD, Australia	Emmaus College	12–13	25	Plate tectonics
26 Aug	0315	Brooklyn NY, USA	Brooklyn Public Library	Adult	20	Teacher education
28 Aug	1000	Brisbane, QLD, Australia	Kenmore State School (STEM) Year 5	10–11	25	Life on the ship, plate tectonics
26 Aug	0350	Tamalpais CA, USA	Tamalpais High School	16–17	30	Oceanography
28 Aug	1515	Sydney, NSW, Australia	Pymble Ladies College	17–18	20	Paleontology, biostratigraphy
29 Aug	0400	Tamalpais CA, USA	Tamalpais High School	16–17	25	Oceanography, stratigraphy
30 Aug	0700	Tamalpais CA, USA	Tamalpais High School	16–17	25	Oceanography, stratigraphy
30 Aug	0500	Tamalpais CA, USA	Tamalpais High School	16–17	25	Oceanography, stratigraphy
30 Aug	0100	Tamalpais CA, USA	Tamalpais High School	16–17	25	Oceanography, stratigraphy
1 Sep	0115	Los Angeles CA, USA	Cerritos College	17–30	30	Education/plate tectonics
2 Sep	0100	Tamalpais CA, USA	Tamalpais High School	16–17	25	Oceanography, stratigraphy
5 Sep	0030	Santiago, Chile	Lycee Jean d'Alembert	17–18	25	Oceanography, stratigraphy
6 Sep	0330	Fairfax VA, USA	Robinson Secondary School	17–18	30	Plate tectonics, biostratigraphy, climate
6 Sep	2300	Bremen, Germany	Osterholz-Scharmbeck	10–11	150	Life on the ship, plate tectonics
7 Sep	0400	Brasilia, Brazil	Technical University of Brasilia	Undergrad	75	Life on the ship, plate tectonics
7 Sep	1000	Victoria, Australia	St Augustine's College, Kyabram	13–14	25	Life on the ship, plate tectonics
7 Sep	1500	Cleveland, QLD, Australia	Cleveland District High School	12–13	50	Life on the ship, plate tectonics
7 Sep	2330	Fairfax VA, USA	Robinson Secondary School	17–18	35	Plate tectonics, biostratigraphy
8 Sep	0315	Fairfax VA, USA	Robinson Secondary School	17–18	70	Plate tectonics, biostratigraphy, ship life
9 Sep	1030	Brisbane, QLD, Australia	Pullenvale State School	9–10	75	Life on the ship, plate tectonics
11 Sep	1230	Brisbane, QLD, Australia	Pullenvale State School	8–9	25	Life on the ship, plate tectonics
11 Sep	0715	Dunedin, NZ	University of Otago	Undergrad	60	Oceanography, stratigraphy, plate tectonics
12 Sep	1130	Cleveland, QLD, Australia	Cleveland District High School	12–13	25	Life on the ship, plate tectonics
12 Sep	0230	Middletown NY, USA	Middletown High School	16–18	25	Plate tectonics, biostratigraphy, climate, ship life
13 Sep	0430	Fairfax, VA, US	Robinson Secondary School	16–17	30	Oceanography, stratigraphy, plate tectonics, ship life
13 Sep	1400	Corinda, QLD, Australia	Corinda State High Library	Teachers	15	Oceanography, stratigraphy, plate tectonics, ship life
13 Sep	0945	Cleveland, QLD, Australia	Cleveland District High School	12–13	100	Oceanography, stratigraphy, plate tectonics
14 Sep	1815	Rome, Italy	Licei Gallei-Oberdan	16–18	300	Oceanography, stratigraphy, plate tectonics
14 Sep	2030	Wellington, NZ	Pukerua Bay School	11–12	25	Life on the ship, plate tectonics
14 Aug	2230	Brisbane, QLD, Australia	Clairvaux Mackillop College	12–13	100	Oceanography, stratigraphy, plate tectonics, ship life
15 Sep	1415	Brisbane, QLD, Australia	Clairvaux Mackillop College	12–13	25	Oceanography, stratigraphy, plate tectonics, ship life
15 Sep	0100	Gayole, France	Lycée Édouard Branly, la Porte Gayole	16–17	35	Oceanography, stratigraphy, plate tectonics
16 Sep	0815	Lower Hutt, NZ	Naenae College, Year 10	15–16	25	Oceanography, stratigraphy, plate tectonics, ship life
18 Sep	1230	Kaitaia, NZ	Ahipara, Primary School	10–11	25	Life on the ship, plate tectonics
18 Sep	1930	Switzerland	Swiss Summer School	14–adult	65	Plate tectonics, biostratigraphy, climate
18 Sep	0200	Monterey Peninsula CA, USA	Monterey Peninsula State College			
19 Sep	0330	Manizales, Caldas, Colombia	Universidad de Caldas	17–21	20	Oceanography, stratigraphy, plate tectonics, ship life

Table T2. (continued).

Date (2017)	Ship time (h)	Location (city, state, and country broadcasting to)	Organization/School name	Age level	Attendees (*N*)	Topic
19 Sep	0600	Queens NY, USA	Reach the World ×2 classes	Staff	30	Oceanography, stratigraphy, plate tectonics, biostratigraphy, ship life
19 Sep	0015	University Park PA, USA	Pennsylvania State University	17–21	18	Stratigraphy, plate tectonics, biostratigraphy, ship life
20 Aug	0100	San Antonio TX, USA	Science Technology Engineering, Maths Early College High School	17–21	200	Stratigraphy, plate tectonics, biostratigraphy
20 Aug	0230	San Antonio TX, USA	Science Technology Engineering, Maths Early College High School	16–17	30	Oceanography, stratigraphy, plate tectonics, ship life
21 Aug	0400	Montvale NJ, USA	Pascack Hills, Pascack Hills High School	16–17	25	Oceanography, stratigraphy, plate tectonics, biostratigraphy, ship life
21 Aug	0400	Bronx NY, USA	Reach the World Classes ×2 classes	10–12	60	Stratigraphy, plate tectonics, biostratigraphy, ship life
21 Aug	1300	Birregurra, VIC, Australia	Birregurra Primary School	5–7	25	Plate tectonics, biostratigraphy, ship life
22 Sep	0345	Cerritos CA, USA	Cerritos Community College	17–adult	25	Oceanography, stratigraphy, plate tectonics, biostratigraphy, ship life
23 Sep	0400	Bremen, Germany	Bremen Cultural Centre	Adult	100	Oceanography, stratigraphy, plate tectonics, biostratigraphy, ship life
				Total attendees:	2583	
Media links						
4 Aug	1900	London, England	BBC, Radio	Public	?	Biostratigraphy, climate change, life on the ship
2 Aug	1300	Spain	La Cadiera, Aragón Radio	Adult		Paleontology, climate, ship life
3 Aug	1030	Texas, USA	KB Radio	Adult	?	Stratigraphy of Zealandia
4 Aug	1030	Houston TX, USA	Maggie Martin, Houston Radio	Adult	?	Stratigraphy of Zealandia
10 Aug	0300	Madrid, Spain	Radio Nacional de España	Adult	?	Oceanography, climate, plate tectonics, ship life
10 Aug	0800	NYC, USA	Press 4 Kids, Children's newspaper	8–12	?	Education
11 Aug	0200	Colombia	Colombia Radio Station	Adult	100 000+	Biostratigraphy, climate change, life on the ship
24 Aug	1415	Madrid, Spain	El Pais, national news and online broadcast	Adult	100,000	Paleontology, climate, ship life

Table T3. Video captured and produced, Expedition 371.

Name	Topics covered	Author	Link
The Adventure Begins: Expedition 371 Tasman Sea Frontier	*JOIDES Resolution*, leaving port at Townsville	Adam Kurtz	**http://joidesresolution.org/video-link-the-adventure-begins-expedition-371-tasman-sea-frontier/**
High above the JOIDES Resolution-Expedition 371 Tasman Sea Frontier	*JOIDES Resolution*, drone footage	Adam Kurtz	**http://joidesresolution.org/video-link-high-above-the-joides-resolution-exp-371/**
Exploring Zealandia-Expedition 371 Tasman Sea Frontier	*JOIDES Resolution*, Zealandia, findings from first drill site	Adam Kurtz	**http://joidesresolution.org/video-link-exploring-zealandia-expedition-371-tasman-sea-frontier/**
Drilling 101-Expedition 371 Tasman Sea Frontier	*JOIDES Resolution*, drilling techniques, core samples	Adam Kurtz	**http://joidesresolution.org/video-link-drilling-101-expedition-371-tasman-sea-frontier/**
First Drill-Expedition 371 Tasman Sea Frontier	*JOIDES Resolution*, drill string setup	Adam Kurtz	**http://joidesresolution.org/video-link-first-drill-expedition-371-tasman-sea-frontier/**
Last Core on Deck-Expedition 371 Tasman Sea Frontier	*JOIDES Resolution*, coring process	Adam Kurtz	**http://joidesresolution.org/video-link-last-core-on-deck-expedition-371-tasman-sea-frontier/**
Unedited footage-Google drive	*JOIDES Resolution*, drone footage, ship footage	Adam Kurtz	**https://drive.google.com/open?id=0B5yIHxTx5RDxLTFmZV9acXp0WXc**
Den of Lore podcast, Episode 050	Stratigraphy of Zealandia	Adam Kurtz/ Gerald Dickens	**https://www.youtube.com/watch?v=Vu3Fu1YAN1Y**

Table T4. Media outlets that ran stories associated with the Townsville port call. (Continued on next two pages.)

Date (2017)	Ship time (h)	Media item type	Media outlet	Media outlet state	Media outlet location	Program/section name
31 Jul	1221	Online news	NEWS.com.au	Outside Australia	Online	Other
30 Jul	2021	Online news	The Silver Ink	Outside Australia	National	**http://www.thesilverink.com**
30 Jul	1931	Online news	Lastusa	Outside Australia	National	**http://www.lastusa.com/health**
30 Jul	1732	Online news	US.Blasting.News	Outside Australia	National	**http://us.blastingnews.com/world**
29 Jul	1613	Online news	Pakistan Today	Outside Australia	National	**http://www.pakistantoday.com.pk**
29 Jul	1548	Online news	Borneo Bulletin	Outside Australia	Online	Other
29 Jul	1354	Online news	Inverse	Outside Australia	National	**http://www.inverse.com**
29 Jul	0725	TV	ABC News	VIC	Melbourne	Weekend Breakfast
29 Jul	0725	TV	ABC News	NSW	Regional NSW	Weekend Breakfast
29 Jul	0725	TV	ABC News	QLD	Brisbane	Weekend Breakfast
29 Jul	0725	TV	ABC News	SA	Adelaide	Weekend Breakfast
29 Jul	0725	TV	ABC News	WA	Perth	Weekend Breakfast
29 Jul	0725	TV	ABC News	QLD	Regional Queensland	Weekend Breakfast
29 Jul	0725	TV	ABC News	TAS	Hobart	Weekend Breakfast

Table T4. (continued). (Continued on next page.)

Date (2017)	Ship time (h)	Media item type	Media outlet	Media outlet state	Media outlet location	Program/section name
29 Jul	0725	TV	ABC News	ACT	Canberra	Weekend Breakfast
29 Jul	0725	TV	ABC News	VIC	Regional Victoria	Weekend Breakfast
29 Jul	0725	TV	ABC News	WA	Regional West Australia	Weekend Breakfast
29 Jul	0725	TV	ABC News	NSW	Sydney	Weekend Breakfast
29 Jul	0454	Online news	Inquisitr	National		Other
29 Jul	0420	Online news	MyRepublica.com	National	Online	Other
29 Jul	0358	Online news	Signs of the Times	National	National	**http://www.sott.net**
29 Jul	0000	Newspaper	Townsville Bulletin	QLD	Townsville QLD	General News
28 Jul	2247	TV	ABC News	VIC	Melbourne	The World
28 Jul	2247	TV	ABC News	NSW	Regional NSW	The World
28 Jul	2247	TV	ABC News	QLD	Brisbane	The World
28 Jul	2247	TV	ABC News	SA	Adelaide	The World
28 Jul	2247	TV	ABC News	WA	Perth	The World
28 Jul	2247	TV	ABC News	QLD	Regional Queensland	The World
28 Jul	2247	TV	ABC News	TAS	Hobart	The World
28 Jul	2247	TV	ABC News	ACT	Canberra	The World
28 Jul	2247	TV	ABC News	VIC	Regional Victoria	The World
28 Jul	2247	TV	ABC News	WA	Regional West Australia	The World
28 Jul	2247	TV	ABC News	NSW	Sydney	The World
28 Jul	2025	Online news	Yahoo! UK & Ireland	National		Other
28 Jul	1944	TV	ABC News	VIC	Melbourne	ABC News Evenings With Grandstand
28 Jul	1944	TV	ABC News	NSW	Regional NSW	ABC News Evenings With Grandstand
28 Jul	1944	TV	ABC News	QLD	Brisbane	ABC News Evenings With Grandstand
28 Jul	1944	TV	ABC News	SA	Adelaide	ABC News Evenings With Grandstand
28 Jul	1944	TV	ABC News	WA	Perth	ABC News Evenings With Grandstand
28 Jul	1944	TV	ABC News	QLD	Regional Queensland	ABC News Evenings With Grandstand
28 Jul	1944	TV	ABC News	TAS	Hobart	ABC News Evenings With Grandstand
28 Jul	1944	TV	ABC News	ACT	Canberra	ABC News Evenings With Grandstand
28 Jul	1944	TV	ABC News	VIC	Regional Victoria	ABC News Evenings With Grandstand
28 Jul	1944	TV	ABC News	WA	Regional West Australia	ABC News Evenings With Grandstand
28 Jul	1944	TV	ABC News	NSW	Sydney	ABC News Evenings With Grandstand
28 Jul	1919	TV	ABC	ACT	Canberra	ABC News
28 Jul	1912	TV	ABC	QLD	Regional Queensland	ABC News
28 Jul	1912	TV	ABC	QLD	Brisbane	ABC News
28 Jul	1911	TV	ABC	SA	Adelaide	ABC News
28 Jul	1814	Online news	New York Times	National	Online	Other
28 Jul	1806	TV	Southern Cross Townsville	QLD	Townsville	Nine News Townsville
28 Jul	1805	TV	WIN Townsville	QLD	Townsville	WIN News
28 Jul	1752	Online news	Brisbane Times	National	Online	Other
28 Jul	1741	Online news	Yahoo! News Australia	National	Online	Other
28 Jul	1738	TV	WIN Riverland	SA	Berri	TEN Eyewitness News
28 Jul	1738	TV	Ten Darwin	NT	Darwin	TEN Eyewitness News
28 Jul	1738	TV	Channel 10	SA	Adelaide	TEN Eyewitness News
28 Jul	1733	TV	WIN Mildura	VIC	Mildura	TEN Eyewitness News
28 Jul	1733	TV	WIN Bendigo	VIC	Bendigo	TEN Eyewitness News
28 Jul	1733	TV	WIN Ballarat	VIC	Ballarat	TEN Eyewitness News
28 Jul	1733	TV	WIN Hobart	TAS	Hobart	TEN Eyewitness News
28 Jul	1733	TV	WIN Gippsland	VIC	Sale	TEN Eyewitness News
28 Jul	1733	TV	WIN Shepparton	VIC	Shepparton	TEN Eyewitness News
28 Jul	1733	TV	Channel 10	VIC	Melbourne	TEN Eyewitness News
28 Jul	1723	TV	ABC News	VIC	Melbourne	News Afternoons
28 Jul	1723	TV	ABC News	NSW	Regional NSW	News Afternoons
28 Jul	1723	TV	ABC News	QLD	Brisbane	News Afternoons
28 Jul	1723	TV	ABC News	SA	Adelaide	News Afternoons
28 Jul	1723	TV	ABC News	WA	Perth	News Afternoons
28 Jul	1723	TV	ABC News	QLD	Regional Queensland	News Afternoons
28 Jul	1723	TV	ABC News	TAS	Hobart	News Afternoons
28 Jul	1723	TV	ABC News	ACT	Canberra	News Afternoons
28 Jul	1723	TV	ABC News	VIC	Regional Victoria	News Afternoons
28 Jul	1723	TV	ABC News	WA	Regional West Australia	News Afternoons
28 Jul	1723	TV	ABC News	NSW	Sydney	News Afternoons
28 Jul	1720	TV	WIN Wagga	NSW	Wagga Wagga	TEN Eyewitness News
28 Jul	1720	TV	WIN Wollongong	NSW	Wollongong	TEN Eyewitness News
28 Jul	1720	TV	WIN Canberra	ACT	Canberra	TEN Eyewitness News
28 Jul	1720	TV	WIN Dubbo	NSW	Dubbo	TEN Eyewitness News
28 Jul	1720	TV	WIN Albury	NSW	Albury	TEN Eyewitness News
28 Jul	1720	TV	Ten Lismore	NSW	Lismore	TEN Eyewitness News
28 Jul	1720	TV	Ten Coffs Harbour	NSW	Coffs Harbour	TEN Eyewitness News
28 Jul	1720	TV	WIN Griffith	NSW	Griffith	TEN Eyewitness News
28 Jul	1720	TV	Ten Gold Coast	QLD	Gold Coast	TEN Eyewitness News

Table T4. (continued).

Date (2017)	Ship time (h)	Media item type	Media outlet	Media outlet state	Media outlet location	Program/section name
28 Jul	1720	TV	Ten Tamworth	NSW	Tamworth	TEN Eyewitness News
28 Jul	1720	TV	Ten Taree	NSW	Port Macquarie	TEN Eyewitness News
28 Jul	1720	TV	Ten Newcastle	NSW	Newcastle	TEN Eyewitness News
28 Jul	1720	TV	WIN Orange	NSW	Orange	TEN Eyewitness News
28 Jul	1720	TV	Channel 10	NSW	Sydney	TEN Eyewitness News
28 Jul	1718	TV	WIN Western Australia	WA	Perth	TEN Eyewitness News
28 Jul	1718	TV	West Digital Television	WA	Albany	TEN Eyewitness News
28 Jul	1718	TV	Channel 10	WA	Perth	TEN Eyewitness News
28 Jul	1713	TV	Channel 10	WA	Perth	TEN Eyewitness News
28 Jul	1713	TV	WIN Sunshine Coast	QLD	Sunshine Coast	TEN Eyewitness News
28 Jul	1713	TV	WIN Townsville	QLD	Townsville	TEN Eyewitness News
28 Jul	1713	TV	WIN Rockhampton	QLD	Rockhampton	TEN Eyewitness News
28 Jul	1713	TV	WIN Cairns	QLD	Cairns	TEN Eyewitness News
28 Jul	1713	TV	WIN Toowoomba	QLD	Toowoomba	TEN Eyewitness News
28 Jul	1713	TV	WIN Mackay	QLD	Mackay	TEN Eyewitness News
28 Jul	1713	TV	Ten Sunshine Coast	QLD	Sunshine Coast	TEN Eyewitness News
28 Jul	1713	TV	WIN Wide Bay	QLD	Bundaberg	TEN Eyewitness News
28 Jul	1713	TV	Channel 10	QLD	Brisbane	TEN Eyewitness News
28 Jul	1624	TV	ABC News	VIC	Melbourne	News Afternoons
28 Jul	1624	TV	ABC News	NSW	Regional NSW	News Afternoons
28 Jul	1624	TV	ABC News	QLD	Brisbane	News Afternoons
28 Jul	1624	TV	ABC News	SA	Adelaide	News Afternoons
28 Jul	1624	TV	ABC News	WA	Perth	News Afternoons
28 Jul	1624	TV	ABC News	QLD	Regional Queensland	News Afternoons
28 Jul	1624	TV	ABC News	TAS	Hobart	News Afternoons
28 Jul	1624	TV	ABC News	ACT	Canberra	News Afternoons
28 Jul	1624	TV	ABC News	VIC	Regional Victoria	News Afternoons
28 Jul	1624	TV	ABC News	WA	Regional West Australia	News Afternoons
28 Jul	1624	TV	ABC News	NSW	Sydney	News Afternoons
28 Jul	1603	FM radio	ABC Tropical North	QLD	Mackay	1600 News
28 Jul	1603	AM radio	ABC North Queensland	QLD	Townsville	1600 News
28 Jul	1603	AM radio	ABC Southern Queensland	QLD	Toowoomba	1600 News
28 Jul	1603	AM radio	ABC Far North	QLD	Cairns	1600 News
28 Jul	1603	AM radio	ABC Capricornia	QLD	Rockhampton	1600 News
28 Jul	1603	AM radio	Radio National	QLD	Brisbane	1600 News
28 Jul	1603	FM radio	ABC Sunshine Coast	QLD	Sunshine Coast	1600 News
28 Jul	1603	FM radio	ABC Gold Coast	QLD	Gold Coast	1600 News
28 Jul	1603	AM radio	ABC Western Queensland	QLD	Longreach	1600 News
28 Jul	1603	FM radio	ABC Wide Bay	QLD	Bundaberg	1600 News
28 Jul	1603	FM radio	ABC North West Qld	QLD	Mt Isa	1600 News
28 Jul	1603	AM radio	ABC Radio Brisbane	QLD	Brisbane	1600 News
28 Jul	1536	FM radio	ABC Western Plains NSW	NSW	Dubbo	NSW Statewide Drive
28 Jul	1536	AM radio	ABC Central West NSW	NSW	Orange	NSW Statewide Drive
28 Jul	1536	FM radio	ABC Coffs Coast	NSW	Coffs Harbour	NSW Statewide Drive
28 Jul	1536	FM radio	ABC North Coast NSW	NSW	Lismore	NSW Statewide Drive
28 Jul	1536	AM radio	ABC New England North West	NSW	Tamworth	NSW Statewide Drive
28 Jul	1536	FM radio	ABC Riverina	NSW	Wagga Wagga	NSW Statewide Drive
28 Jul	1536	AM radio	ABC South East NSW	NSW	Bega	NSW Statewide Drive
28 Jul	1536	FM radio	ABC Illawarra	NSW	Wollongong	NSW Statewide Drive
28 Jul	1536	FM radio	ABC Mid North Coast	NSW	Taree	NSW Statewide Drive
28 Jul	1532	AM radio	ABC Radio Canberra	ACT	Canberra	Drive
28 Jul	1516	Online news	Viva.co.id	National		Other
28 Jul	1456	Online news	Yahoo! UK & Ireland	National		Other
28 Jul	1324	Online news	Ten Network	National		Other
28 Jul	1324	Online news	Georgia Newsday	National	National	**http://www.georgianewsday.com/news/regional**
28 Jul	1302	Online news	TravelWireNews	National	National	**http://travelwirenews.com**
28 Jul	1301	Online news	Tech Investor News	National	National	**http://www.techinvestornews.com/Tech-News/Tech-Bloggers**
28 Jul	1254	Online news	Mashable	National		Other
28 Jul	1153	Online news	Daily Mail Australia	National	Online	Other
28 Jul	0952	FM radio	ABC Central Coast	NSW	Erina	Mornings
28 Jul	0952	AM radio	ABC Radio Sydney	NSW	Sydney	Mornings
28 Jul	0924	Online news	Business Insider Australia	National		Other
28 Jul	0800	Online news	Lastusa	National	National	**http://www.lastusa.com/science**
28 Jul	0019	Online news	WA Today	National	Online	Other
28 Jul	0000	Online news	Canberra Times	National	Online	Other
28 Jul	0000	Newspaper	Age	VIC	Melbourne	General News
28 Jul	0000	Newspaper	Sydney Morning Herald	NSW	Sydney	General News
28 Jul	0000	Newspaper	Herald Sun	VIC	Melbourne	General News
27 Jul	1400	Online news	Herald Sun	National	Online	Other

Figure F1. Location of Izu-Bonin-Mariana and Tonga-Kermadec subduction systems in the western Pacific.

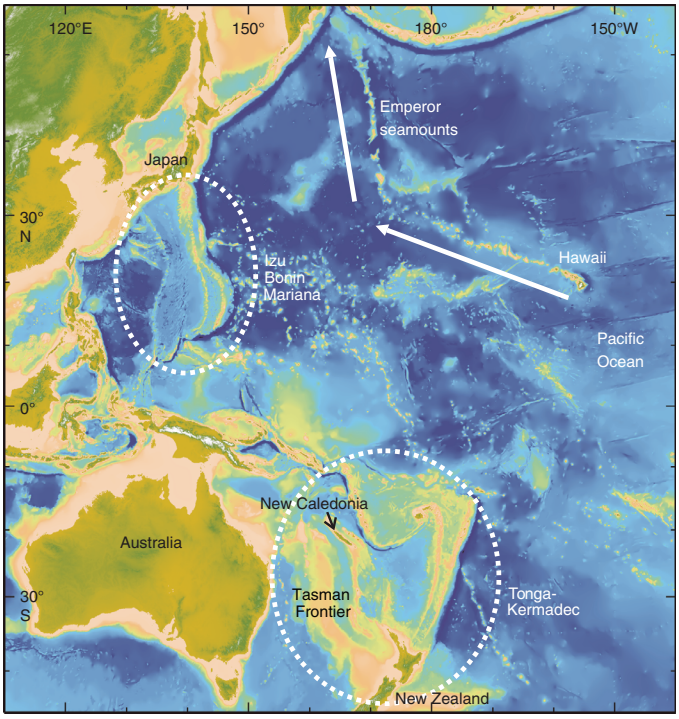

Figure F2. Location of Sites U1506–U1511 (stars) in the southwest Pacific. Circles = relevant DSDP and ODP sites. The expedition departed from Townsville and returned to Hobart. Dashed line = approximate location of Zealandia (Mortimer et al., 2017).

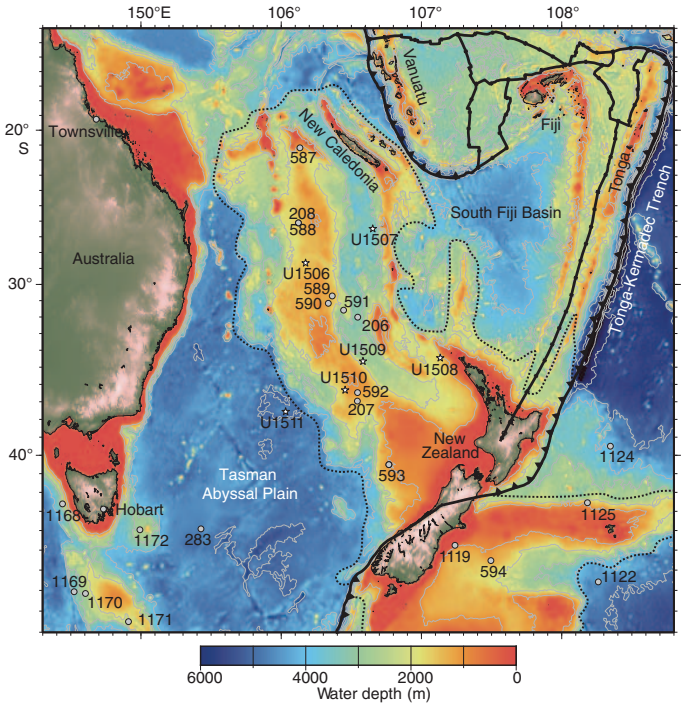

Figure F3. Location of Sites U1506 and U1507 (stars) in northern part of Tasman Frontier in relation to New Caledonia, submarine physiographic features, and DSDP sites (circles).

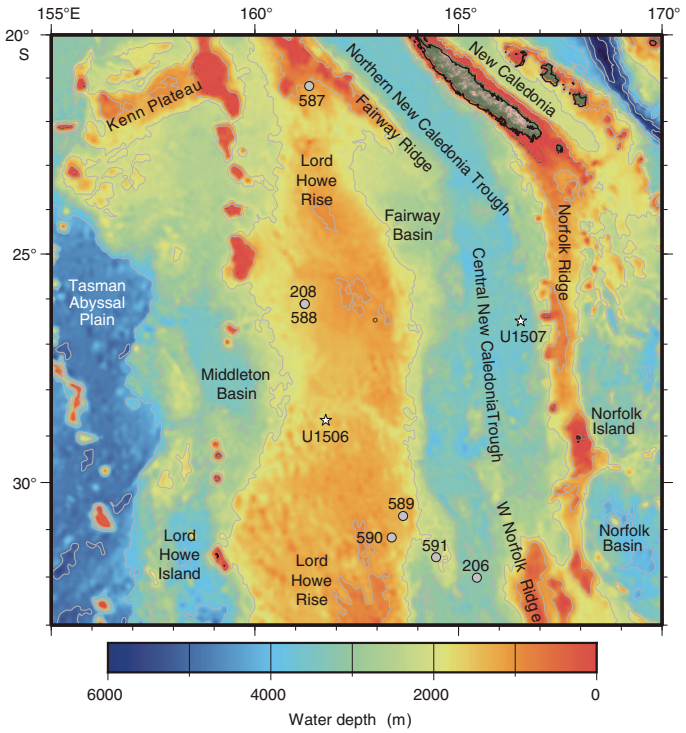

Figure F4. Location of Sites U1508–U1511 (stars) in southern part of Tasman Frontier in relation to New Zealand, submarine physiographic features, and DSDP sites (gray circles). White circles = petroleum boreholes.

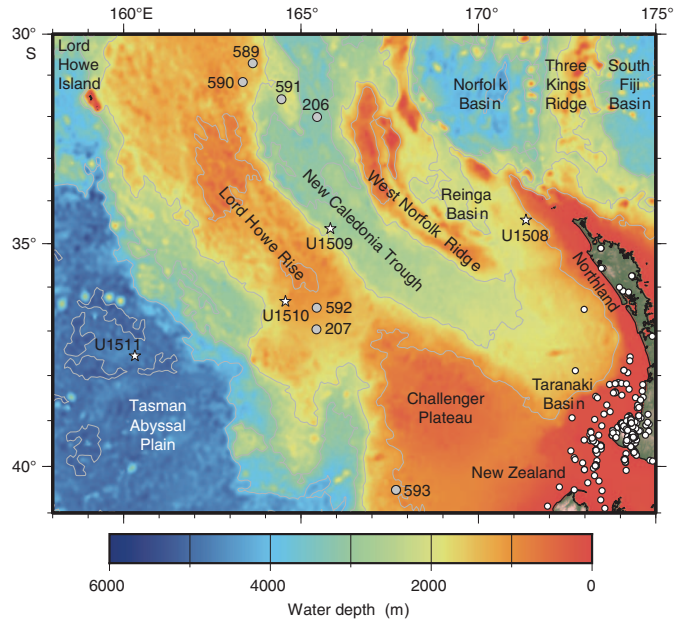

Figure F5. Stable carbon and oxygen isotope compositions of Cenozoic benthic foraminifers (Zachos et al., 2008) compared to global climate/ocean events and regional tectonism. Note that the long-term decrease in $\delta^{18}O$, interpreted as global cooling and greater continental ice volume, begins during the EECO at ~53–49 Ma and thus coincides with significant tectonic change around the Tasman Sea. Oi1 = Oligocene isotope Event 1, MECO = Middle Eocene Climatic Optimum, PETM = Paleocene/Eocene Thermal Maximum.

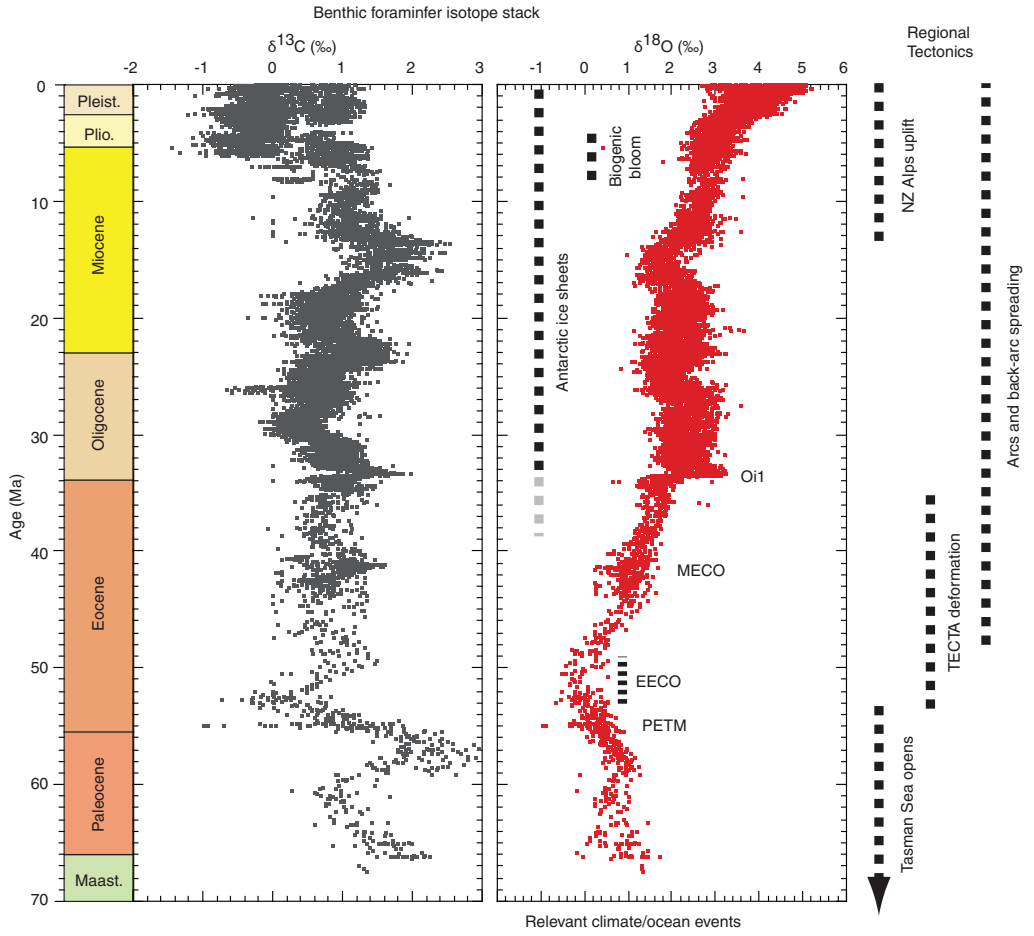

Figure F6. Induced vs. spontaneous subduction initiation models with possible examples (Stern, 2004; Arculus et al., 2015a).

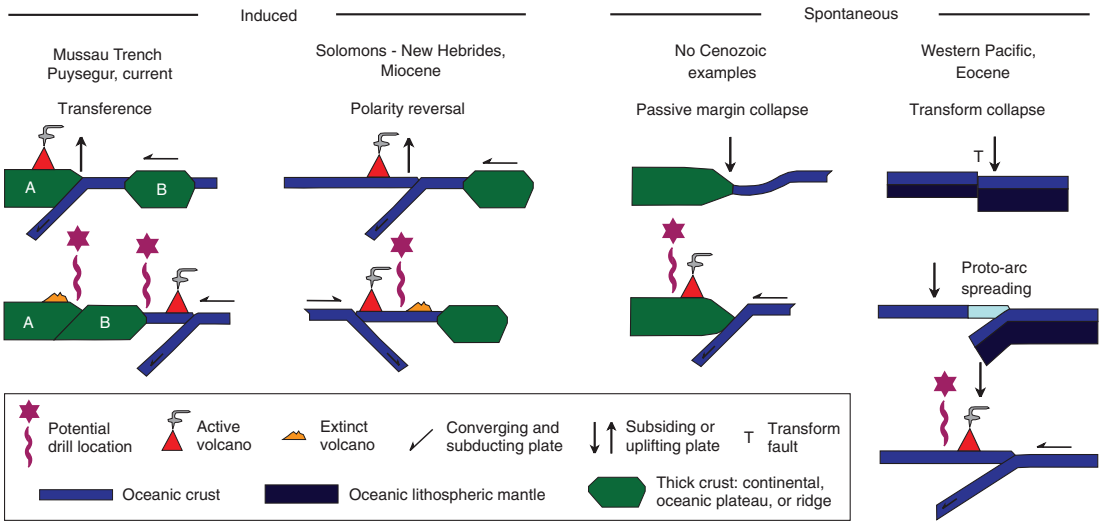

Figure F7. Primary ocean currents (C), fronts (F), and gyres (G) of the Southern Ocean (Rintoul et al., 2001). The Tasman Sea sector is affected by the ACC and EAC.

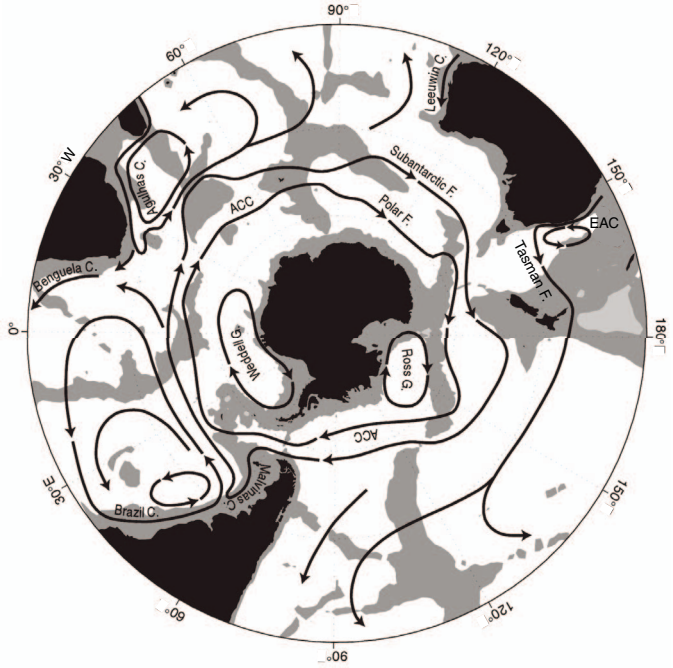

Figure F8. Australia-Pacific relative plate motion history plotted on Tasman Frontier bathymetric features (NC = New Caledonia, R = ridge) (after Bache et al., 2012). Australian plate points are reconstructed relative to a fixed Pacific plate at 1 My intervals. Dashed lines = relocated positions of Norfolk Ridge at 5 My intervals, revealing that plate motion rates were low within New Zealand during the interval 45–25 Ma.

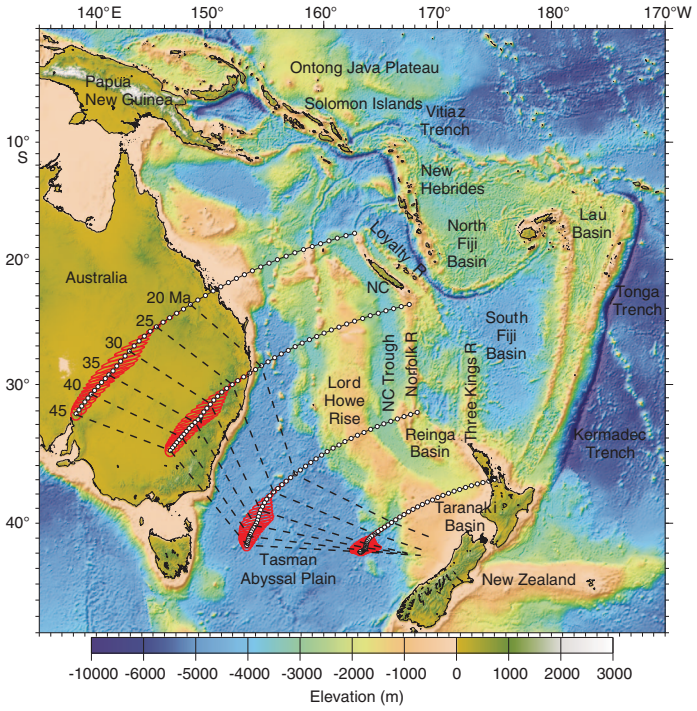

Figure F9. Scales of observation in relation to physical processes. Timing of events relative to each other, to plate motion parameters, and to global events will be used as a discriminator between alternate tectonic models. Arrows = drill site locations.

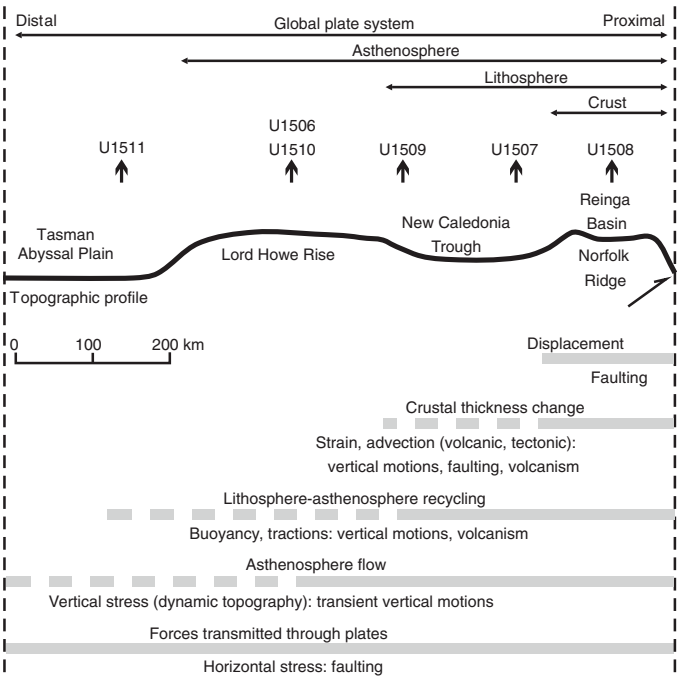

Figure F10. Lithostratigraphic comparison of sites cored during Expedition 371. Arrows = approximate location of ooze–chalk transition.

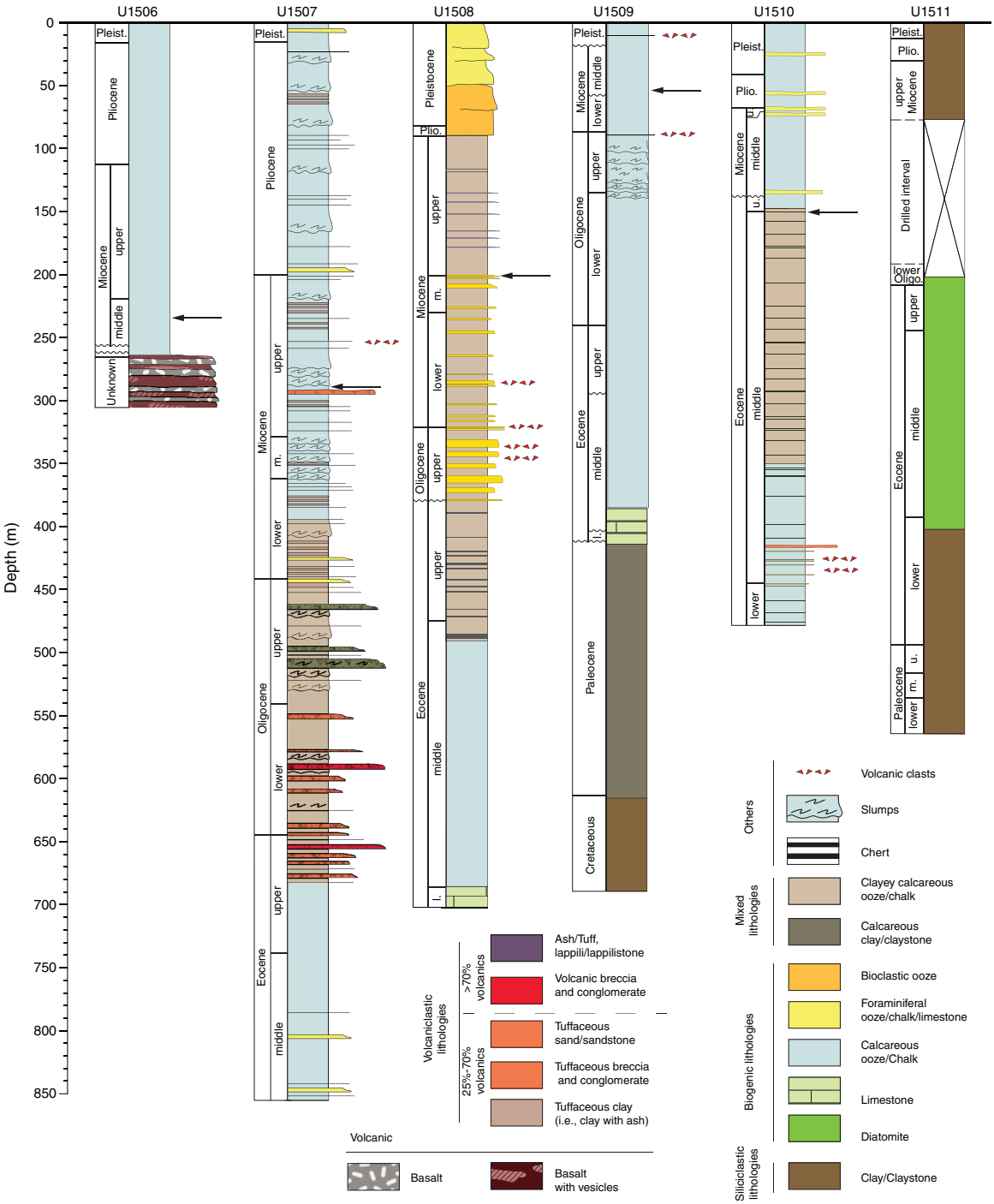

Figure F11. Age-depth models for each site drilled during Expedition 371.

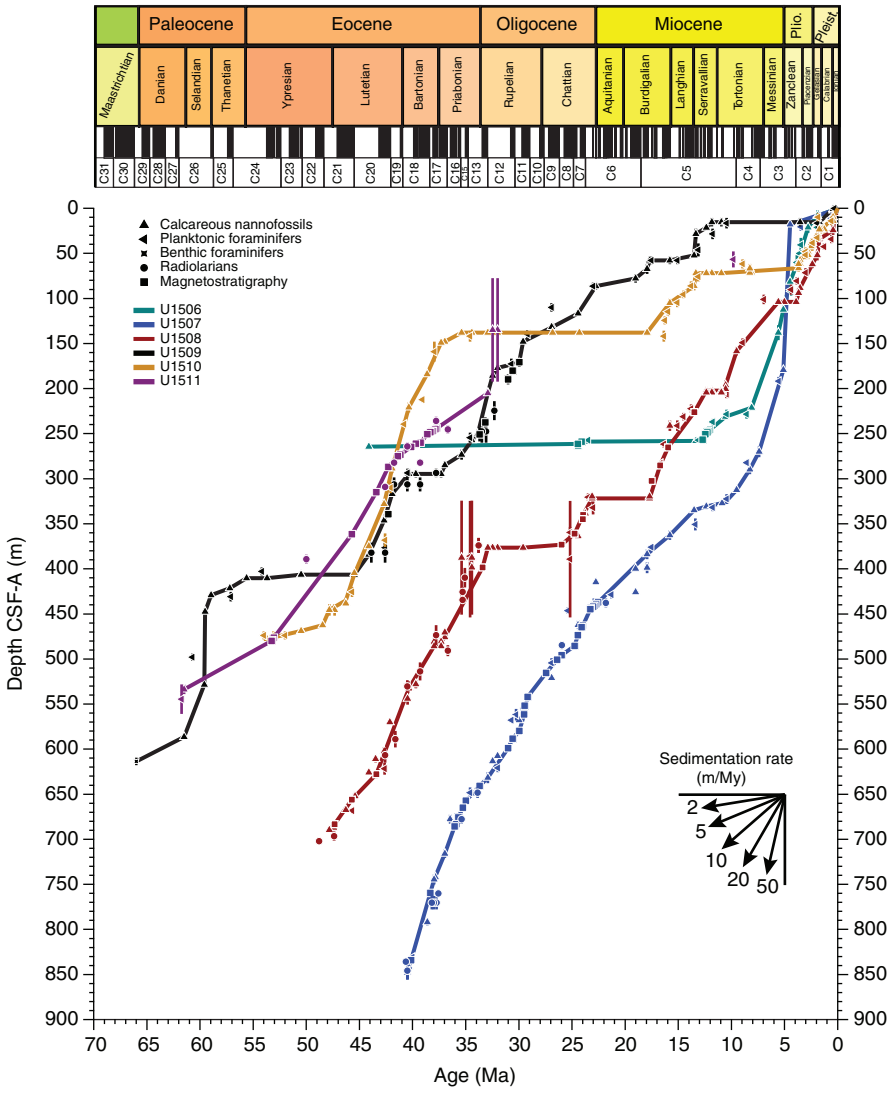

Figure F12. Linear sedimentation rates (LSRs) determined during Expedition 371 compared to previously drilled sites in the region.

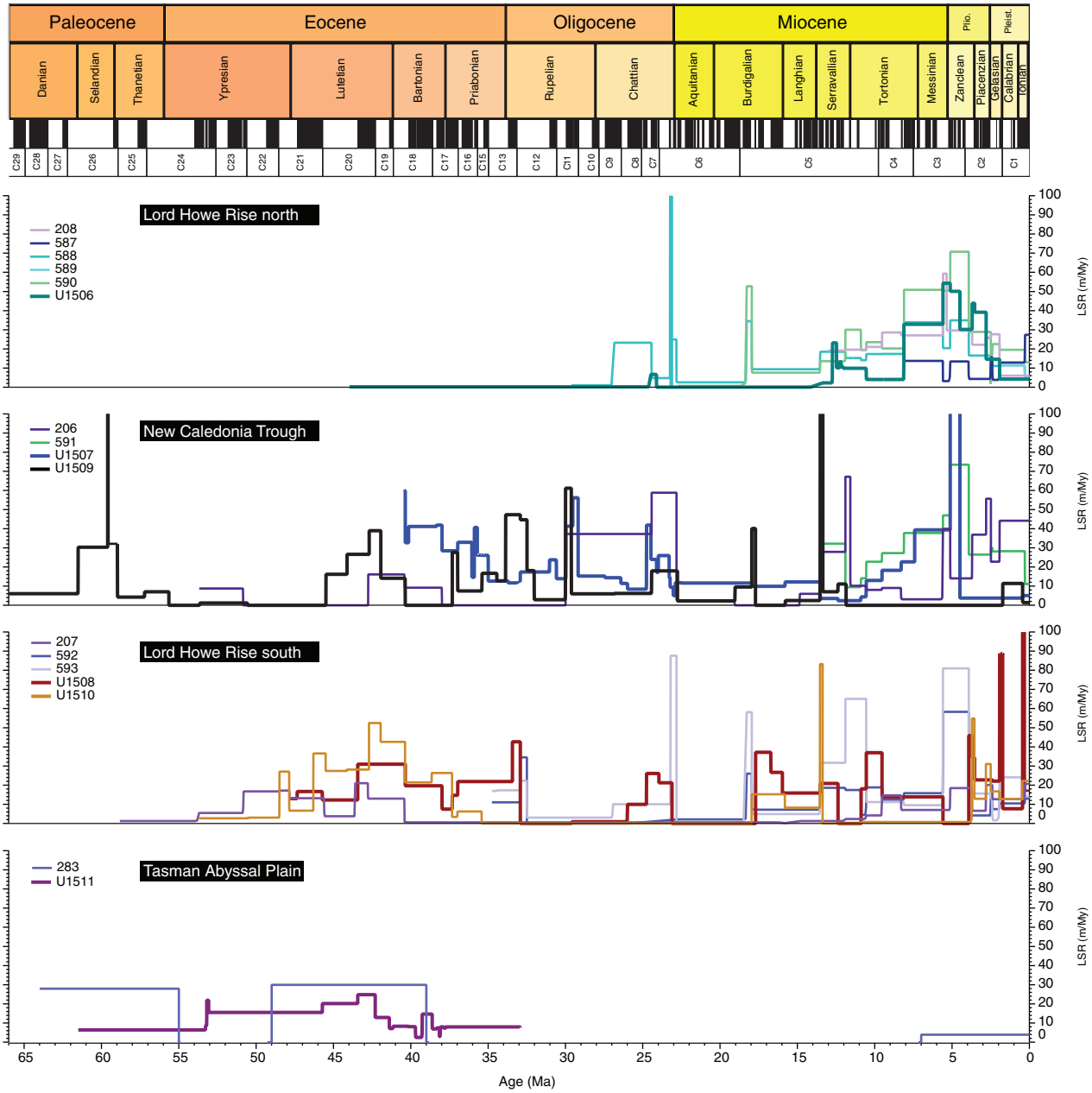

Figure F13. Summary of porosity data collected during Expedition 371.